WATER CHARACTERISTICS AND CURRENT STRUCTURE OF THE INTERMEDIATE WATERS IN THE ARABIAN SEA

Thesis Submitted to the University of Cochin

For the Degree

of

DOCTOR OF PHILOSOPHY

IN

PHYSICAL OCEANOGRAPHY

UNDER THE FACULTY OF MARINE SCIENCES

By

P. MADHUSOODANAN, M. Sc.

NAVAL PHYSICAL AND OCEANOGRAPHIC LABORATORY,

COCHIN 682 004

OCTOBER 1985

C E R T I F I C A T E

This is to certify that this Thesis is an authentic record of research work carried out by Sri P. Madhusoodanan, M.Sc. under my supervision and guidance in Naval Physical and Oceanographic Laboratory for the Ph.D. Degree of the University of Cochin and no part of it has previously formed the basis for the award of any other degree in any University.

Dr. G.S. SHARMA
(Supervising Teacher)
Professor of Physical Oceanography
School of Marine Sciences
University of Cochin

Cochin 682 016,
October, 1985

ACKNOWLEDGEMENT

I am highly indebted and wish to record my deep sense of gratitude to Dr. G. S. Sharma, Professor of Physical Oceanography, School of Marine Sciences, University of Cochin, for suggesting the problem, the valuable guidance, the constant encouragements and critical scrutiny of the manuscript.

My thanks are due to the Director, Naval Physical and Oceanographic Laboratory, Cochin, for providing the necessary facilities. I am also thankful to Dr. Basil Mathew and Mr. C. K. B. Kurup for their persistent encouragement, courtesy and kindness.

Finally, my thanks are due to Mr. P. Suseelan, Naval Physical and Oceanographic Laboratory, for typing the thesis.

CONTENTS

PREFACE

Circulation and water characteristics in the upper layers of the ocean, to a large extent, depend on the atmospheric conditions. In the North Indian Ocean, the atmospheric circulation changes semi-annually during the southwest and northeast monsoons and this in turn reflects in the circulation and water characteristics in the northern part of the Indian Ocean.

At intermediate depths of the Arabian Sea, the circulation and characteristics of water are more influenced by the high saline waters from the north and low saline waters from the south of equator. The interaction of these waters which greatly differ in characteristics is less understood compared to that at the upper layers. An understanding of the nature of the intermediate waters is of vital importance not only because of the unusual characteristics of the waters but also due to the influx of the different water masses from the neighbouring Red Sea and Persian Gulf. Hence, in the present investigation, it is proposed to study the water characteristics and current structure of the intermediate waters in the Arabian Sea through the distribution of the water properties on the isanosteric surfaces of 100, 80, 60 and 40-cl/t, vertical sections, and scatter diagrams.

An attempt is also made to present the potential vorticity between different steric levels to understand the circulation and mixing processes. Data collected during and subsequent to International Indian Ocean Expedition (IIOE) are used for this study. The thesis has been divided into six chapters with further sub divisions.

Chapter one consists of two sections. Section one presents the general introduction while section two describes the materials and methods of the present investigation.

Distribution of properties on different isanosteric surfaces are presented in chapter two.

Chapter three deals with the vertical sections.

The scatter diagrams of potential temperature against salinity for various representative areas forms chapter four.

The distribution of potential vorticity between different steric surfaces are discussed in the fifth chapter.

The last chapter concerns summary of the investigation and conclusion arrived at.

C H A P T E R - I

CHAPTER - I

SECTION 1 - INTRODUCTION

Indian Ocean is the only one not connected to the north pole due to the presence of Asiatic Continent, amongst the major oceans of the world. The northern boundary causes differential heating of land and sea during summer and winter producing the southwest and northeast monsoons. The water characteristics and circulation of the upper layers in the North Indian Ocean are greatly influenced by the monsoon atmospheric circulation. Some aspects of the monsoon influence on the upper layers of the sea are still to be understood, though considerable advances are made in many aspects of the circulation in the upper layers of the North Indian Ocean in recent years. Using observed wind data Luther and O'Brien (1985) modelled the seasonal circulation in the Arabian Sea with remarkable success.

The intermediate layers of the sea which lie below the wind-driven layer are dominated by thermohaline effects. In the Arabian Sea evaporation greatly exceeds precipitation on an annual basis and hence, the salinity of the water increases. The Red Sea and Persian Gulf are areas where immense evaporation takes place. The warm, saline water of the Red Sea flow into the Arabian Sea through the Gulf

of Aden and disperse to intermediate depths. Besides, comparatively less saline waters are transported to the intermediate depths of the Arabian Sea from south of equator. The interaction of these waters, which greatly differ in characteristics is less understood compared to the water characteristics and circulation of the upper layers. Hence, a detailed study of the water characteristics and current structure of the intermediate waters in the Arabian Sea is attempted in the present investigation.

1.1. Earlier studies on the intermediate waters

1.1.1. Studies before IIOE

Much of our knowledge on the water characteristics and current structure in the Arabian Sea, as indeed of the entire Indian Ocean, was derived on the basis of data collected during several expeditions, like, Valdiva(1898-99), Planet (1906), Dana (1920-30), Snellius (1929), John Murray (1933-34), Swedish Deep Sea Expedition (1947-48), Norsel I and II (1955-56). However, the information available from these expeditions is rather limited in space and time.

Using the data of Planet (1906), Dana (1929) and other earlier expeditions in the equatorial and central Indian Ocean, Moller (1929) identified four water masses

namely, subsurface water of subtropical origin, low salinity intermediate water of Antarctic origin, warm saline water flowing towards south, and northward moving Antarctic Water. Schott (1926) and Thomsen (1933) investigated the spreading of Red Sea Water in the Indian Ocean from the then available data. Thomsen (1935) gave a systematic classification of the characteristic water masses in the Indian Ocean. Clowes and Deacon (1935) identified Red Sea Water along the African Coast upto 40°S. Sverdrup et al. (1942) while summarising the studies on the water masses in the Indian Ocean attributed the intermediate salinity maximum in the Arabian Sea to the subsurface outflow from the Red Sea.

1.1.2. Studies based on IIOE data

The first systematic knowledge of the Indian Ocean came from the IIOE (1960-65) when several ships from different nations participated. It is the first of its kind for such a large scale oceanographic survey of any ocean that was taken up. During this expedition, an enormous amount of data were collected which greatly enhanced our knowledge of the oceanography of the Indian Ocean. Based on the data collected during and earlier to IIOE, several studies were carried out.

Taft (1963) while studying the property distributions on isanosteric surfaces suggested the penetration of low salinity water from the Banda and Timor seas into the South Indian Ocean on 125-cl/t surface extending westward to 60°E at 10°S. He attributed this low salinity water to the salinity minimum observed in the Somali Basin at intermediate depths. The incursion of Pacific Water into the Indian Ocean through Banda and Timor seas was earlier identified by Wyrtki (1957) and further confirmed by Wyrtki (1961), Rochford (1961, 1966), Sharma (1972) and Sharma et al. (1978).

Rochford (1964) made an independent study of the salinity maxima in the upper 1,000 m of the North Indian Ocean. He identified five water masses. Three of them are named according to their origin, Red Sea, Persian Gulf and Arabian Sea. The other two could not be assigned the exact origin although one is confined largely to the northern part of the Arabian Sea and the other to the equatorial region of the Indian Ocean.

Warren et al. (1966) studied the water mass structure of the Somali Basin from observations of temperature, salinity and dissolved oxygen content made during the southwest monsoon. They identified the sources of the waters responsible for the water mass structure in the Somali Basin. They discussed the probable vertical influence

of Red Sea Water in the Somali Basin.

Gallagher (1966) described the various water masses and their movement in the Indian Ocean. According to him, high salinity water from the Gulf of Aden enters the Arabian Sea at depths of 400-600 m and is mixed with adjacent water and forms the intermediate water of the Arabian Sea. The salinity of this water mass decreases gradually from west to east and from north to south.

Robinson (1967) demonstrated the spread of Red Sea Water by means of T-S diagrams. Beneath the surface, the salinity decreases with depth until the influence of Persian Gulf and Red Sea waters are encountered and below 1,500 m, cold, less saline Antarctic waters are found.

Using the hydrographic data available upto 1965, Duing and Schwill (1967) identified two distinct salinity maxima in the Arabian Sea below 200 m, contrary to Rochford (1964). They considered that the Red Sea Water spreads around 500-700 m depth. They also suggested that the distribution of salinity in the central part of the Arabian Sea is essentially maintained by large scale mixing processes.

Wooster et al. (1967) presented the water properties at 300, 150 and 100-cl/t surfaces in the Arabian Sea. They

considered 100-cl/t surface as representative of Red Sea Water. The fine structure of the Red Sea Water in the Indian Ocean was investigated by Hamon (1967), Krause (1968) and Federov (1978).

The results of the IIOE were presented in the Oceanographic Atlas of the International Indian Ocean Expedition (Wyrtki, 1971). Mean distributions of the water masses are given in this atlas. The high salinity water leaving the Red Sea through the Strait of Bab-el-Mandeb spreads as a well developed core layer into the Gulf of Aden and the Arabian Sea at depths between 500 and 800 m. The water mass characteristics were described by Wyrtki (1973) based on the IIOE data. He discussed the various sources of water masses affecting the intermediate layers of the Indian Ocean. Sastry and D'Souza (1972) described the distribution of salinity in the Arabian Sea during the southwest monsoon by presenting vertical sections and spatial distribution charts.

Sharma (1972) studied the water characteristics at 200-cl/t surface in the intertropical Indian Ocean by presenting the distribution of the physical properties on this surface. He inferred the transport of low salinity water from the Pacific through Banda and Timor seas into the western Indian Ocean along the South Equatorial Current.

In a latter paper, Sharma et al. (1978) demonstrated clearly the intrusion of the low salinity water of Pacific origin in the western Indian Ocean in the layers above 100-cl/t surface. They also showed that the Somali Basin intermediate salinity minimum is obviously of Pacific origin.

Sharma (1976) critically examined the transequatorial movement of water masses in the Indian Ocean and studied the water characteristics along $5^{\circ}N$, equator, and $5^{\circ}S$ using volumetric analysis and interrelationships of potential temperature-salinity and potential temperature-oxyty in bivariate classes.

Rochford (1964) derived the paths of flow of various water masses in the Indian Ocean from salinity maxima. Warren et al. (1966) inferred the probable flow pattern from the property distributions in the Somali Basin. The current structure in the Somali Basin was discussed by Swallow and Bruce (1966) from both direct measurement and indirect method. Currents at depths around 1,000 m are more variable, and appear to have southward components. The southwestward motion indicated by the geostrophic profile below 500 m seem to be significant. They pointed out that the flow at intermediate depths was irregular and complex in nature.

Bruce and Volkmann (1969) described the geostrophic and direct current measurements off the Somali Coast. They reported an evidence of anticyclonic subsurface motion in the northern Somali Basin prior to the onset of the southwest monsoon. They speculated that this might be a remainder of the northern Somali Gyre of the previous year. Dynamic topographic charts of Bruce (1968) indicated that there was considerable eddy activity in the western Arabian Sea. Bruce (1970) suggested that the currents in the Somali region were part of the anticyclonic circulation formed during the southwest monsoon. Duing (1970) derived the surface circulation of the North Indian Ocean by dynamic computations and discussed at length the vertical extent of the monsoon influence on current structure.

Wyrtki (1973) also described the current structure of the Indian Ocean. During the northeast monsoon, the surface flow does not appear to penetrate much beyond the thermocline whereas during the southwest monsoon, the circulation appears to penetrate below the thermocline. Large parts of the Somali Current are recirculated in an intense eddy, the centre of which is about 300 km offshore. This elongated elliptical eddy stretches for about 100 km parallel to the coast and is intimately connected with the dynamics of the Monsoon Gyre.

1.1.3. Studies after IIOE

After the IIOE survey, a joint Indo-Soviet Meteorological Experiment (ISMEX) was conducted in the Arabian Sea during the summer of 1973. Subsequently, an OCEANOVEX Programme was carried out in the northeast Arabian Sea during 1973-74. A monsoon sub-programme known as MONEX was conducted during 1979 as a part of the Global Atmospheric Research Programme (GARP). As a pre-MONEX build up activity, the Monsoon-77 Experiment on a limited scale was also conducted during 1977.

During the First GARP Global Experiment (FGGE) 1979, a large oceanographic experiment called the Indian Ocean Experiment (INDEX) was conducted in the western Indian Ocean. Preliminary results of this experiment were reported by Swallow (1980). The behaviour of the Somali Current during the spring transition period was documented by Leetmaa et al. (1982). The vertical structure and variability of the Somali Current system were studied using current and temperature observations from moored instruments(Schott and Quadfasel, 1982; Quadfasel and Schott, 1983). Quadfasel and Schott(1982) described the water mass distributions at intermediate layers off the Somali Coast during the southwest monsoon. They discussed the importance of equatorial and near-coastal under-currents in the large-scale redistribution of water masses in the intermediate layers.

The waters carried by the South Equatorial Current and crossing the equator towards north during the south-west monsoon may also be playing an important part in the distribution of properties at intermediate layers in the Arabian Sea. Swallow (1984) suggested that the volume transport of water coming into the Arabian Sea at intermediate depths from south of equator must, generally, exceed that coming in from the northern source. Godfrey and Golding (1981) suggested that the influence of Banda Intermediate Water in the western Indian Ocean is much greater than what was earlier expected. The intermediate waters that are carried by the South Equatorial Current in the later stages of the southwest monsoon goes directly as far as $8^{\circ}N$ under the Somali Current (Swallow and Bruce, 1966) but probably most of it is carried eastwards under Equatorial Counter Current and then westwards in the subsurface westward jets (Luyten et al., 1980)before it reaches the Arabian Sea. Hence, the mixing process at the intermediate waters of the Arabian Sea is much more vigorous than in any other oceans (Swallow, 1984).

Quadfasel and Schott (1982) described an outflow of relatively high saline water in the depth range of 500 to 1,000 m, crossing the equator close to the western boundary under the Somali Current. The southflowing current was about 100 km wide. Beyond it, there could be another boundary current flowing in the opposite direction(Swallow, 1984).

Levy et al. (1982) reported that the mean current in a 14-month record from a current meter at 750 m depth at 0° 47°E was 4 cm s^{-1} towards 350°. Farther east along the equator, at leas as far as 60°E, the mean currents at 750 m were predominantly westward, with only weak and variable meridional components. It seems possible that advection across the equator at intermediate depth is confined to the western boundary, may be in the form of a pair of opposing boundary currents, with the north-going one offshore (Swallow, 1984).

From all the above studies it is understood that there are some conflicting views on the spatial extent of the various water masses at intermediate depths and also in the current structure in the Arabian Sea. The salinity minimum observed at intermediate depths of the western Arabian Sea makes a lot of controversy among the various investigators. In view of the diversity of views expressed by various researchers, the author is tempted to study in detail the water characteristics and current structure of the intermediate waters in the Arabian Sea.

1.1.4. Description of the area

The Arabian Sea is bounded by the land masses of Asia and Africa with an opening in the south. It is connected to the Persian Gulf through the Gulf of Oman through a sill

depth of 50 m at the Hormuz Strait. Similarly, it is connected to the Red Sea through a sill depth of 125 m at the Strait of Bab-el-Mandab through the Gulf of Aden.

The atmospheric and oceanic circulation in the Arabian Sea vary seasonally. During northern summer, a low pressure area developed over the Indian Sub-continent causes the winds to blow persistently from southwest, whereas during winter the wind system over the Arabian Sea is northeasterly due to the influence of high pressure developed over Tibetan Plataue. The winds are weak and unsteady during the transition periods between two monsoons i.e. March-April and October-November. Of the two monsoons, the southwest monsoon lasts over a longer period and the wind speeds are much higher and steadier than the northeast monsoon, causing profound changes in the dynamics of the Arabian Sea.

The surface currents are mainly induced by the monsoon winds resulting in the reversal of the surface circulation semi-annually. During the southwest monsoon, a strong anticyclonic flow is found whereas a weak cyclonic flow is observed during the northeast monsoon. The most notable current in the Arabian Sea is the Somali Current which is found only during the southwest monsoon and perhaps is the strongest current with speeds exceeding 350 cm s^{-1} (Warren et al., 1966; Swallow and

Bruce, 1966; Schott, 1983). Besides, strong upwelling takes place off the coasts of Somalia, Arabian and southwest India.

For the present investigation, the area north of the Equator is considered. Red Sea and Persian Gulf are excluded.

SECTION - II - MATERIALS AND METHODS

The water characteristics and current structure of the intermediate waters of the Arabian Sea are studied by presenting the distributions of salinity and acceleration potential on constant potential thermosteric anomaly surfaces and their topography, vertical sections of potential temperature and salinity along the various latitudes and longitudes, scatter diagrams of potential temperature against salinity at different representative areas, and the distribution of potential vorticity between different isanosteric surfaces.

1.2.1. Isanosteric analysis

The flow of water takes place along the steric surfaces rather than along the geometric surfaces. The use of steric surfaces for the study of the water characteristics and circulation was introduced by Montgomery (1938) and Parr (1938). In their studies they worked out the distribution of conservative properties on the surfaces of constant sigma-T to study the circulation. The method is very useful for studying the water characteristics and flow pattern as revealed from the studies of Montgomery(1938), Taft(1963), Reid(1965),

Tsuchiya (1968) and Sharma (1972). An advantage of the steric surfaces for mapping of oceanographic properties lies in the elimination of depth as an independent variable, whereby the short term vertical displacements in the water column, such as internal waves are eliminated.

The movement of water from a particular source along the steric surface may form, in the maps of salinity and temperature, patterns that indicate the path of flow. The interpretation of tongues of high and low concentrations as evidence of flow is in many cases sound, but it has been recognized that tongues need not always represent the axis of flow in every case and that under some conditions the flow may parallel the isolines of a property (Sverdrup et al.,1942). Thus, core method always need not give an unambiguous picture. It is all the more inapplicable in the Indian Ocean because of the inflow of various water masses at different levels (Sharma, 1976). But Montgomery and Wooster (1954) suggested thermosteric anomaly surfaces to study the water characteristics and flow pattern in place of steric surfaces with the assumption that the pressure effect is much less. Nevertheless, to compensate the pressure effect, constant potential thermosteric anomaly surfaces are employed in the present study.

The main aim of the present investigation being the

study the water characteristics and current structure in the intermediate waters, it is found from the literature that the intermediate waters are covered within the isanosteric surfaces of 100 and 40-cl/t and therefore it is preferred to present the distribution of properties and the flow pattern on 100, 80, 60 and 40-cl/t potential thermosteric anomaly surfaces.

1.2.2. Geostrophic flow

The geostrophic flow along the isanosteric surfaces was deduced from the gradient of acceleration potential (Montgomery, 1937; Montgomery and Sphilhas, 1941; Montgomery and Stroup, 1962), commonly called Montgomery function (Reid, 1965). The expression of acceleration potential used for numerical computation is

$$\int_{\delta_{\theta_o}}^{\delta_\theta} P \, d\delta_\theta + P_o \, \delta_{\theta_o}$$

where δ_{θ_o} is potential thermosteric anomaly at the reference pressure (Po). The reference pressure for this numerical integration has been chosen to be 2,000 db.

1.2.3. Vertical sections of potential temperature and salinity

The surface and intermediate layers of the Arabian Sea are composed of several high and low salinity water masses.

Each water mass has originated from the surface water in a particular area and has carried the characteristics of that area to the positions appropriate to their density, where they lie beneath the sea surface in the Arabian Sea. Mixing between and along these layers modifies the original characteristics, but some of these layers can be recognized over very long distances in the Arabian Sea.

In order to study the water characteristics of the Arabian Sea, seven vertical sections have been chosen. Five of them are zonal; along the equator, $5^{o}N$, $10^{o}N$, $15^{o}N$, $20^{o}N$, while rest of the two are meridional; along $58^{o}E$ and $70^{o}E$ from equator to $15^{o}N$ and $18^{o}N$ respectively. Station positions are given in Fig.1. The water properties presented are potential temperature and salinity.

1.2.4. Scatter diagrams of potential temperature against salinity

The potential temperature-salinity characteristics offer a useful view of the qualitative description of the waters of the region under study. The value of potential temperature is plotted against salinity at the levels of 30, 40, 50, 60, 70, 80, 90, 100, 110, 120, 130, 140, 150, 160, 180, 200, 240, 280, 320, 360, 400, 440, 480, 520, 580, etc., cl/t at the surface and the deepest sampling level. Scatter diagrams for θ-S are prepared at different

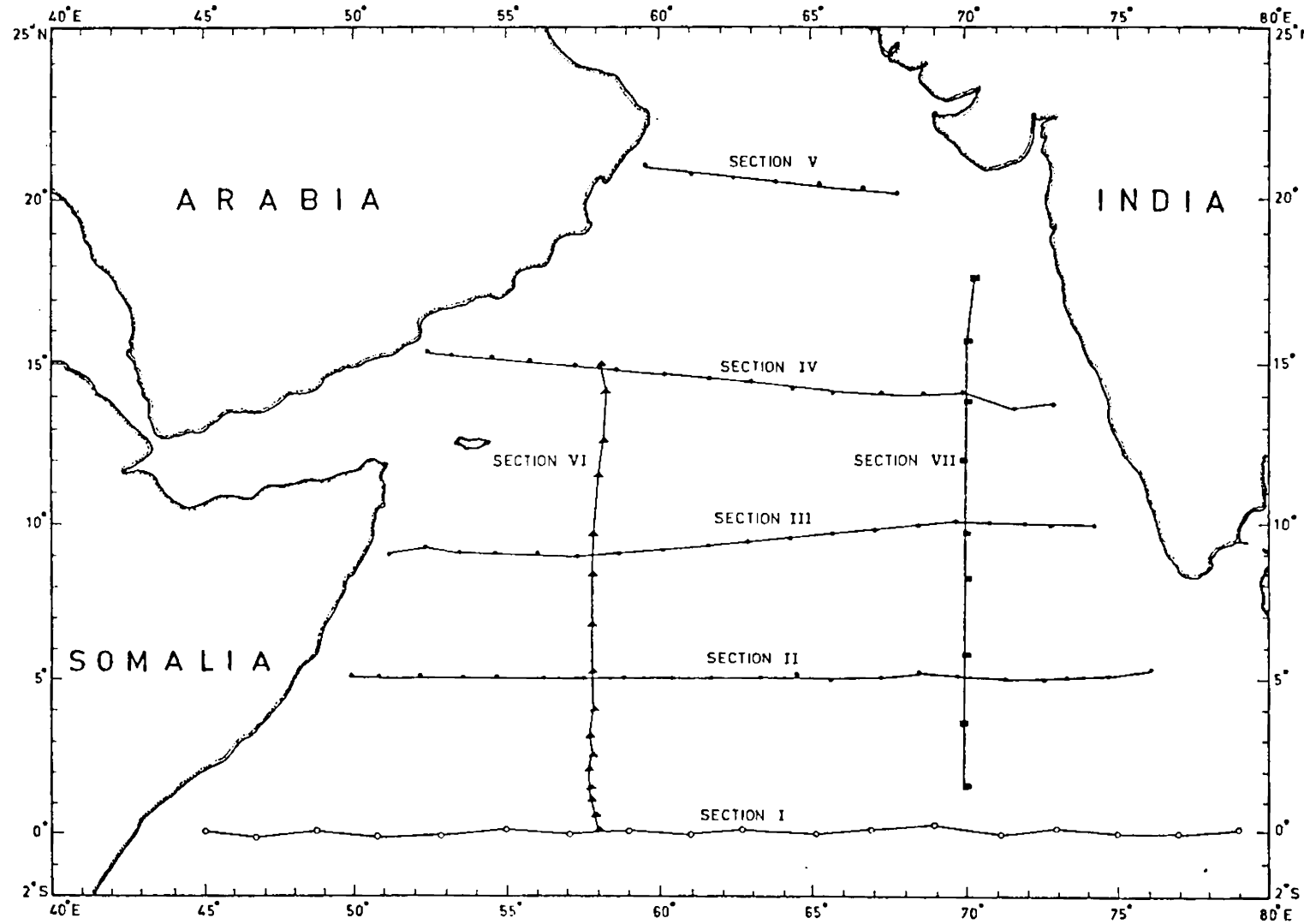

FIG. 1 STATION POSITIONS USED FOR VERTICAL SECTIONS.

areas as shown in Fig.2. This method is advantageous in that the number of representative points is the same for each station, and the relative distribution of properties at each steric level is well depicted (Sharma, 1976).

1.2.5 Potential vorticity

Vorticity is a characteristic of the kinematics of fluid flow which expresses the tendency for portions of the fluid to rotate (Pond and Pickard, 1983). When it is measured relative to the earth, it is called relative vorticity. For a rotating solid object, the vorticity is twice the angular velocity, $2\Omega \sin \phi$ and is known as planetary vorticity. The sum of the relative and planetary vorticities is the absolute vorticity.

For a layer of thickness D in the sea, where the density is unform, the absolute vorticity divided by D is a constant for the motion of a water body, provided that there is no input of vorticity such as might come from wind stress or other frictional effects. The quantity absolute vorticity divided by D is called the potential vorticity of the water (Pond and Pickard, 1983).

Behringer (1972) produced maps of potential vorticity for two density intervals in the intermediate depths in the South Atlantic Ocean. Sarmiento et al. (1982)presented maps

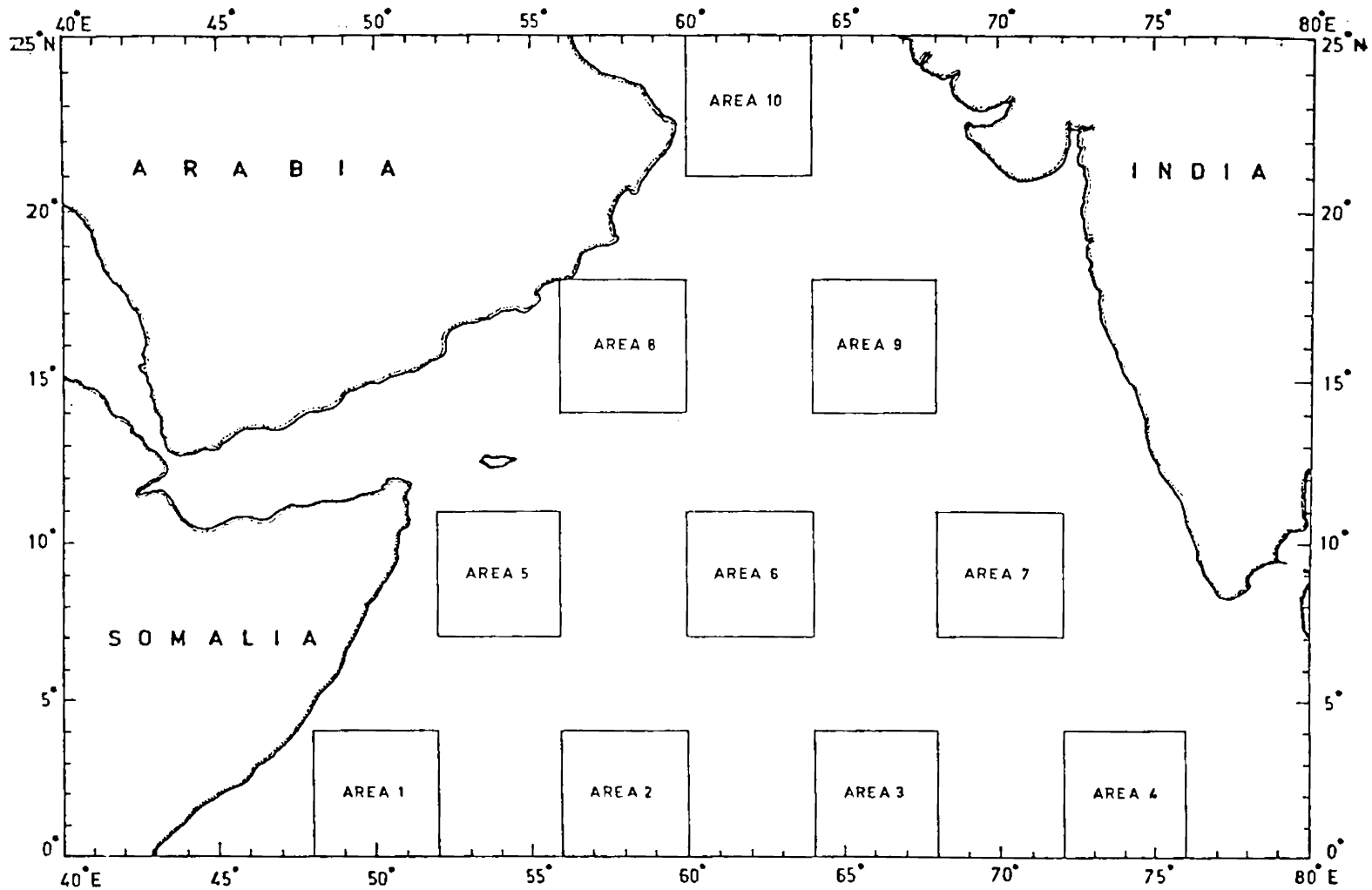

FIG.2 REPRESENTATIVE AREAS FOR WHICH SCATTER DIAGRAMS ARE PRESENTED

of potential vorticity on density surfaces to study the distribution of tritium in the North Atlantic Ocean. The vertical minimum in potential vorticity was used as the primary tracer of Labrador Sea Water by Talley and McCartney (1982). McDowell et al. (1982) presented maps and sections of the large scale North Atlantic potential vorticity in relation to the general circulation. Maps of potential vorticity derived from smoothed density profiles were studied by Stramma (1984).

In the interior of the ocean, for large-scale processes, relative vorticity is negligible compared to planetary vorticity. Under these conditions McDowell et al. (1982) showed that the potential vorticity, q , can be determined from hydrographic measurements of the potential density, $\bar{\rho}$ (in 10^3 kg m^{-3}) alone. In this case,

$$\bar{q} \cong \frac{f}{\rho_o} \frac{\partial \bar{\rho}}{\partial z}$$

where f is the coriolis parameter, ρ_o is the mean density of the layer and z is the vertical coordinate (positive downward).

Using this relationship, potential vorticity is computed and maps of potential vorticity between the isanosteric surfaces, 110 and 90 cl/t, 90 and 70 cl/t and 70 and 50 cl/t are prepared.

1.2.6. Data

The data used in the present investigation are from those collected on board various research vessels during the International Indian Ocean Expedition and subsequently. The details of the oceanographic data used are given in Table 1 and their geographical positions are shown in Fig.3. The stations were chosen on the basis of their geographical distribution, maximum depth of observation and vertical spacing of samples. Stations for which observations, made beyond 1,000 m were only selected.

The study of Duing (1970) reveals that the seasonal influence in the North Indian Ocean is limited only to the upper 400 m. Since the present study of the water characteristics and current structure of the intermediate waters pertains to water below 400 m, the seasonal variation is expected to be negligible. Therefore, no attempt is made to select the data on seasonal basis.

1.2.7. Procedure

For each hydrographic station, the potential temperature for each sample are computed using the equation given by Fonoffof (1962).

Potential temperature $\Theta = T - \Delta T$

where $\Delta T = \Sigma\Sigma\Sigma A_{ijk}\, p^i\, S^j\, T^k$

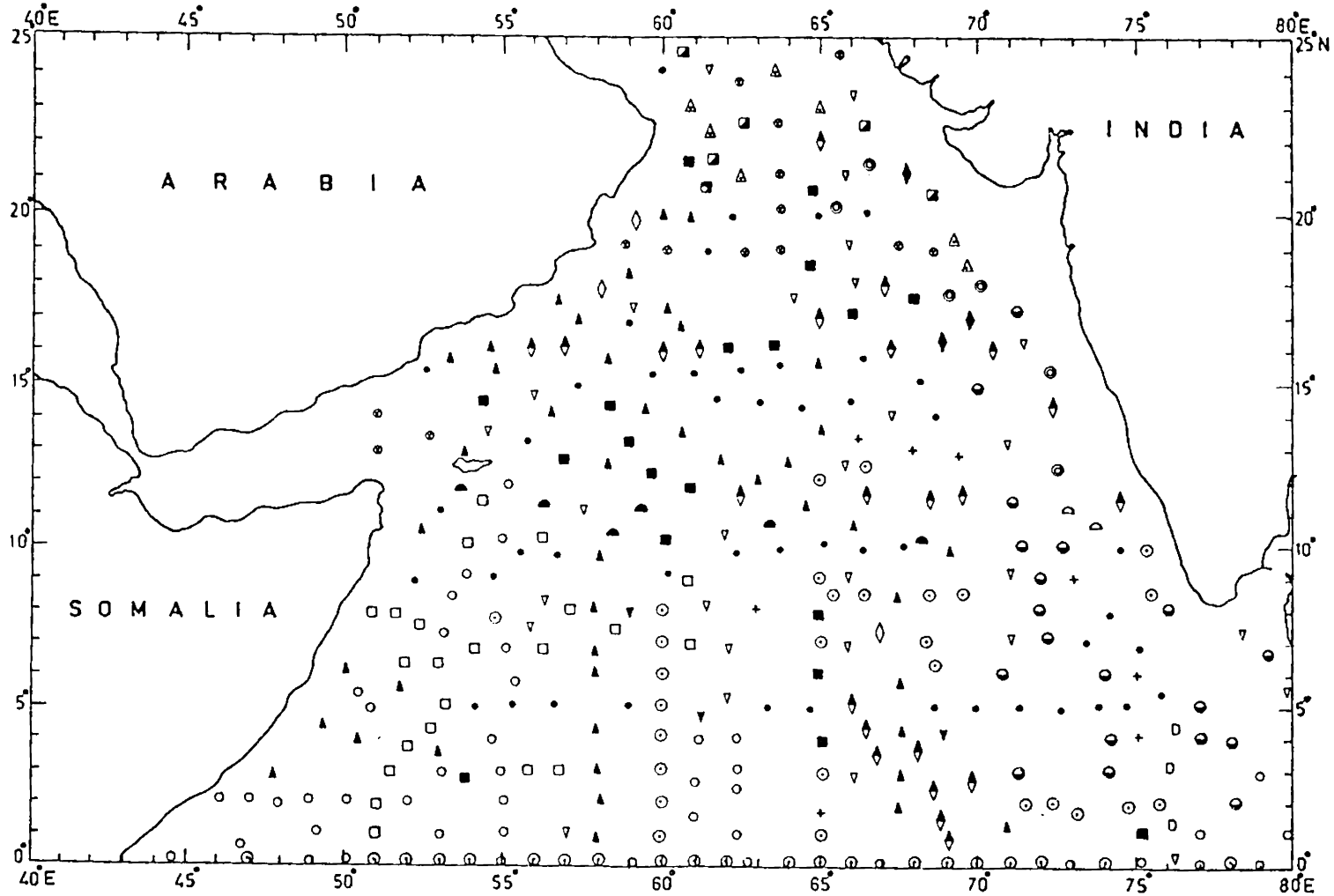

FIG.3 MAP SHOWING LOCATION OF STATION POSITIONS

TABLE 1

Ship	Number of stations used	Months and Year	Symbol used	Abbre-viation
Atlantis II	112	Aug.-Sep. 1963 Feb.-Apr. 1965	●	AN
Anton Bruun	26	Mar., May, Aug., Oct., Nov. 1963 Jan., May 1964	■	AO
Argo	64	Jul.-Aug. 1962 Aug. 1964	⊙	AR
Commandant R. Giraud	15	Sep. 1960 Apr.-May 1961 Jul.-Dec. 1962	⊗	CG
Columbus Iselin	21	Aug.-Sep. 1970	□	CI
Darshak	7	Dec. 1973 Jan.-Feb. 1974	▲	D
Discovery	58	Jul.-Aug. 1963 Mar., May, Jun., Aug., Sep. 1964	▲	DI
Diamantina	3	May 1965	D	DM
Kalva	2	Feb. 1958 Apr. 1959	◘	KA
Kistna	8	Nov.-Dec. 1962 Mar. 1965	+	KI
Meteor	7	Feb.-Mar. 1965	◆	ME
Mikhal Lomonosov	6	May-Jul. 1966	⊙	ML
Okean	54	Jun.-Jul. 1973 Jun.-Jul. 1977	⊙	OK

Ship	Number of stations used	Months and	Year	Symbol used	Abbre-viation
Priliv	20	May,Jul.	1973	◆	PL
		Jun.	1977		
Robert D. Conrad	4	Jun.	1965	◊	RD
Requisite	5	Feb.-Mar.	1961	◪	RE
Shakalsky	7	Jun.	1973	●	SH
Varuna	17	Sep.-Dec.	1962	◒	VA
Vema	3	May-Jun.	1958	▼	VE
Vityaz	29	Jan.-Apr.	1960	▽	VI
		Oct.-Dec.			
		Sep.	1962		
Total	468				

TABLE 1 The details of the oceanographic data used

Using the equation, a computer program was written in PDP-11/60 computer in FORTRAN IV PLUS language, the input values being temperature T in ^{o}C, salinity S in ‰ , depth D in metres and latitude Ø in degrees.

For each station, curves are drawn with a common abscissa of potential temperature against the ordinate of salinity and depth with an overprinted isopleths of thermosteric anomaly. Smooth curves are drawn through the plotted points. Some apparently questionable observed values, such as those indicating hydrostatic instability or abnormal deviation from neighbouring stations are rejected. The values of depth and salinity at each chosen potential thermosteric anomaly surface are read directly from the station curves.

Station values, thus, obtained are plotted on each map, and smooth isopleths are drawn. If a station value is incompatible with nearby stations, the station curves are revised without ignoring the observed values, in such a way that the station value fits better with the nearby stations. The isopleths on the maps are drawn not strictly following the station values, and some points are ignored in the interest of smoothness. This is particularly true for the salinity and depth maps on which the station values show certain deviations.

Since, temperature on an isanosteric surface is uniquely defined by salinity, the salinity maps can be alternatively interpreted as temperature maps. The values of temperature corresponding to the values of salinity for the isohalines drawn on the maps are listed in Table 2. The value of sigma-θ equivalent to those of potential thermosteric anomaly are also listed in Table 2.

The numerical integration of the acceleration potential is carried out at intervals of 10-cl/t to yield the acceleration potential at chosen potential thermosteric anomaly surfaces. The unit of acceleration potential chosen is joule per kilogram (J/Kg). Like the salinity and depth maps, prepared for the chosen four isanosteric surfaces, the maps are also prepared for the acceleration potential. Since, 2,000 db has been chosen as the reference pressure for the computation of acceleration potential and not all stations extend to 2,000 m depth, the number of stations used in the presentation of acceleration potential are less compared to those of the depth and salinity.

Salinity, per mil	Potential temperature, Celsius			
	δ_θ, cl/t	100	80	60	40
	σ_θ, g/l	27.07	27.28	27.49	27.70
34.8					3.47
34.9				6.03	4.23
35.0		9.41	8.01	6.62	4.94
35.1		9.88	8.59	7.18	5.60
35.2		10.33	9.08	7.72	6.22
35.3		10.77	9.55	8.24	6.80
35.4		11.19	10.01	8.74	
35.5		11.60	10.46	9.22	
35.6		12.01	10.89	9.69	
35.7		12.41	11.31	10.15	
35.8		12.81			

TABLE 2 Values of potential temperature corresponding to the values of salinity for the isohalines drawn on the maps of the isanosteric surfaces. The values of σ_θ equivalent to the values of potential thermosteric anomaly are included.

C H A P T E R - II

CHAPTER - II

DISTRIBUTION OF PROPERTIES ON POTENTIAL THERMOSTERIC ANOMALY SURFACES

The spatial distributions of potential temperature and salinity in the intermediate layers of the ocean reflect the combined effect of advection and mixing of different water masses. The large scale distributions of these conservative properties often indicate qualitatively the current structure in the oceans and therefore the circulation must be consistent with the distributions of these properties.

The topography of 100, 80, 60 and 40-cl/t surfaces, and the distribution of acceleration potential relative to 2,000 db and the salinity on these surfaces are shown in Figs. 4 to 15.

2.1. The 100-cl/t surface

2.1.1. Topography

The topography of the 100-cl/t surface deepens to a conspicuous trough structure along 1^{o}-2^{o}N between 46^{o} and 55^{o}E and from 68^{o} to 74^{o}E, with depths exceeding 600 m. These troughs are possibly associated with the northern boundary of the westward flowing undercurrent, discussed by Luyten and Swallow (1976) and Luyten *et al.*

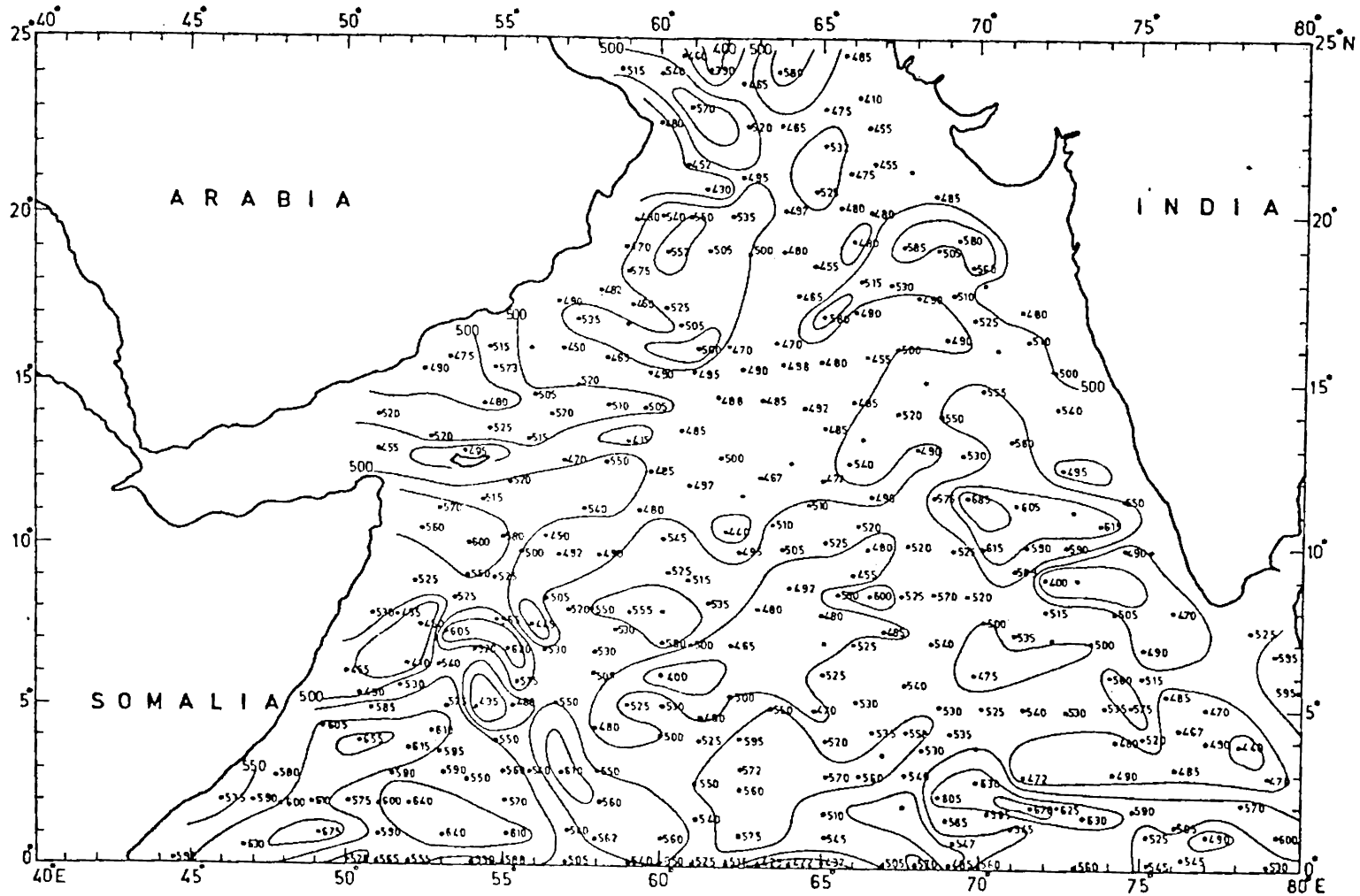

FIG.4 TOPOGRAPHY of 100-cl/t SURFACE

(1980). Off the coast of Somalia, at about 7^{o}N from 53^{o} to 55^{o}E a prominent trough, surrounded by ridges on the east, west and south is obsrved. The southern ridge is located at about 4^{o}-5^{o}N along 54^{o}E. These ridges and the trough may be associated with the boundaries of the southward flowing undercurrent carrying the high salinity water and northward flowing low salinity water (Quadfasel and Schott, 1982). Off the southwest coast of India, a trough is noticed around 11^{o}N between 69^{o} and 74^{o}E and a ridge centered around 9^{o}N, 73^{o}E. These, probably, indicate the boundaries of the southerly flow as confirmed on the distribution of acceleration potential.

Besides, there are a number of troughs and ridges in the depth range of 450 to 650 m in the various regions of the Arabian Sea on this surface. These ridges and troughs suggest the possible occurrence of cyclonic and anticyclonic eddies. Duing (1970) found several cells of low and highs in the dynamic topographic charts which he attributes to the cyclonic and anticyclonic eddies at the surface in the Arabian Sea.

The depth of 100-cl/t surface in the central Arabian Sea is more or less uniform with values slightly less than 500 m. Another region of fairly uniform depth is between 4° and 8°N from 66° to 74°E. In general, the depth of 100-cl/t surface varies from slightly less than 450 m to more than 650 m.

2.1.2. Geostrophic flow

The circulation suggested by the topography of this surface is more or less agreeing with the pattern of acceleration potential. A westerly undercurrent near the equator is clearly indicated except west of 45°E and east of 75°E This appears to be the westward flowing intermediate equatorial current. The westward current below the eastward undercurrent is named as Intermediate Equatorial Current (Hisard and Rual, 1970) in the Pacific Ocean. Its presence in the Indian Ocean was identified from the current meter observations by Luyten and Swallow (1976) at 0°, 53°E. Prominent westward flow at these depths was reported by Leetmaa et al. (1982). A westward flowing undercurrent with jet-like structure is known to exist along the equator between 1° 30'N and 1° 30'S (Luyten and Swallow, 1976; Luyten et al., 1980). North and south of the westward undercurrent, an eastward flow of about 200 km wide, having a vertical structure similar to that of the

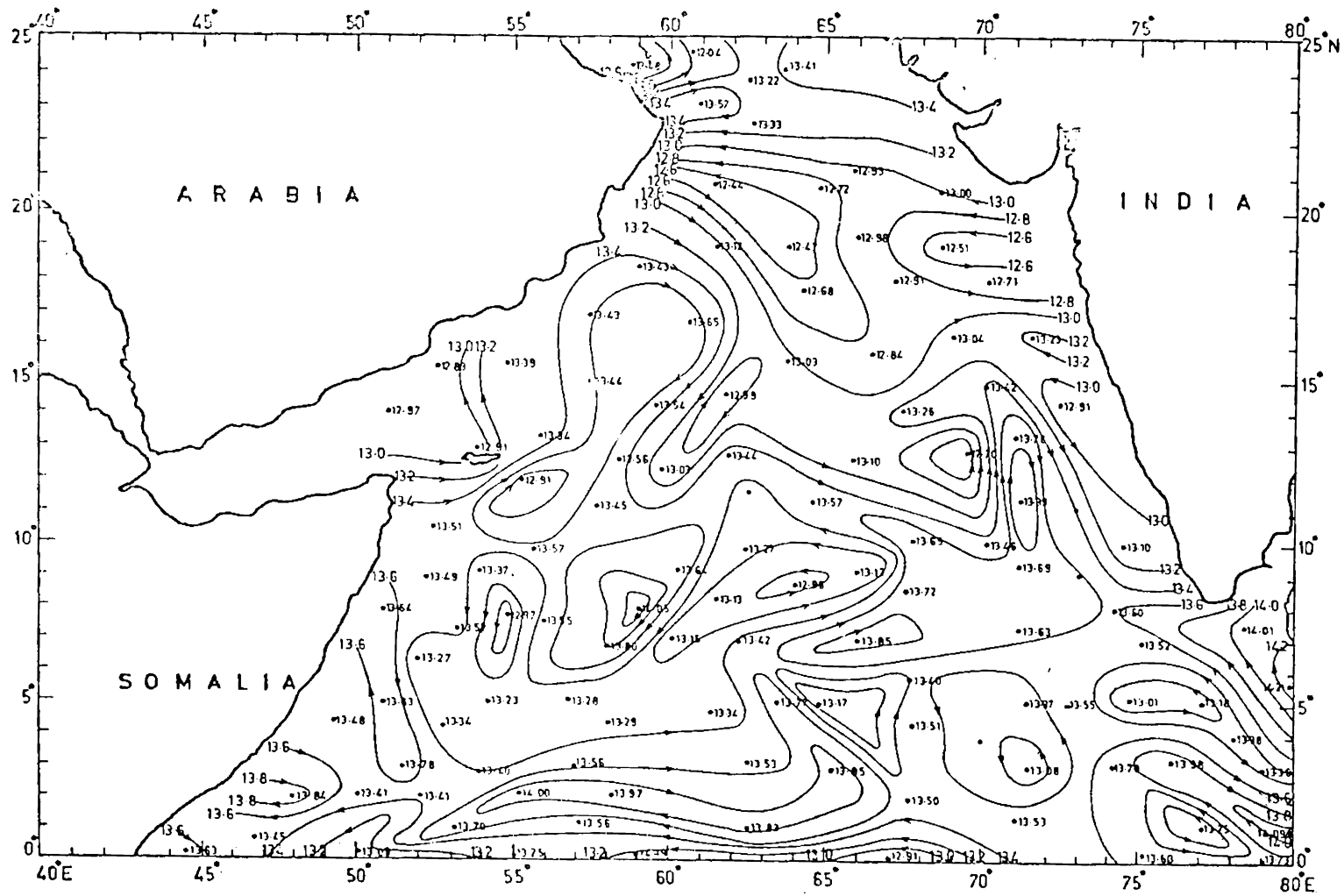

FIG.5 DISTRIBUTION OF ACCELERATION POTENTIAL (joules/kg) RELATIVE TO 2000 db AT THE 100-cl/t SURFACE

westward undercurrent at the equator was reported by Spencer et al. (1980).

Off the coast of Somalia, meridional flow is predominant. This can probably be attributed to the southward flowing undercurrent off Somalia. Measurements by Swallow and Bruce (1966) at 8^{o} 30'N indicate the presence of southward flowing undercurrent. Observations with moored instruments (Duing, 1977; Schott and Quadfasel, 1982) also show strong southward subsurface flow. Such an undercurrent is not seen south of 4^{o}N and north of 8^{o}N (Leetmaa et al., 1982). The existence of the undercurrent at different times of the year suggests that it is a permanent feature of the subsurface circulation rather than a transient phenomenon (Leetmaa et al., 1982). The presence of a southward flowing current beneath the northern part of the Somali Current is also documented in a 2½ year time series observations of currents at moored stations near 5^{o}N, about 30 km off the Somali Coast (Quadfasel and Schott,1983).

An anticyclonic flow pattern is noticed near the southern Somali Coast between 1^{o} and 3^{o}N from 46^{o} to 49^{o}E that can, probably, be attributed to the recirculation of the westward flowing equatorial undercurrent near the

East African Coast. Quadfasel and Schott (1982) report that equatorial water which is nearly homogeneous in the vertical is carried by the westward flowing equatorial undercurrent and before it reaches the East African Coast, it is recirculated to the east just north and south of the equator. These subsequently drift as anticyclonic subsurface eddies away from the equator into the northern and southern parts of the Somali Basin.

A southerly flow is observed off the southwest coast of India. Wyrtki's maps (1971) did not show such a flow at 500 m relative to 3,000 db, perhaps, due to lack of adequate number of stations or might have been masked in the averaging.

Zonal flow is predominant in the northern Arabian Sea while northerly prevails off the southeast coast of Arabia and at the mouth of Gulf of Oman.

Similar to the topography map, the distribution of acceleration potential on 100-cl/t surface exhibits a number of high and low values in different regions of the Arabian Sea. The occurrence of the complex pattern of highs and lows are indicative of anticyclonic and cyclonic eddies and are seen in the earlier works of Swallow and Bruce (1966), Bruce (1968), Bruce (1970) and Duing (1970),

Duing (1970) stated that even if one takes into account the fact that the data are of very heterogeneous quality, there can be little doubt that this complex distribution really exists.

2.1.3. Salinity

The salinity distribution on the 100-cl/t surface shows significant spatial variation. The salinity values range from 34.94 to 35.89‰. The lower salinities are encountered near the equator because of the influence of low salinity water from the southern hemisphere as well as advection of equatorial Pacific Ocean Water that flows along the South Equatorial Current to the western Indian Ocean (Wyrtki, 1957, 1961; Taft, 1963; Sharma, 1972; Sharma et al., 1978). Salinity values above 35.80‰ are noticed in the northern Arabian Sea. Relatively high salinity values observed in the central western Arabian Sea are clearly due to the influence of Red Sea Water.

The isohalines are zonal near the equator, whereas they are meridional off the northern Somali Coast. Tongue-like structure observed off the northern Somali Coast suggests the southward advection of Red Sea Water (Quadfasel and Schott, 1982). Off the west coast of India, similar tongue-like structure is noticed indicating southerly flow as found on the distribution of acceleration potential.

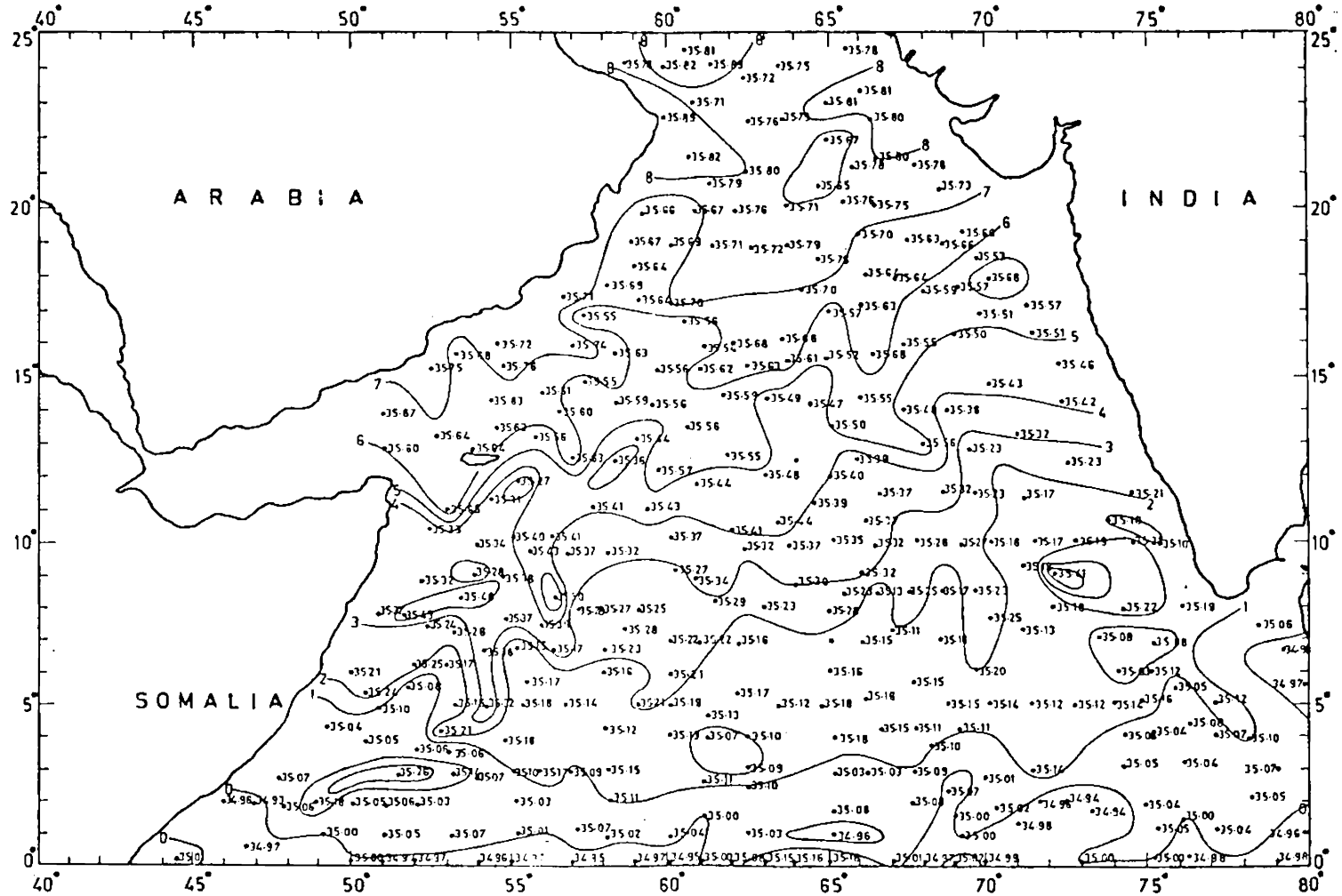

FIG.6 SALINITY (‰) OF 100-cl/t SURFACE

Another interesting feature is the presence of two cells of high salinity water, one along the southern Somali Coast and the other along the southwest coast of India. Rapid decrease of salinity from the east of the Gulf of Aden towards south and southeast of Socotra Island may be due to horizontal advection. In general, salinity decreases from north to south and from west to east on this surface.

2.2. The 80-cl/t surface

2.2.1. Topography

The topography of the 80-cl/t surface closely resembles that of 100-cl/t surface in many respects. The troughs and ridges associated with the boundaries of the currents observed on the 100-cl/t surface are all found on this surface also. The depth of the surface, in general, varies from 600 to 925 m.

A comparison between the topography of 100 and 80-cl/t surfaces shows relatively lower thickness (less than 200 m) between these two surfaces off the southern Somali Coast, east of the Gulf of Aden, central Arabian Sea and off the west coast of India. Such a condition indicates higher stability of the waters between these two isanosteric surfaces. On the contrary, greater thickness (more than 250 m) is found near Socotra Island, northern and southeastern Arabian Sea where the vertical stability is less.

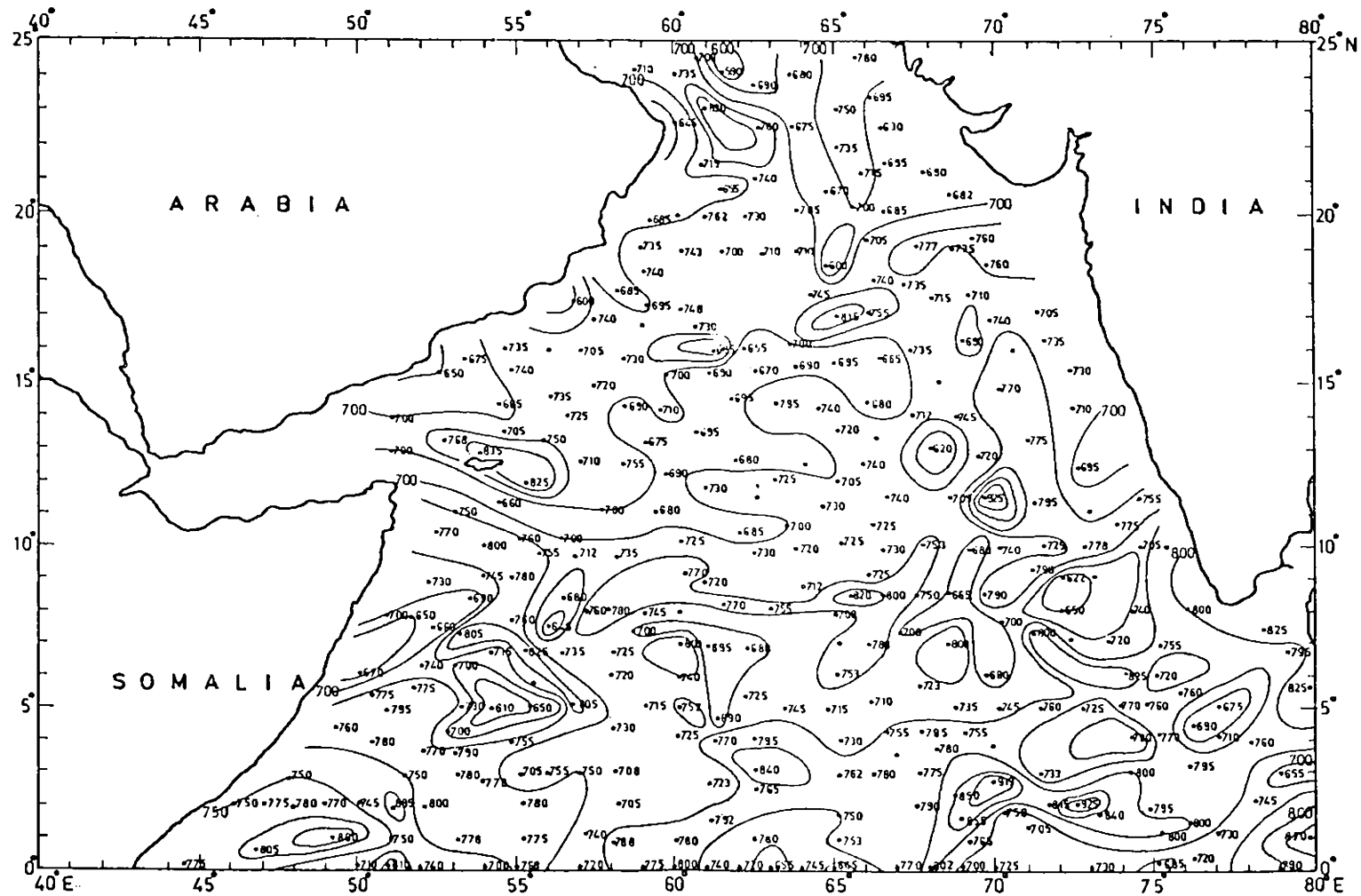

FIG.7 TOPOGRAPHY of 80-cl/t SURFACE

2.2.2. Geostrophic flow

The flow pattern on 80-cl/t surface is, in general, similar to that on the 100 cl/t. The westward undercurrent near the equator, easterly flow north of it, southward undercurrent along the Somali Coast, anticyclonic flow near the southern Somali Coast and southerly flow along the southwest coast of India are all evident on 80-cl/t surface also. The occurrence of complex pattern of lows and highs in the distribution of acceleration potential suggests the presence of cyclonic and anticyclonic eddies.

2.2.3. Salinity

The distribution of salinity on the 80-cl/t surface exhibits significant spatial variation just as on 100-cl/t surface. Salinity varies from 34.91 to 35.78‰ . The regions of occurrence of lower and higher salinities are same as that of the upper surface. Most of the other features, noticed are similar to that of the 100-cl/t surface. However, the isohalines display meridional orientation in the southeastern Arabian Sea and are almost meridional in the northern Arabian Sea. Besides, cells of low and high salinities are noticed in different regions of the Arabian Sea.

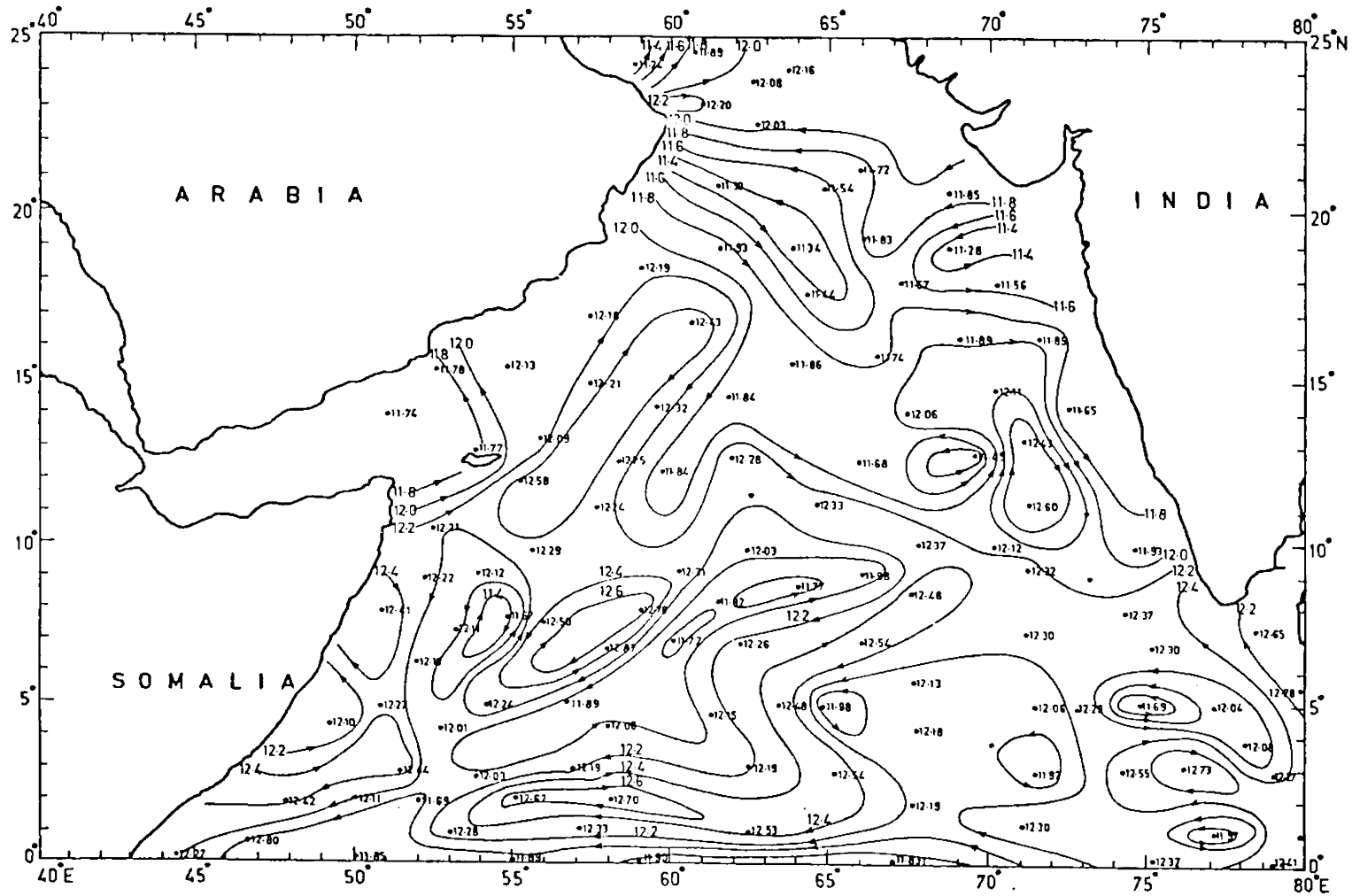

FIG. 8 DISTRIBUTION OF ACCELERATION POTENTIAL (joules/kg) RELATIVE TO 2000 db AT THE 80-cl/t SURFACE

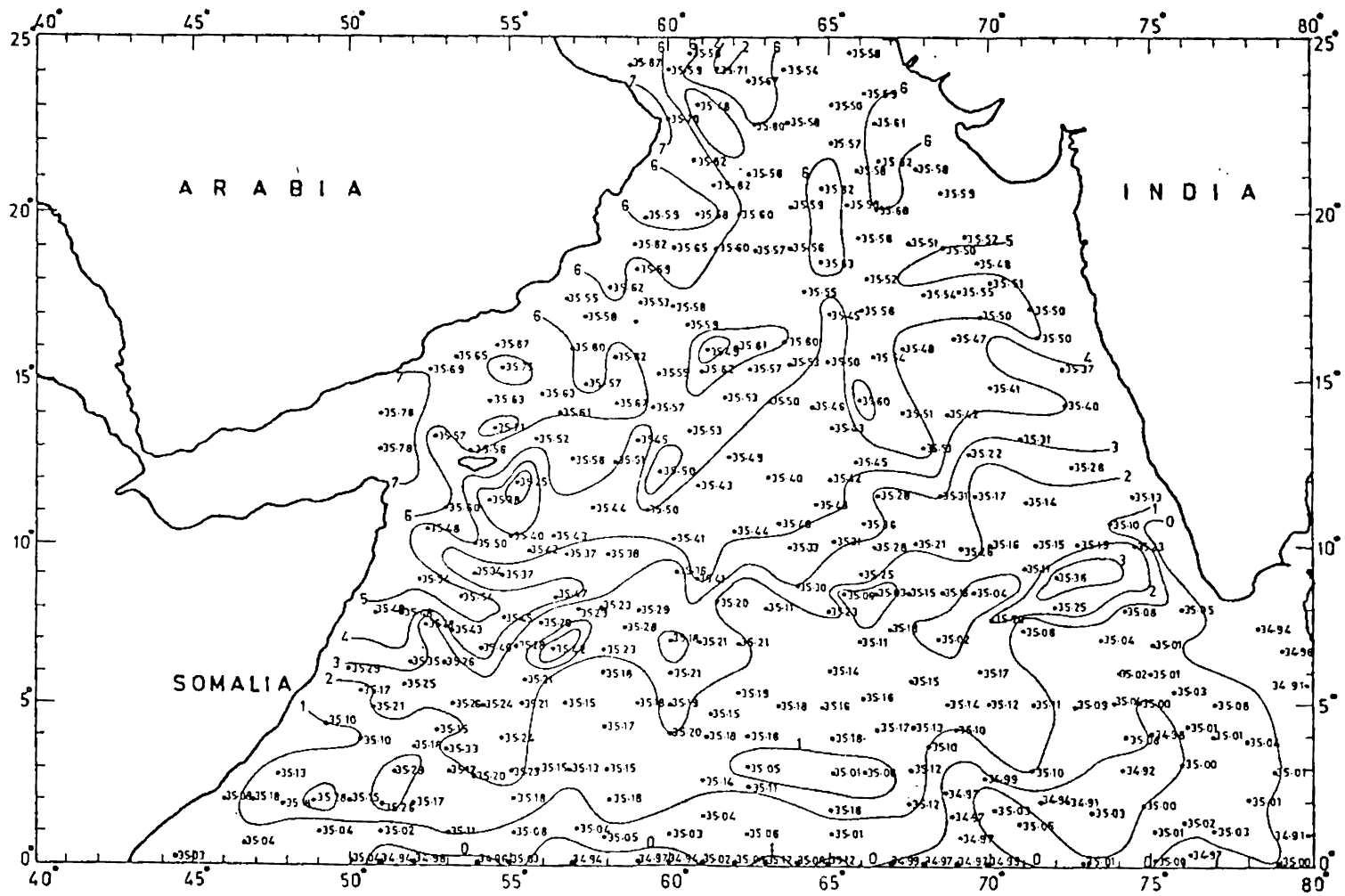

FIG.9 SALINITY (‰) OF 80-cl/t SURFACE

The horizontal gradients in salinity are relatively higher off the Somali Coast, east of the Gulf of Aden and eastern Arabian Sea, coinciding with the lower thickness (less than 450 m) between the topography of the 100 and 60-cl/t surfaces, where horizontal mixing predominates due to higher stability. Similarly less horizontal salinity gradients in the northern, central and southeast Arabian Sea where greater thickness (more than 500 m) between the 100 and 60-cl/t surfaces indicating the presence of relatively less stratified water are noticed. Such a situation arises out of vertical mixing.

2.3. The 60-cl/t surface

2.3.1. Topography

The topography of the 60-cl/t surface resembles that of the 100 and 80-cl/t surfaces in many respects. The troughs and ridges associated with the boundaries of the currents found on the upper two surfaces are all evident on this surface, but their positions are slightly altered. Contrary to the upper two surfaces, the topography of this surface in the central Arabian Sea is uniform. The depth of the surface, in general, varies from 860 to 1,260 m.

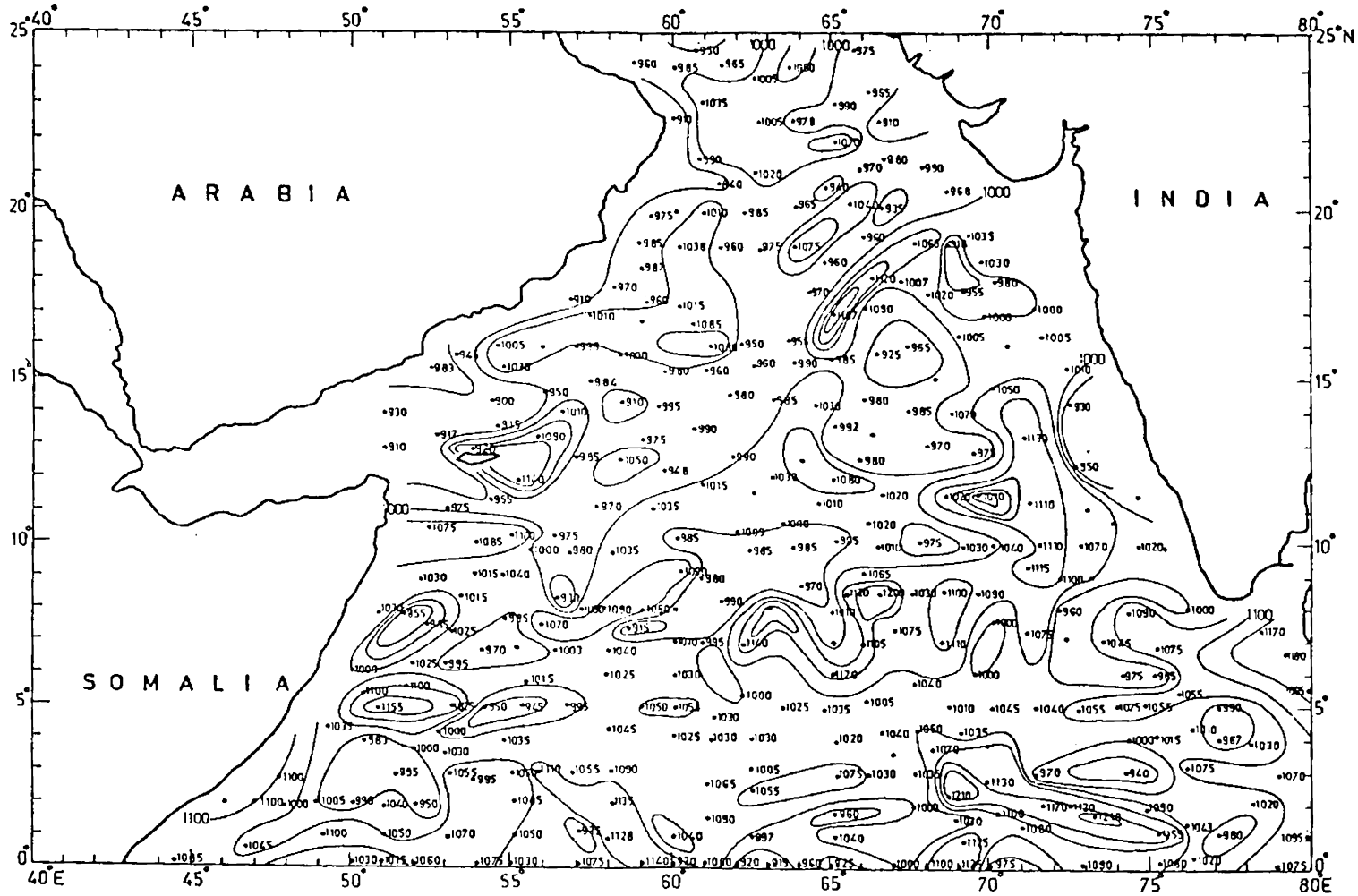

FIG.10 TOPOGRAPHY of 60-cl/t SURFACE

The thickness of the layer between 80 and 60-cl/t surface is more (greater than 300 m) off the Somali Coast, southeast of Socotra Island, central and southeastern Arabian Sea indicating lower stability between these surfaces. Relatively lower thickness (less than 250 m) is noted on the eastern side of Gulf of Aden and in the eastern and northern Arabian Sea suggesting more stratified water between these two isanosteric surfaces.

2.3.2. Geostrophic flow

The flow pattern more or less shows similar features as on the upper two surfaces, though the intensity is comparatively less. The zonal flows near the equator and meridional flows along the Somali Coast and southwest coast of India are observed on this surface. Cyclonic and anticyclonic eddies are also noted as on the upper two surfaces. Unlike on the two upper surfaces, there are strong meridional components in the northern Arabian Sea on 60-cl/t.

2.3.3. Salinity

The salinity distribution on the 60-cl/t surface displays remarkable spatial variation, similar to the two upper surfaces. The salinity values range from 34.83 to 35.74‰. The lower and higher values of salinity are found near the equator and in the central western Arabian Sea respectively, like in the upper two surfaces.

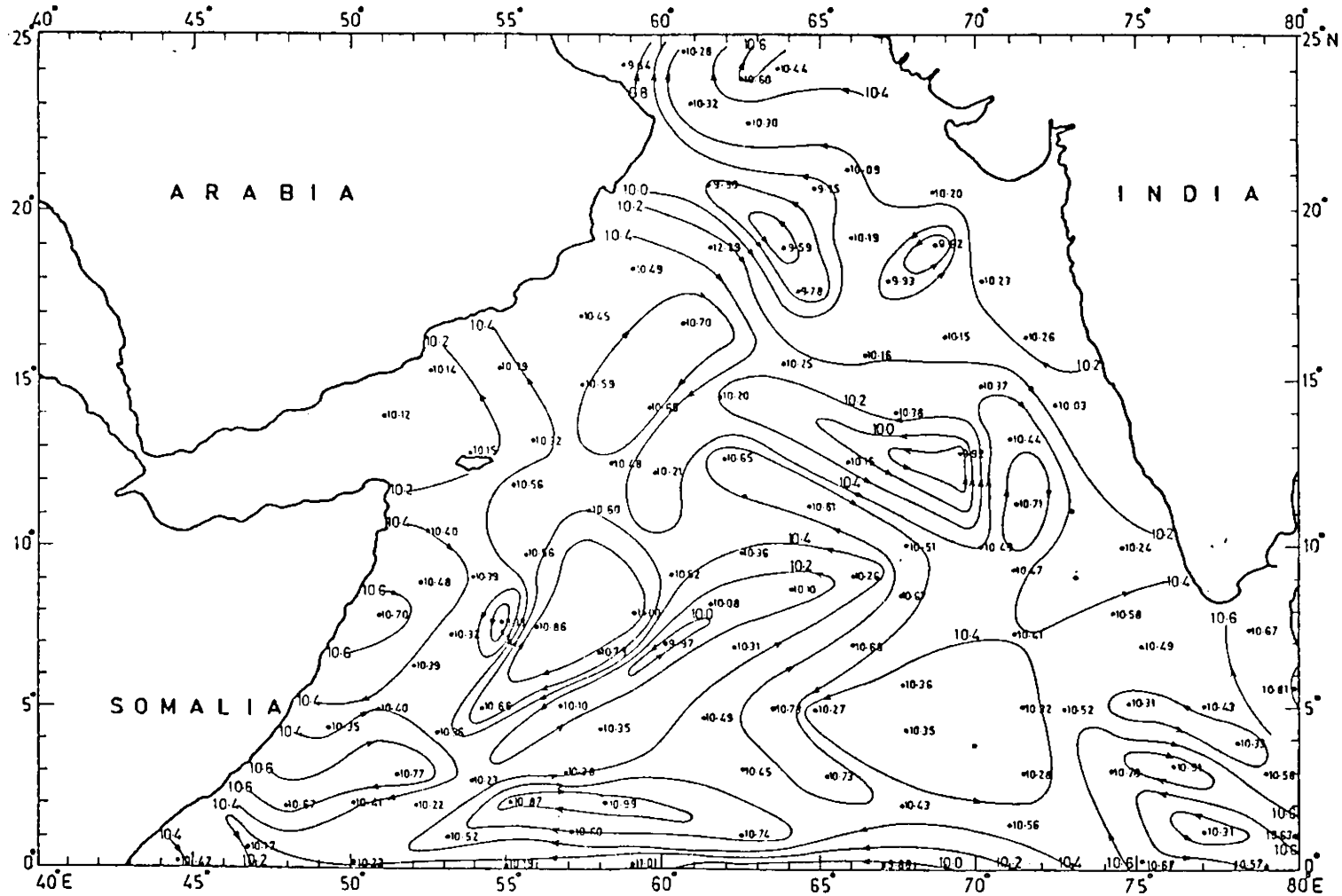

FIG.11 DISTRIBUTION OF ACCELERATION POTENTIAL (joules/kg) RELATIVE TO 2000 db AT THE 60-cl/t SURFACE

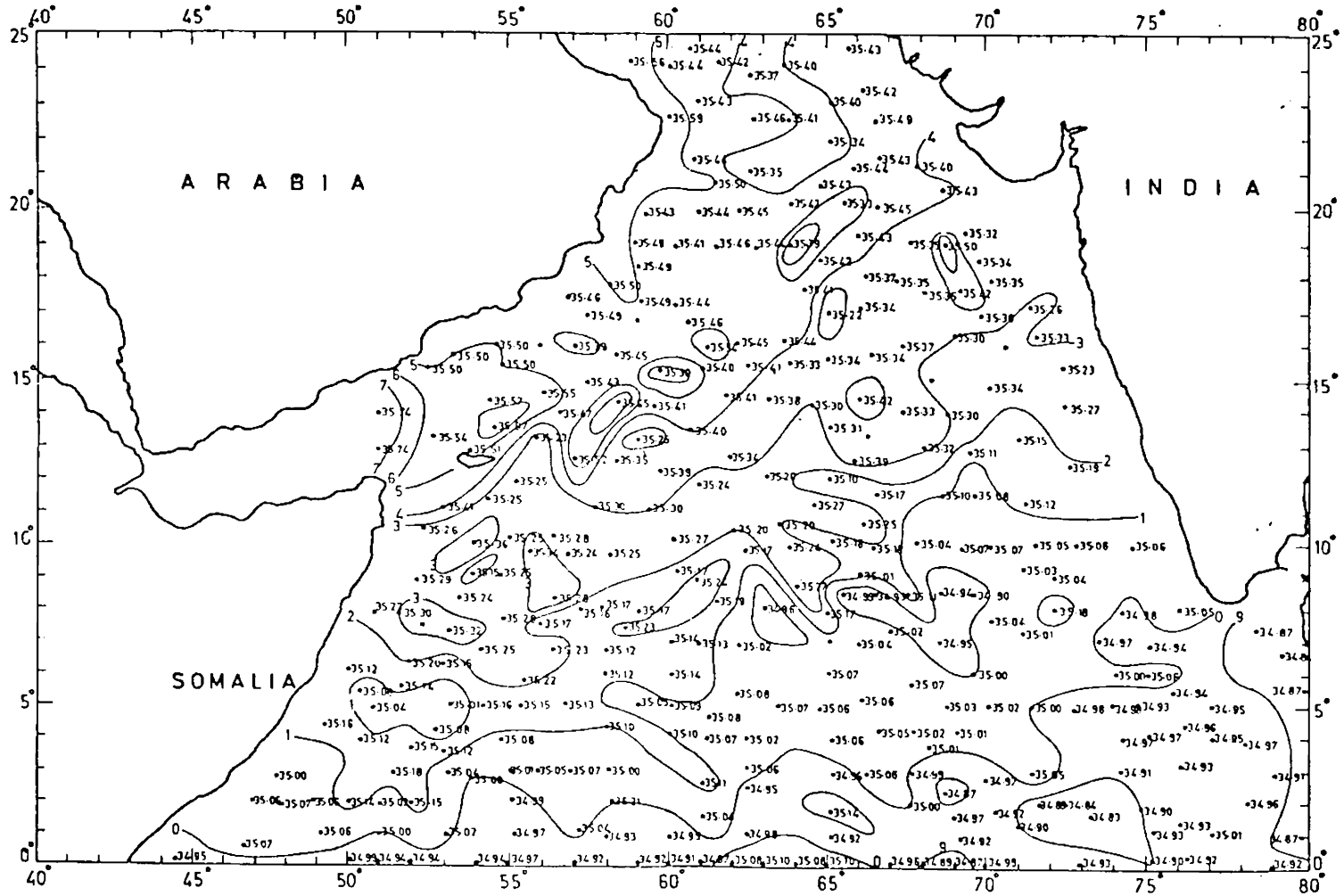

FIG.12 SALINITY (‰) OF 60-cl/t SURFACE

The pattern of isohalines near the equator is almost similar to that found on 80-cl/t surface, They exhibit an irregular pattern in the central Arabian Sea. The high salinity noticed off the northeastern Arabia Coast which is a predominant feature at 100 and 80-cl/t surfaces is weakened on this surface.

The horizontal salinity gradients are comparatively higher from east of Gulf of Aden to 60°E (around Socotra Island) and central Arabian Sea, matching with the lower thickness (less than 700 m) between the topography of 80 and 40-cl/t surfaces, where the prominence of horizontal mixing occurs due to higher stability. Less horizontal salinity gradients are noticed at northern and southeastern Arabian Sea indicating the predominence of vertical mixing which agrees with relatively greater thickness (more than 800 m) between 80 and 40-cl/t surfaces because of less stable water.

2.4. The 40-cl/t surface

2.4.1. Topography

The topography of the 40-cl/t surface exhibits significant differences from that of the upper three surfaces. The depth of this surface is very uneven compared to the other surfaces and hence contouring is

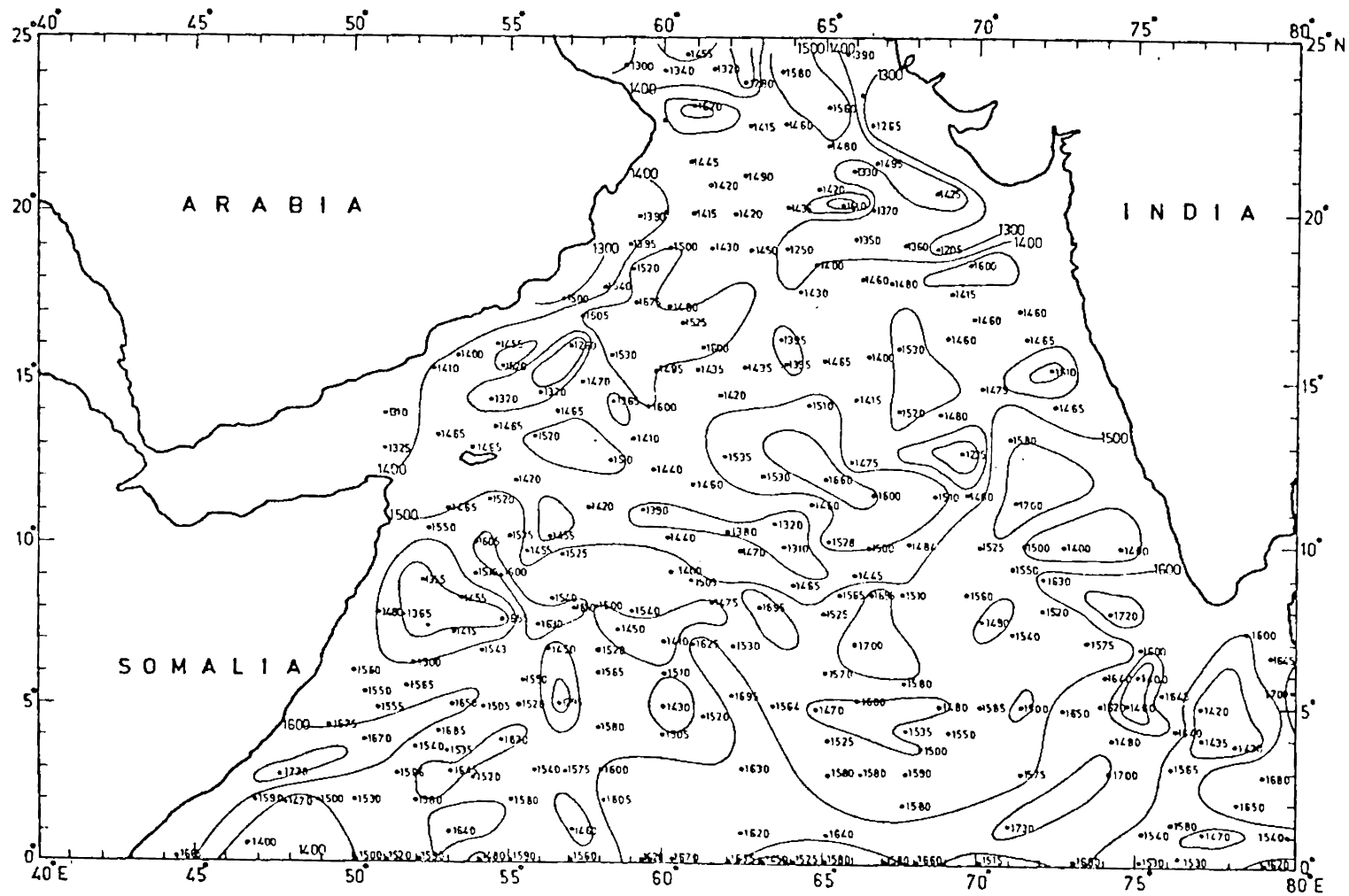

FIG.13 TOPOGRAPHY of 40-cl/t SURFACE

done with 100 m interval. The depth of this surface ranges from 1,230 to 1,730 m. In the central Arabian Sea, a trough with depth exceeding 1,600 m is observed while no trough is found on the upper three surfaces. Alternate troughs and ridges are noticed along the northern Somali Coast and the central and southwest coast of India.

The thickness of the layer between 60 and 40-cl/t surfaces reveals relatively lower thickness (less than 500 m) in the region east of the Gulf of Aden around Socotra Island and central Arabian Sea indicating stable waters between the two isanosteric surfaces. The thickness is comparatively high (more than 550 m) off the southern Somali Coast and eastern Arabian Sea suggesting that waters are less stratified.

2.4.2. Geostrophic flow

The circulation noticed on the 40-cl/t surface displays remarkable differences from that of the upper three surfaces. The westerly flow near the equator which is a conspicuous feature of the 100, 80 and 60-cl/t surfaces is completely absent on this surface. Instead, meridional components of flow are evident near the equator. This weak northerly flow pattern suggests the advection of

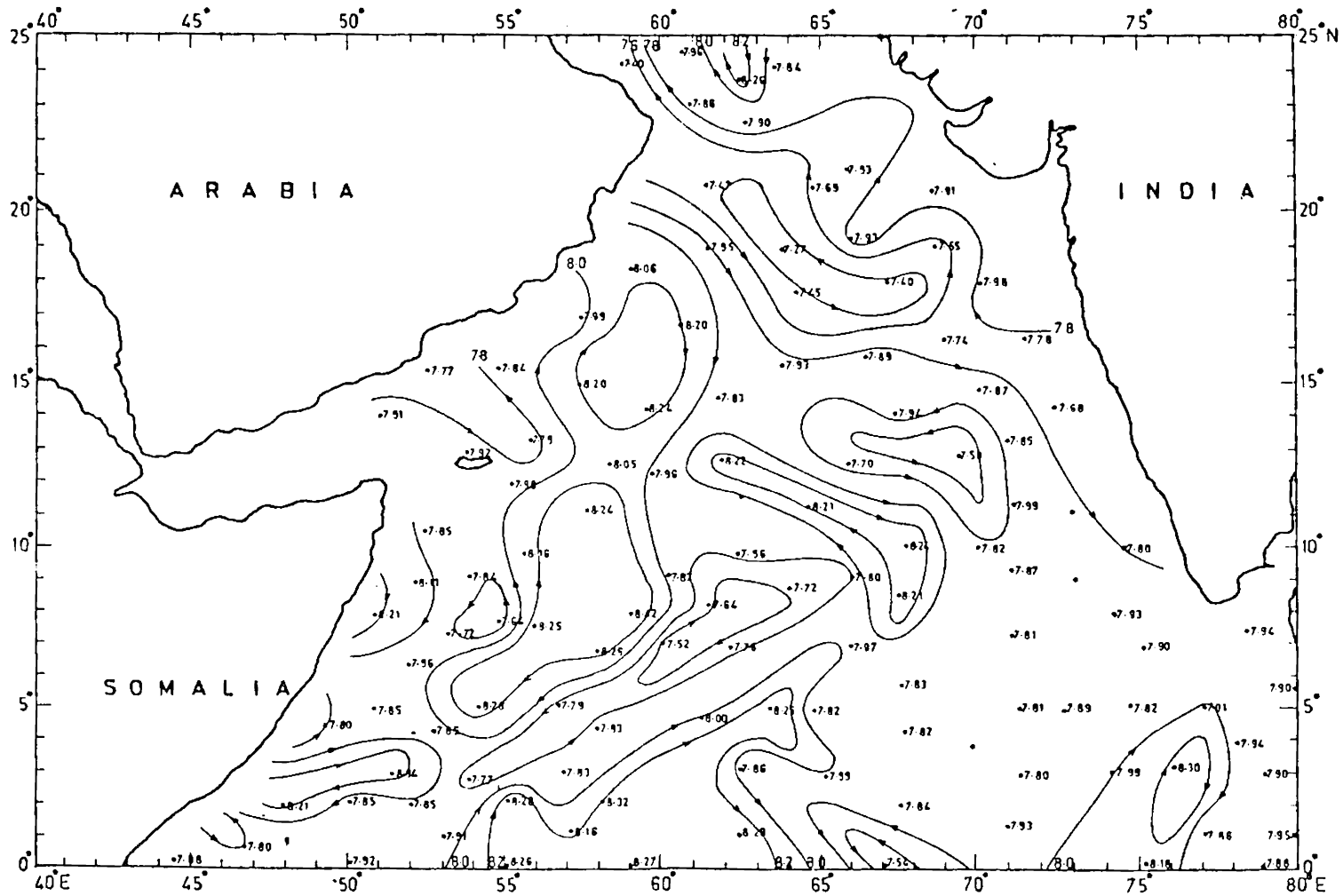

FIG.14 DISTRIBUTION OF ACCELERATION POTENTIAL (joules/kg) RELATIVE TO 2000 db AT THE 40-cl/t SURFACE

water from the southern hemisphere. Warren et al. (1966) found that the deep waters of the Somali Basin are filled with the Circumpolar Water and indicated that the flow is weak and not well defined. Northward advection of cool, less saline water from the south to the northern Indian Ocean was suggested by Warren (1978, 1981).

The southward undercurrent found along the Somali Coast on the upper three surfaces is restricted to the northern Somali Coast between 9° and 7°N with much reduced strength. As on the upper surfaces, anti-cyclonic flow pattern along the southern Somali Coast and southerly flow along the southwest coast of India are noted with reduced intensity. Unlike the upper three surfaces, the meridional components of currents are more prominent than the zonal components on this surface.

2.4.3. Salinity

The spatial variation of salinity on the 40-cl/t surfaces is much less compared to the upper three surfaces. The salinity varies from 34.78 to 35.33‰. The lower salinities are observed between 1° and 7°N whereas higher values are noticed in the northern Arabian

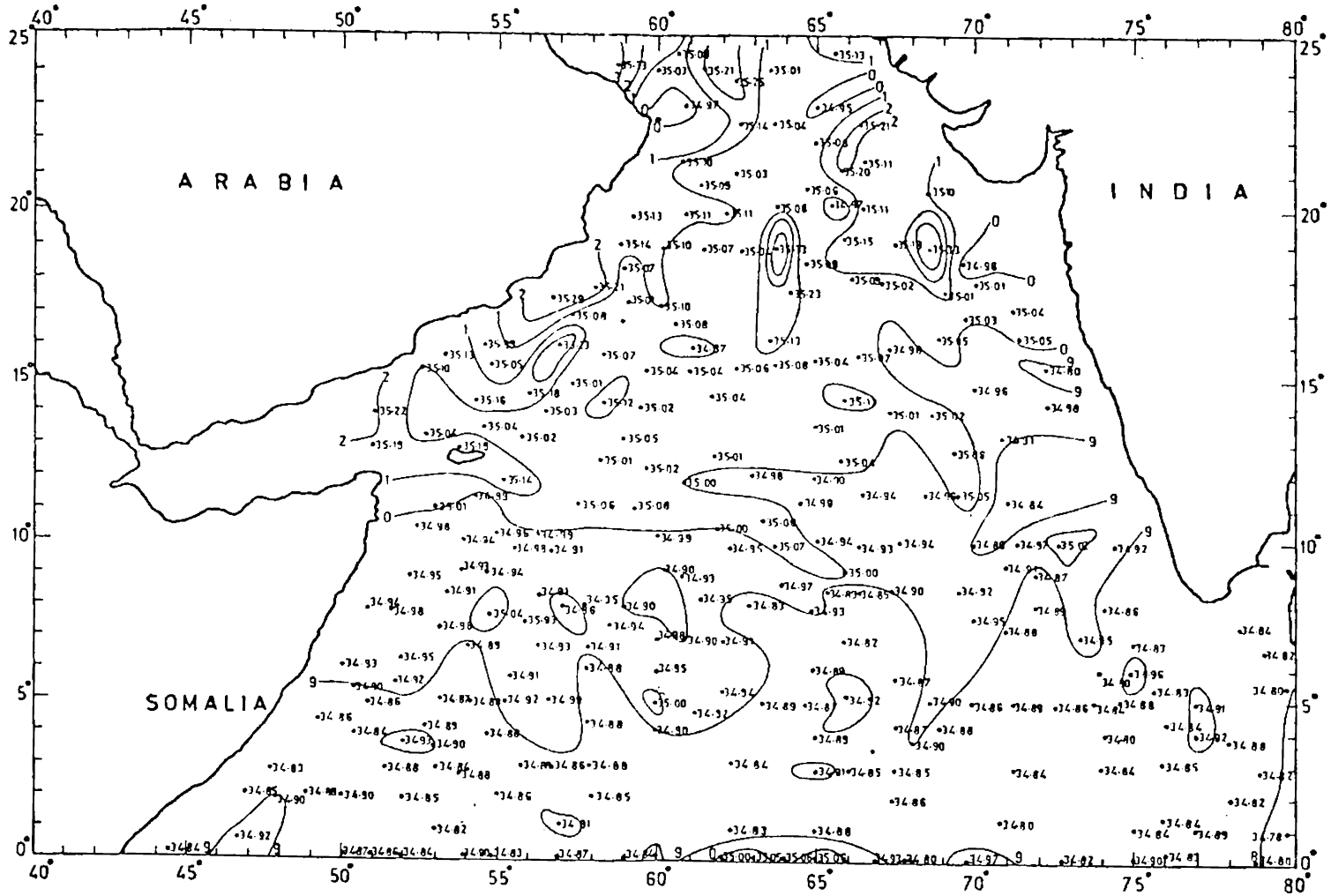

FIG.15 SALINITY (‰) OF 40-cl/t SURFACE

Sea. The zonal pattern of isohalines found on the upper three surfaces is almost absent and is replaced by meridional pattern indicating the northward movement of low salinity water from the south. Warren et al. (1966) reported the northward advection of water into the Somali Basin from the south.

Uniform salinity values are found off the Somali Coast whereas relatively higher values are observed in the central western Arabian Sea. Cells of comparatively high salinity are also found in the northern Arabian Sea.

C H A P T E R - III

CHAPTER - III

VERTICAL SECTIONS OF POTENTIAL TEMPERATURE AND SALINITY

The water characteristics of the Arabian Sea are influenced by the presence of several sources of low and high salinity waters. An attempt is made in this chapter to study the cross-sectional flow pattern and water characteristics of the intermediate waters in the Arabian Sea by presenting vertical sections of potential temperature and salinity. The sections are presented in Figs. 16 to 29.

3.1.1. Section I - 45° to 79°E along 0°

The temperature distribution along the equator does not vary much horizontally at any depth below 300 m indicating a homogeneous nature, although the surface waters are warmer in the eastern region. The homogeneity may be because of mixing.

The salinity distribution also shows nearly homogeneous water in the intermediate layers. The vertical variation of salinity from 200 to 1,700 m depth is only 0.30‰ . Relatively homogeneous water in the equatorial region is shown in the meridional sections of the IIOE atlas (Wyrtki, 1971). Sharma (1976) reported homogeneous

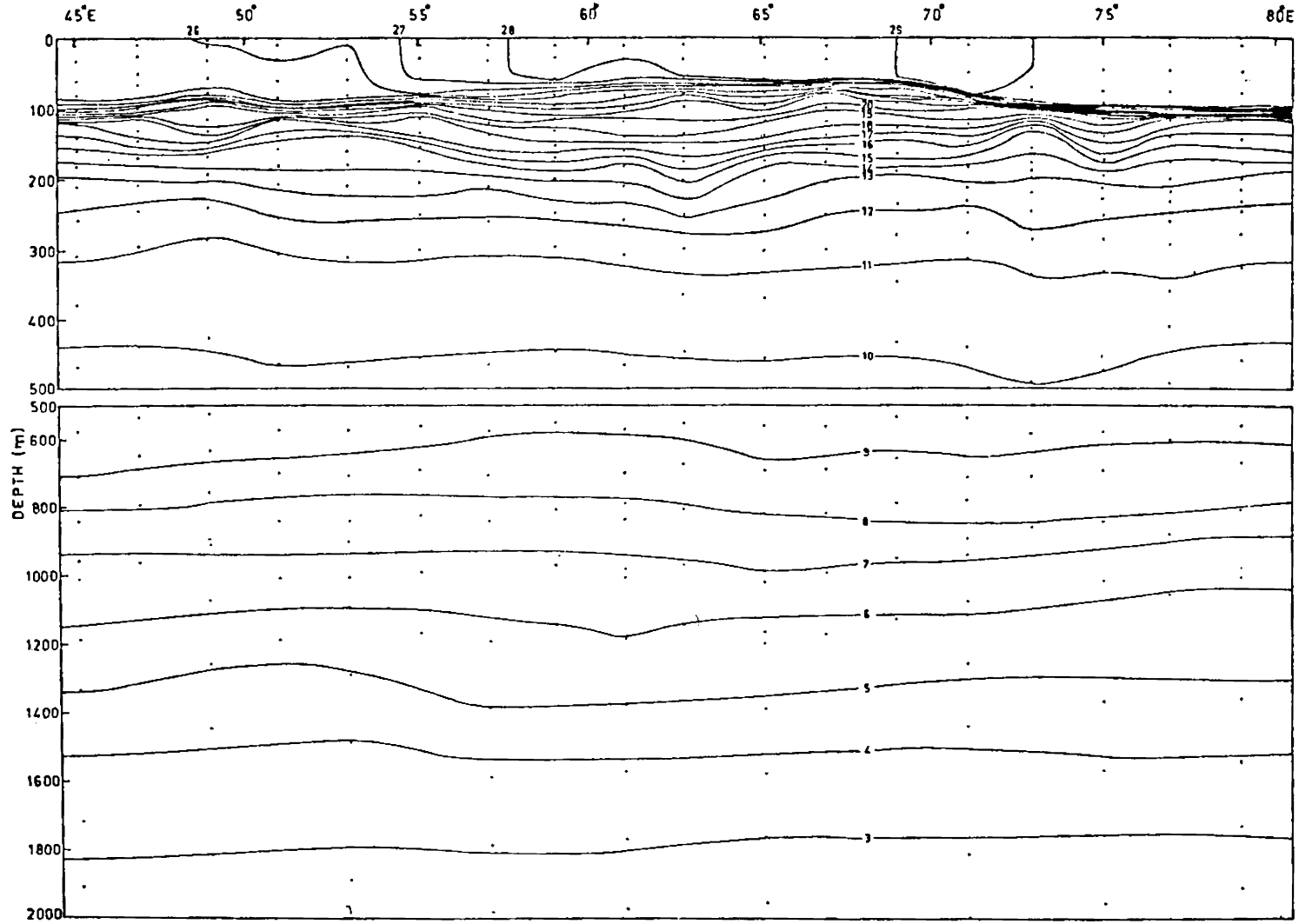

FIG 16 : DISTRIBUTION OF POTENTIAL TEMPERATURE ALONG SECTION I

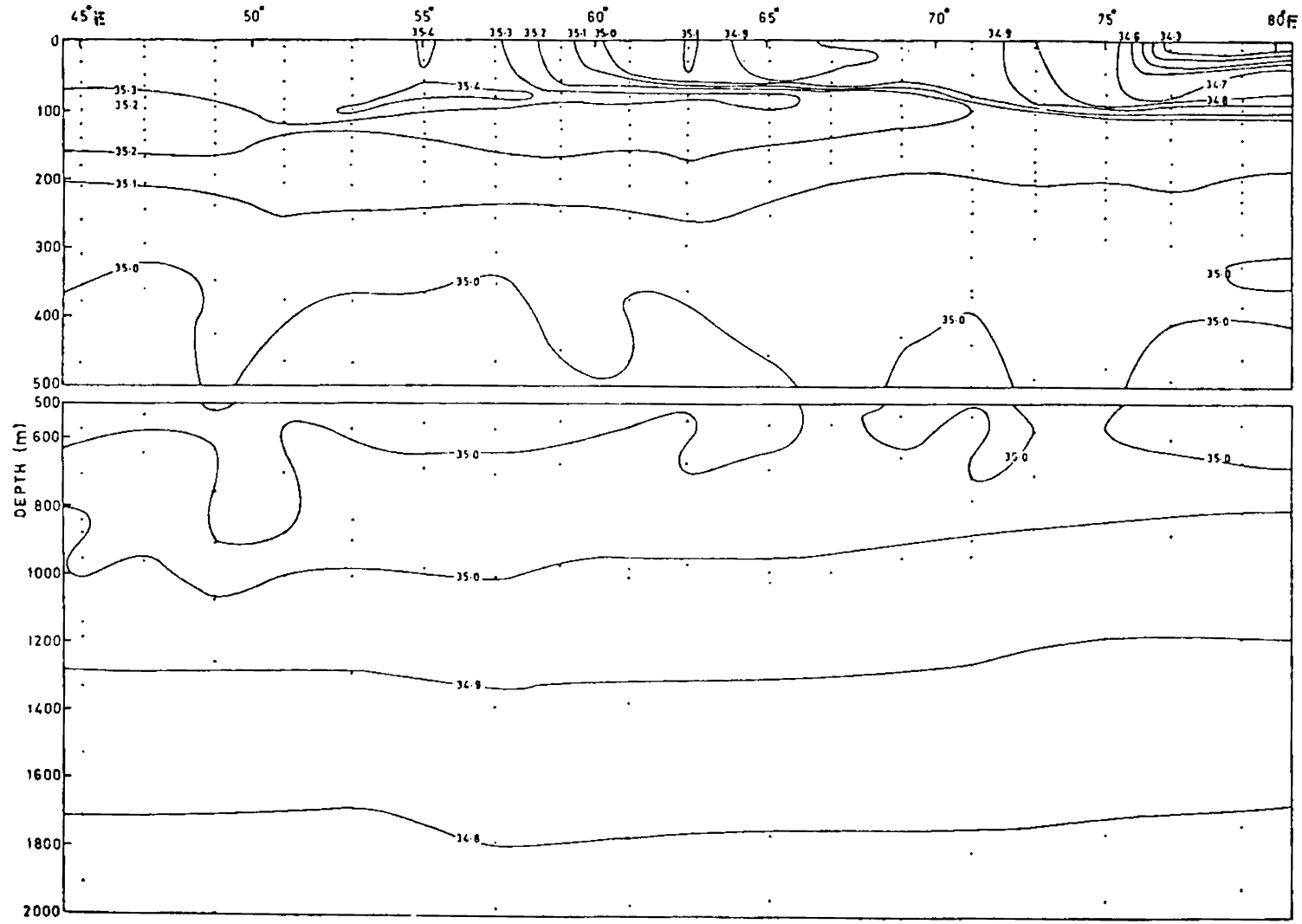

FIG 17 : DISTRIBUTION OF SALINITY ALONG SECTION I

water in the equatorial region, vertically extending from 100 to 1,000 m depth. He called it Equatorial Indian Ocean Water and suggested that it is an admixture of various water masses of the northern and southern hemispheres, and the water mass of the Pacific Ocean. However, Quadfasel and Schott (1982) referred it as Equatorial Water of the Indian Ocean.

A close examination of the salinity distribution reveals a weak salinity minimum in the depth range of 325 to 650 m with values less than 35.00‰ . The salinity minimum is more conspicuous in the western side. A comparison of the vertical sections of the IIOE atlas (Wyrtki, 1971) confirms that the salinity minimum is prominent only in the western region but not in the east. Probably the salinity minimum is caused in the west due to the influx of the Pacific Ocean Water which is carried to the west along with the South Equatorial Current that crosses the equator in the western region of the Indian Ocean (Sharma, 1972; Sharma et al., 1978).

3.1.2. Section II - 50° to 76°E along 5°N

The distribution of temperature on this section confirms that zonal variation of temperature in the intermediate depth is less. The temperature varies significantly on either side of the ridge situated along 60°E, particularly in the deeper layers.

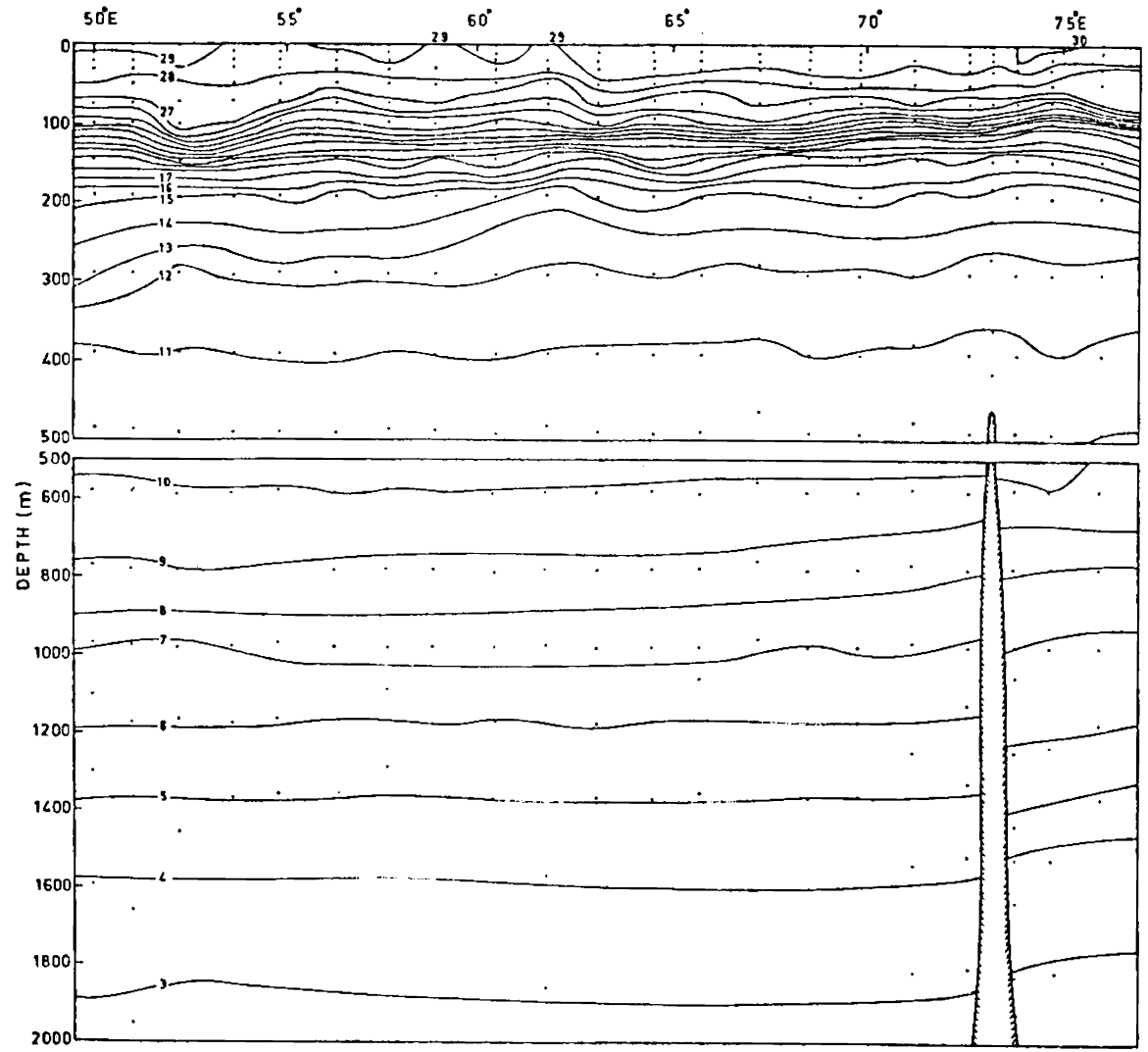

FIG 18 : DISTRIBUTION OF POTENTIAL TEMPERATURE ALONG SECTION II

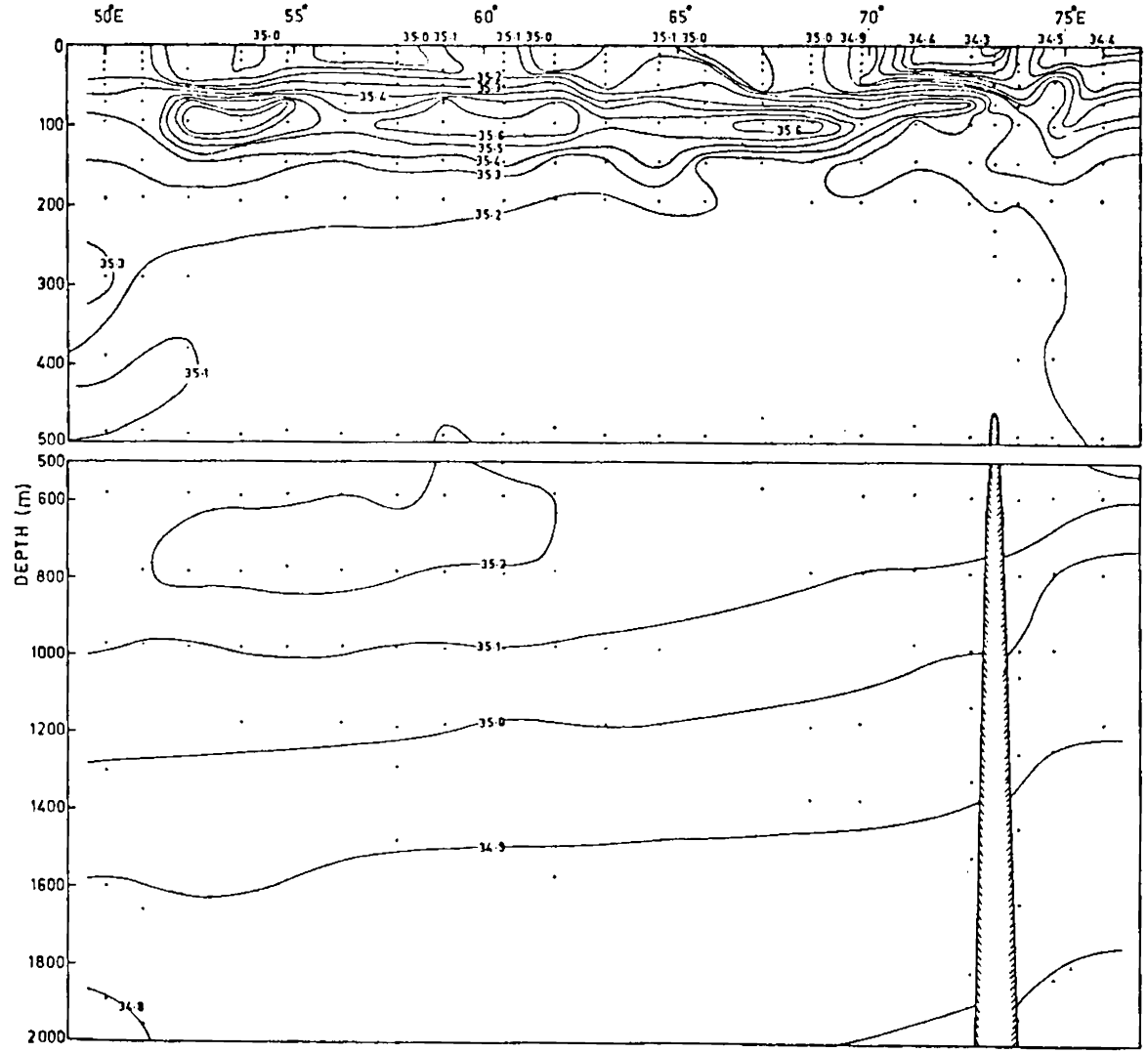

FIG 19 : DISTRIBUTION OF SALINITY ALONG SECTION II

A conspicuous feature in the salinity distribution is the intrusion of relatively high salinity water around 600-800 m depth in the western side. This is due to the spreading of Red Sea Water (Rochford, 1964; Wyrtki, 1971; Quadfasel and Schott, 1982). Nearly homogeneous water is found in the depth interval of 250 to 600 m. The homogeneity may be because of lateral as well as vertical mixing. A weak salinity minimum is noticed around 400 m depth in the western side, probably, due to the influence of Pacific Ocean Water as discussed in the previous section. However, the value of salinity minimum is increased to 35.10‰ due to mixing with high salinity waters from the north. The other remarkable feature is the presence of low salinity water in the eastern part of the section in the depth range of 100 to 300 m. This is attributed to the influence of the Bay of Bengal Water. Below 900 m, the isohalines show an upward tilt towards the east.

3.1.3. Section III - 51° to 75°E along 10°N

The horizontal variation of temperature on this section is low in the intermediate depths except in the western side. In the eastern part, the isotherms exhibit an upward tilt towards the west coast of India indicating

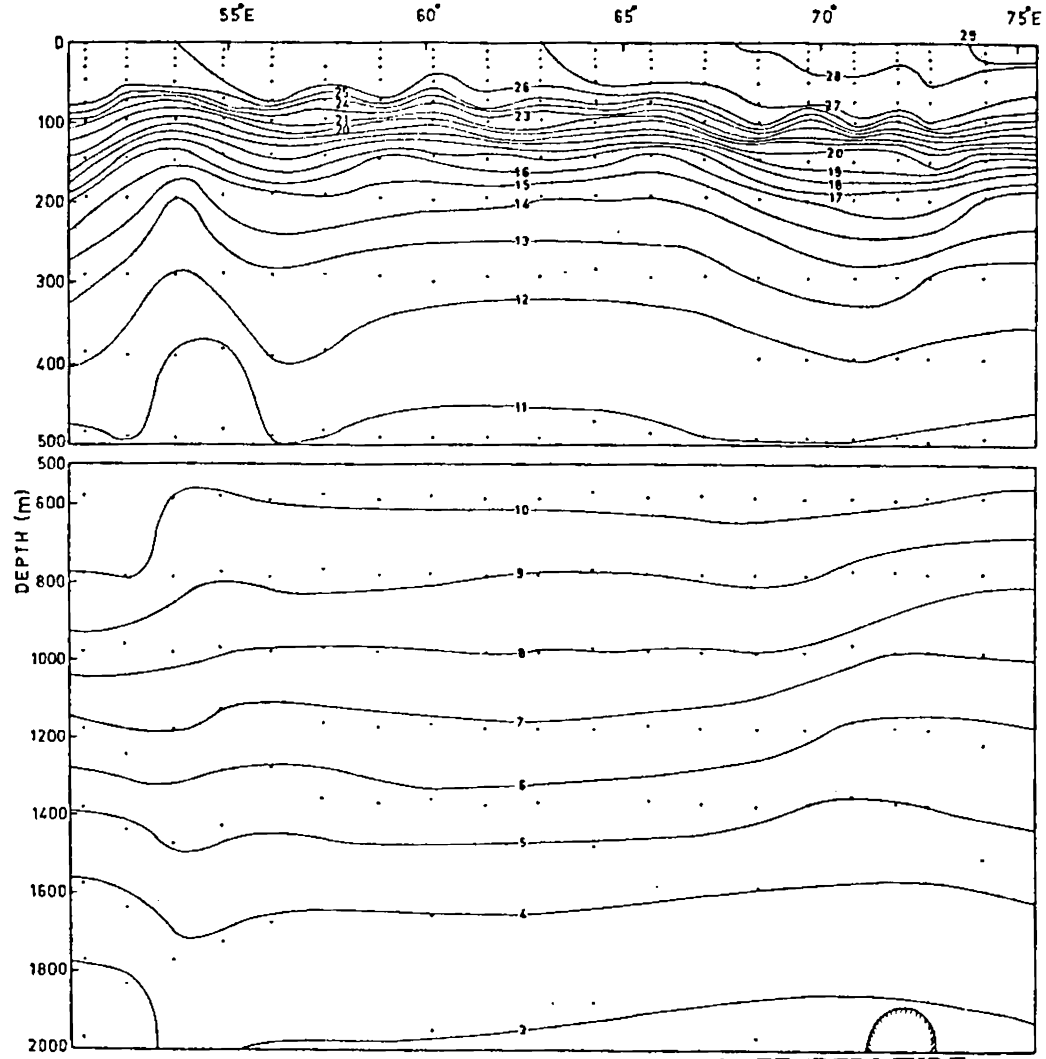

FIG 20 : DISTRIBUTION OF POTENTIAL TEMPERATURE ALONG SECTION III

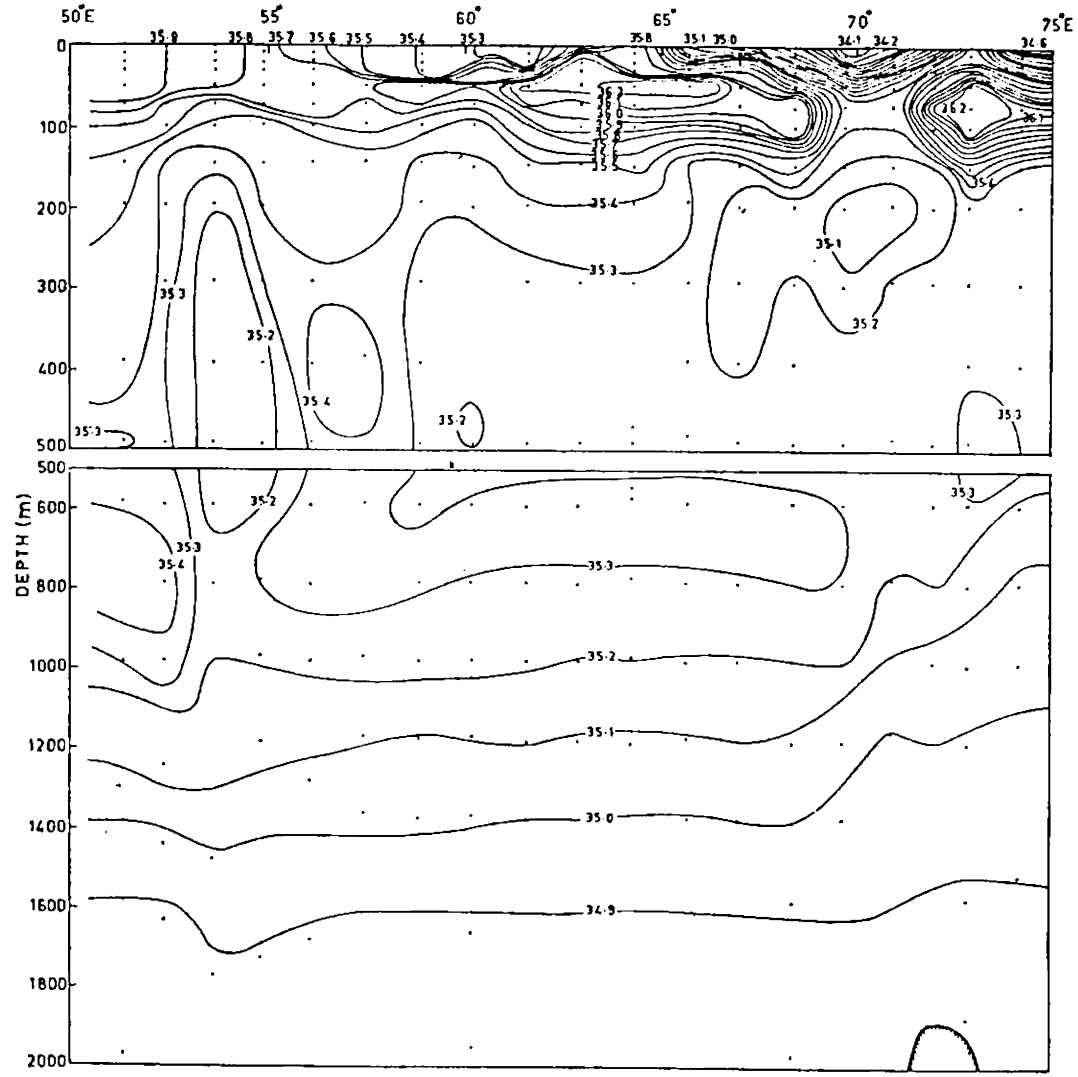

FIG 21 : DISTRIBUTION OF SALINITY ALONG SECTION III

the southerly flow as found on the acceleration potential maps. In the western part, a southerly flow west of 54°E between 200 and 1,000 m and a northerly flow east of 54°E in the depth interval of 200 to 500 m are evident. This is in agreement with the southward flow along the Somali Coast carrying the Red Sea Water and northward flowing low salinity water found on the distributions of properties on potential thermosteric anomaly surfaces of the present study. Below 1,000 m, weak northerly and southerly flows are indicated in the western side.

The influence of Red Sea Water which is limited to the western side of the previous section is more predominant and widely spread on this section. One branch of Red Sea Water spreads horizontally in the western side in the depth range of 600 to 1,000 m. It is interesting to note a low salinity layer around 54°E in the depth interval of 200 to 600 m. It indicates strong vertical mixing. The salinity minimum is probably due to the influence of water of Pacific origin from south as discussed in Section I.

Another branch of Red Sea Water, east of the salinity minimum, spreads vertically downward in the layer between 400 and 900 m around 56° to 58°E again

spreads horizontally upto 70°E in the depth range of 500 to 800 m. The horizontal spreading of Red Sea Water in the intermediate depths noticed on this section is in confirmation with the predominant horizontal mixing found on the distribution of salinity on the potential thermosteric anomaly surfaces.

The homogeneous water noticed in Section II is also present in this section east of 59°E in the depth limits of 300 and 500 m, indicating an admixture of various waters. The influence of Bay of Bengal water is also felt in the upper layers, on the eastern side. Below 1,000 m horizontal variation of salinity is less except in the eastern side, which agrees with the horizontal mixing found in the salinity distribution on the steric surfaces.

3.1.4. Section IV - 52° to 73°E along 15°N

The horizontal variation of temperature is less in the intermediate depths except in the east. The upward slope of isotherms towards the west coast of India suggests southerly flow as revealed on the distribution of acceleration potential.

Noticeable differences are found in the distribution of salinity on the section compared to the previous one. The Red Sea Water found as a predominant feature in Section III is restricted to western side around 400 to

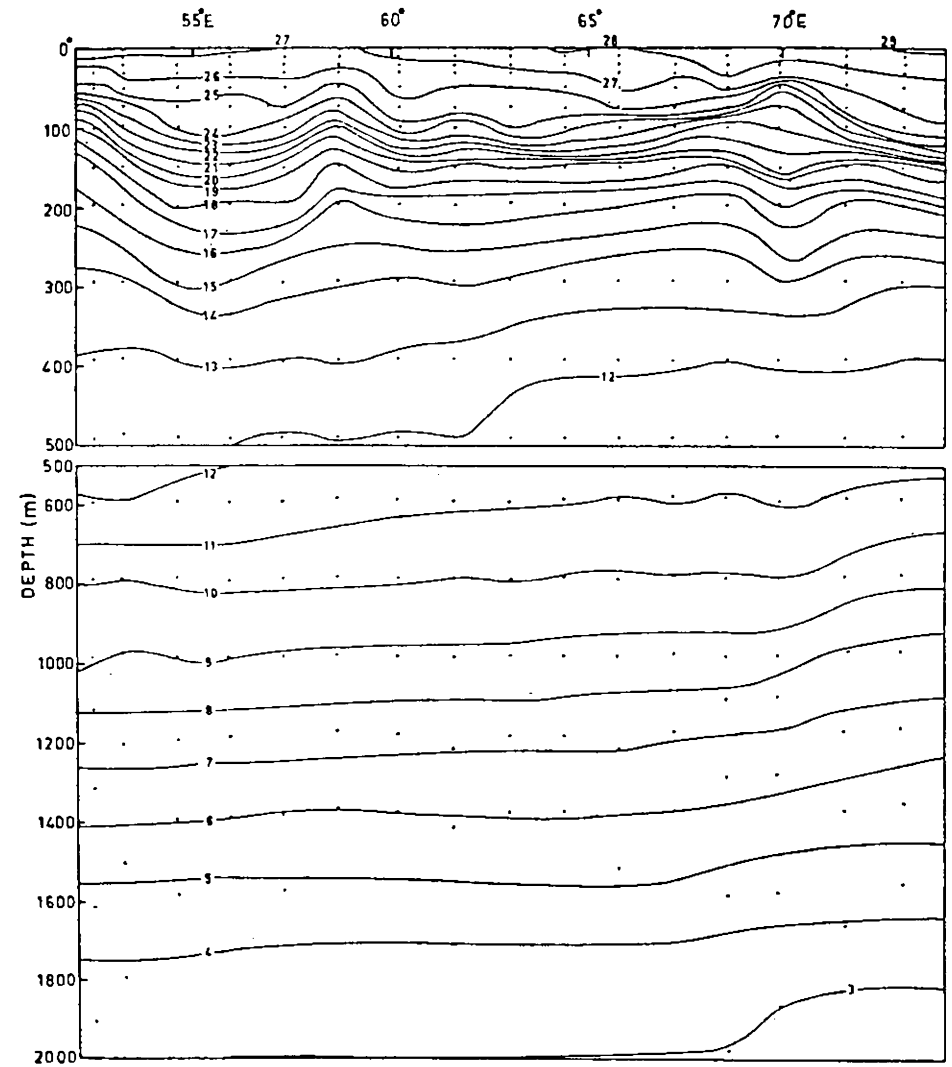

FIG 22 : DISTRIBUTION OF POTENTIAL TEMPERATURE ALONG SECTION IV

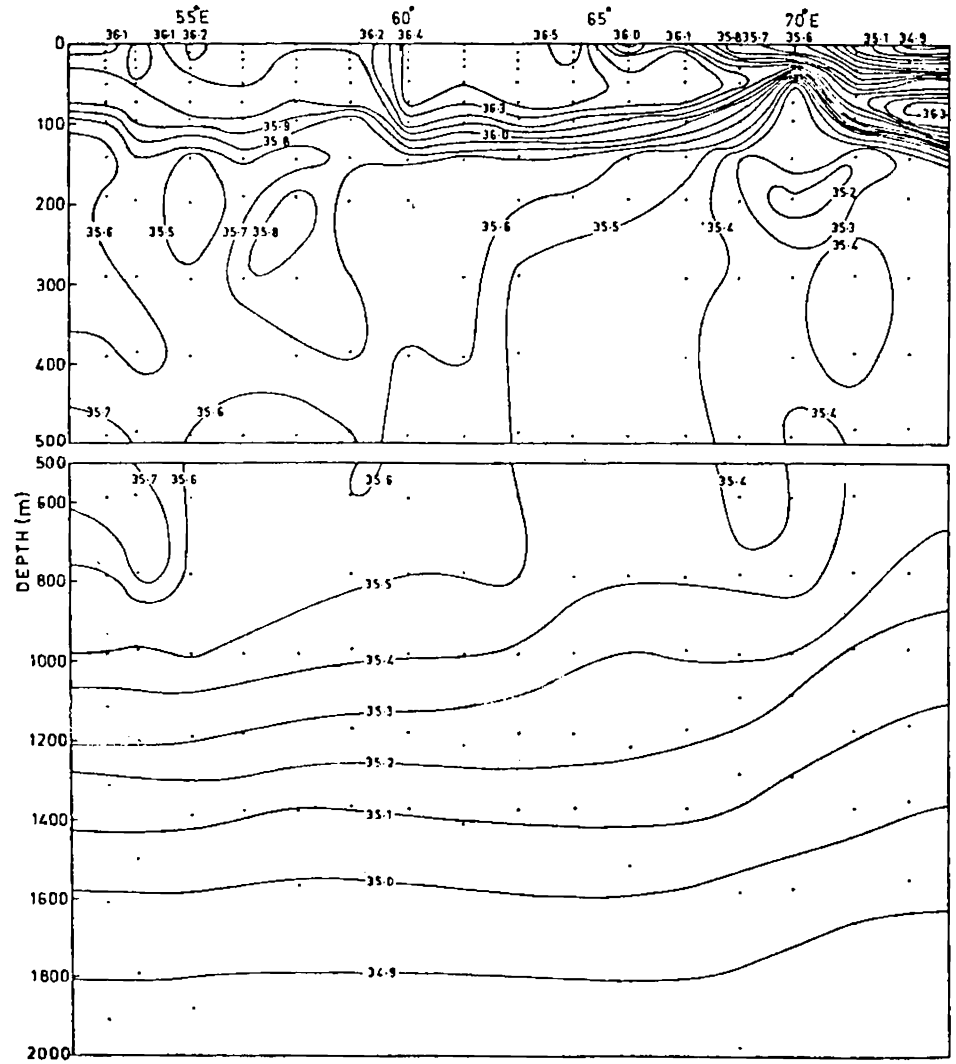

FIG 23 : DISTRIBUTION OF SALINITY ALONG SECTION IV

800 m. The influence of Persian Gulf Water is observed around 55° to 59°E in the depth range of 200 to 400 m. As in the earlier sections east of 60°E, a homogeneous water is found between 200 and 800 m. Below 1,000 m, salinity does not vary much horizontally except in the east. The spreading of Persian Gulf Water is in agreement with the horizontal mixing found in the eastern Arabian Sea in the distribution of salinity on the steric surfaces.

3.1,5. Section V - 59° 30' to 68°E along 20°N

The temperature distribution indicates less horizontal variation in the intermediate depths below 500 m, although weak gradients are found around 300 to 400 m.

Remarkable differences are noticed in the distribution of salinity compared to the previous sections. The Red Sea Water found in the earlier three sections is totally absent.

Below the Arabian Sea Water, Persian Water is noticed in the depth range of 200 to 400 m. Premchand (1982) reported the spreading and mixing of Persian Gulf Water around the same depth interval in the northern Arabian Sea. Below 500 m, horizontal salinity gradients are low indicating the vertical mixing as found in the salinity distribution maps on the steric surfaces.

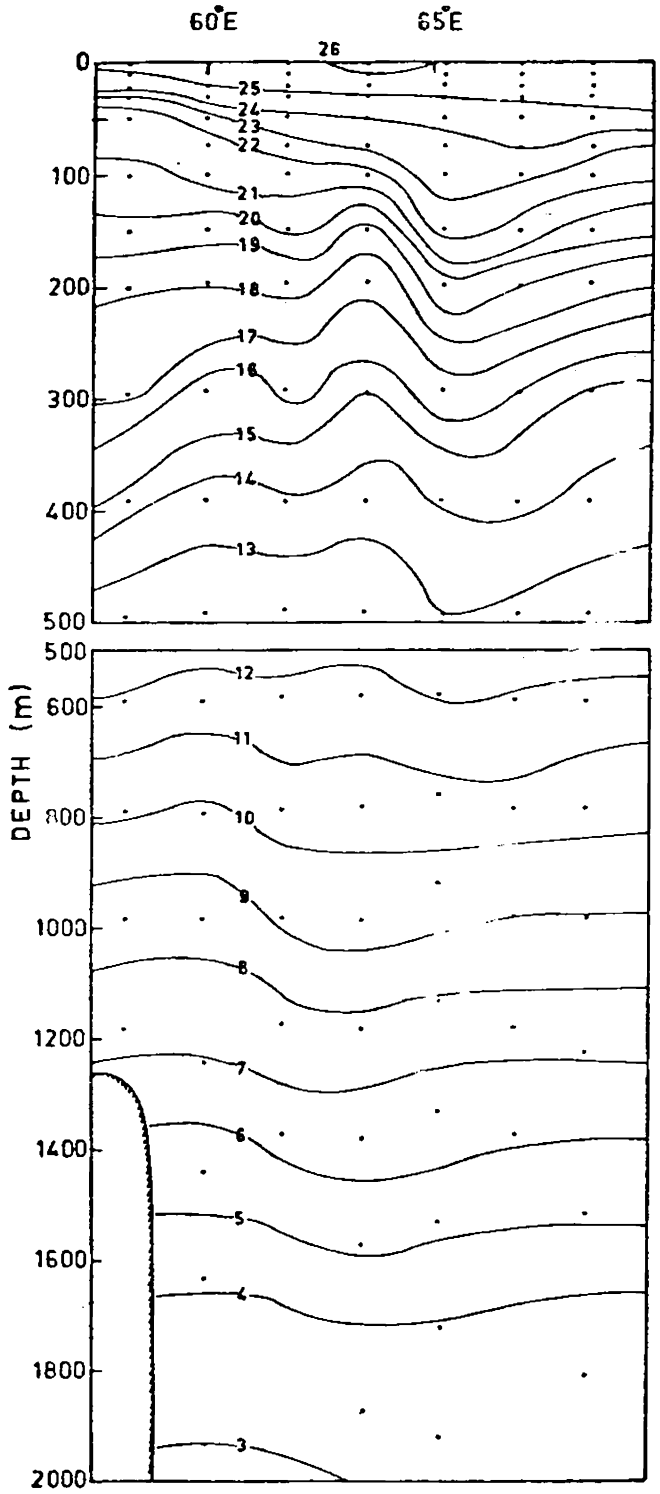

FIG 24 : DISTRIBUTION OF POTENTIAL TEMPERATURE ALONG SECTION V

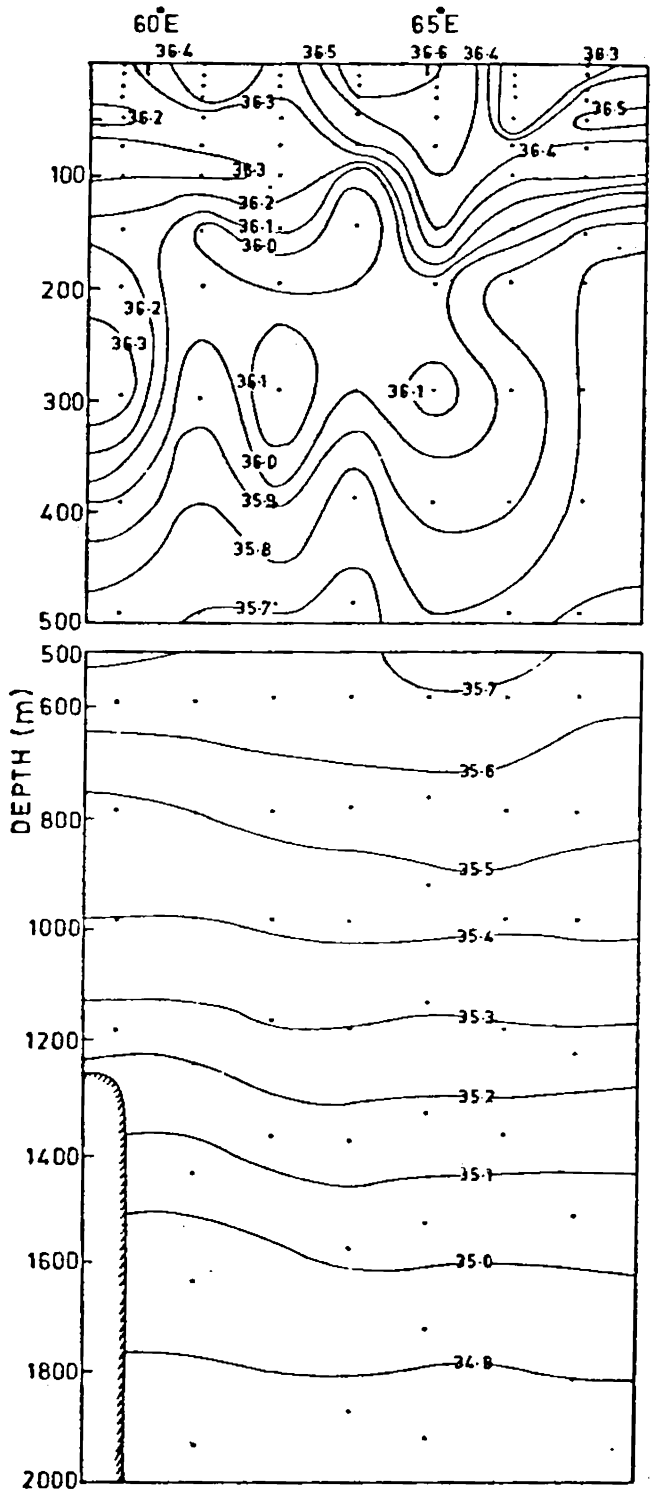

FIG 25 DISTRIBUTION OF SALINITY ALONG SECTION V

3.1.6. Section VI - 0° to 15°N along 58°E

Compared to the zonal sections so far discussed, the distribution of temperature on meridional section shows significant horizontal variation in the intermediate depths except near the equator where a homogeneous nature is indicated. The upward trend of isotherms from north to south observed in the intermediate depths suggests the presence of westerly flow. This is in confirmation with the distribution of acceleration potential on 100, 80 and 60-cl/t surfaces.

The prominent feature in the salinity distribution is the horizontal and vertical mixing of Red Sea Water in the intermediate depths. One branch of Red Sea Water around 13-15°N at 500m mixes vertically downward to deeper regions while another branch around 10°N spreads horizontally towards south in the depth range of 400 to 900 m. This is in agreement with the horizontal mixing found in the distribution of properties on potential thermosteric anomaly surfaces.

Low salinity water from the south spreads towards north in the depth interval of 200 to 500 m and Persian Gulf Water is restricted to 15°N around 200-300 m along 58°E. The low salinity water from the south is trapped into a cell around 300 m at 11° 30'N surrounded by high salinity

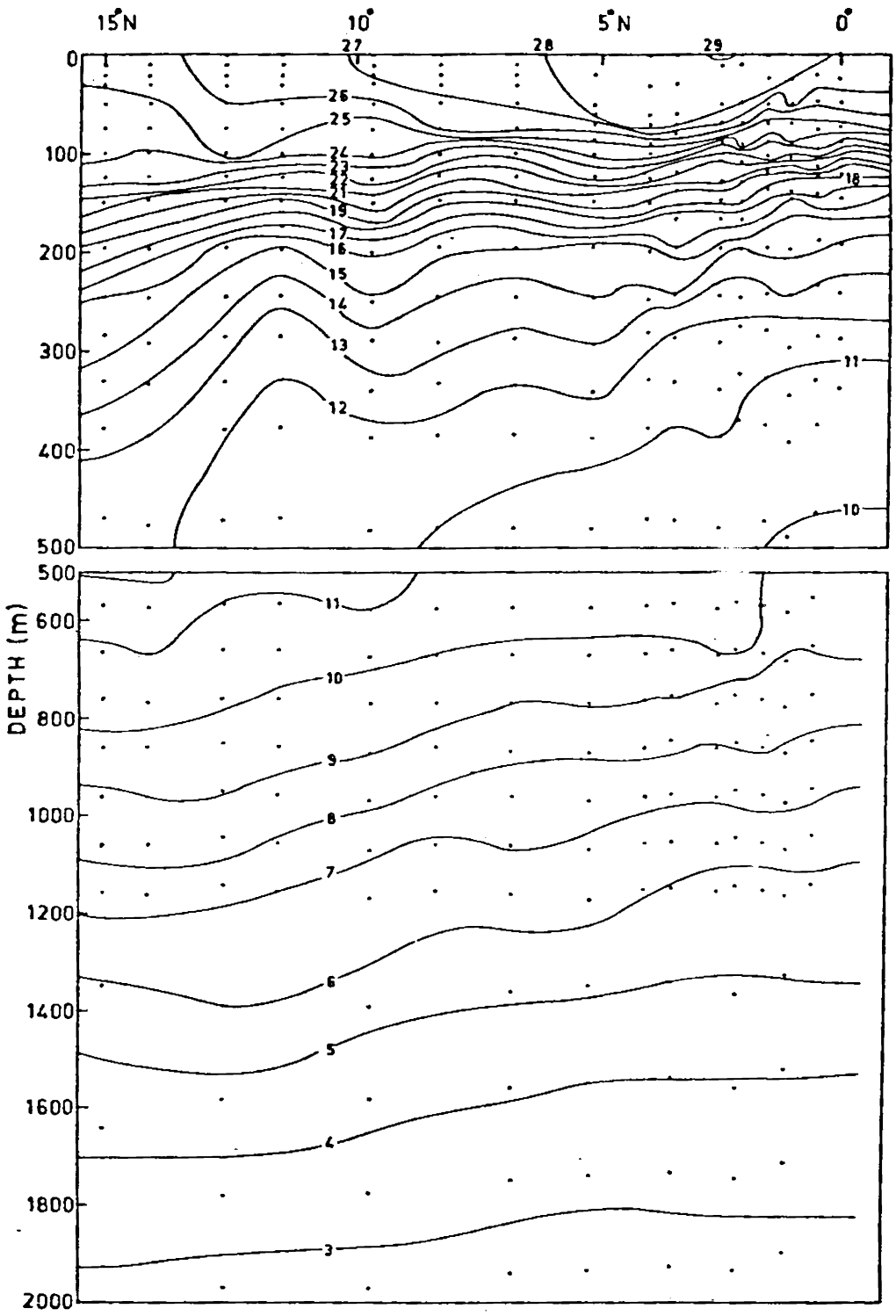

FIG 26. : DISTRIBUTION OF POTENTIAL TEMPERATURE ALONG SECTION VI

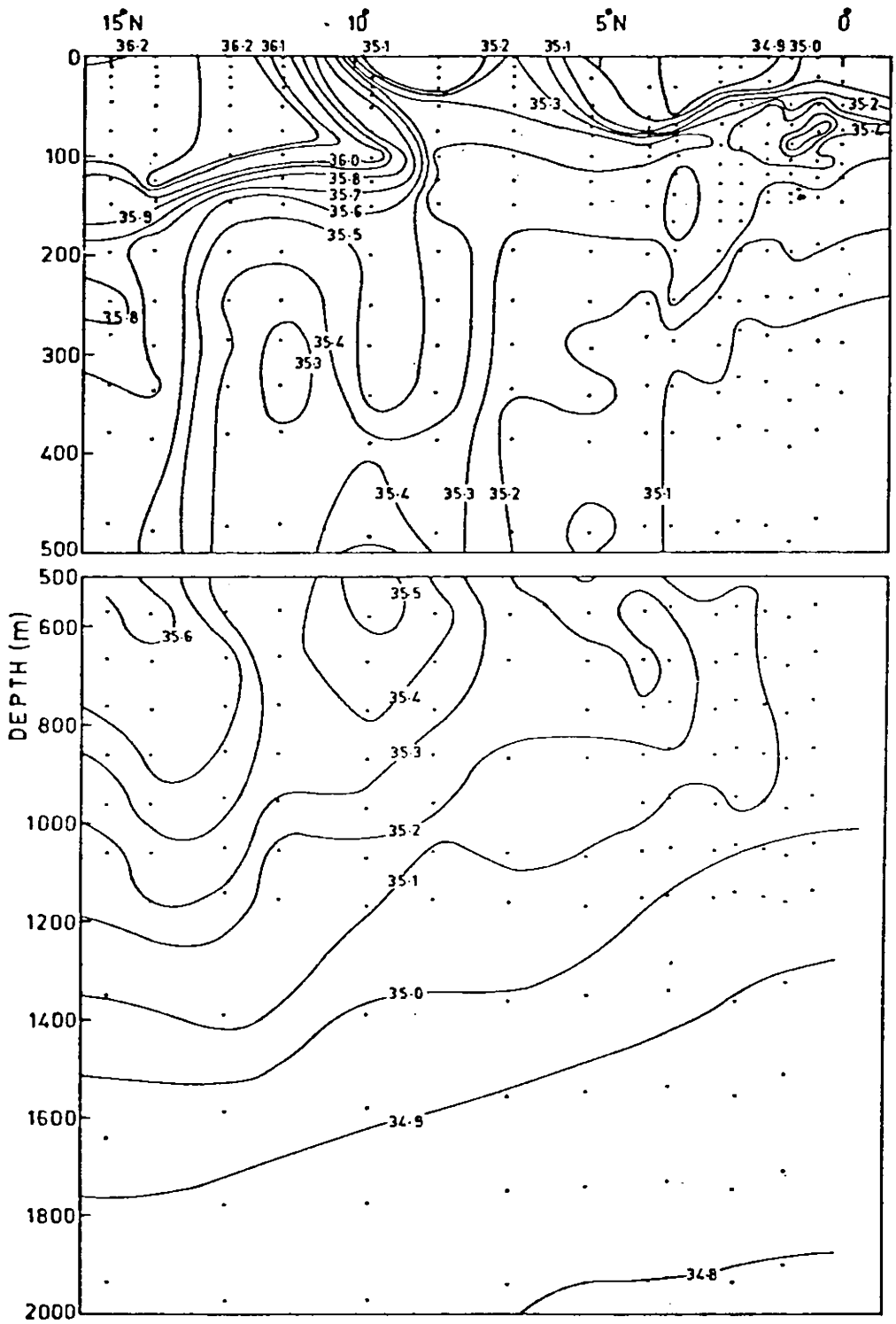

FIG 27 :- DISTRIBUTION OF SALINITY ALONG SECTION VI

waters. The presence of nearly homogeneous water is also found near the equator.

3.1.7. Section VII - 1° 30' to 18°N along 70°E

The temperature distribution on this section is nearly similar to the previous one showing significant horizontal variation in the intermediate depths and indicating the presence of westerly flow.

The distribution of salinity also reveals somewhat similar features as that of Section VI. Red Sea Water, found south of 15°N around 400-600 m spreads horizontally towards south upto 3°N and its influence is found to a depth of 900 m. The spreading of Red Sea Water is in confirmation with the horizontal mixing found in the salinity distribution maps on steric surfaces.

Above the southward spreading Red Sea Water, low salinity water from the south spreads horizontally towards north until the influence of highly saline Arabian Sea Water is encountered in the upper layers. The Arabian Sea Water is very well represented by tongue-like structure around 100 m from north to 6°N.

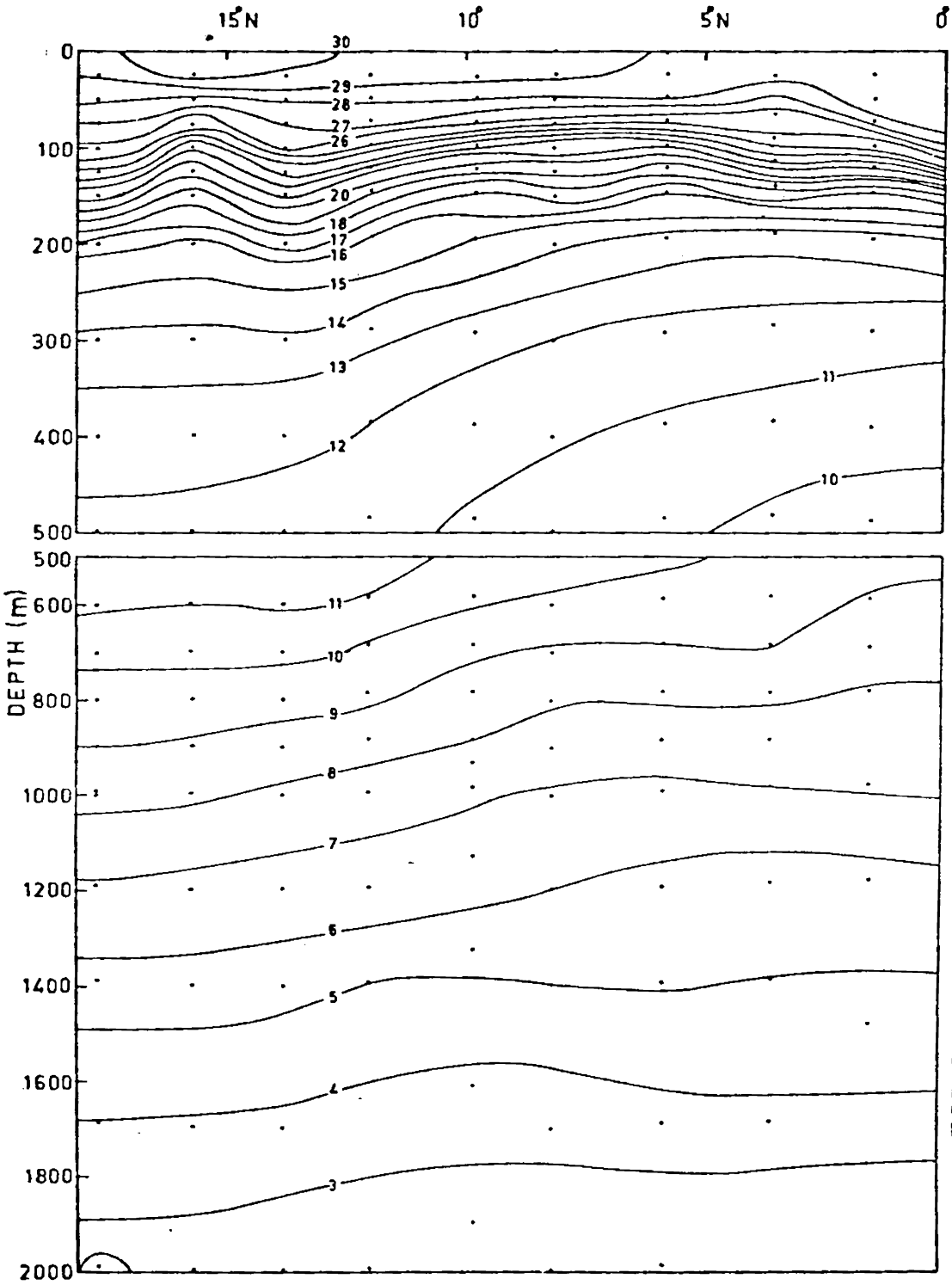

FIG 28 : DISTRIBUTION OF POTENTIAL TEMPERATURE ALONG SECTION VII

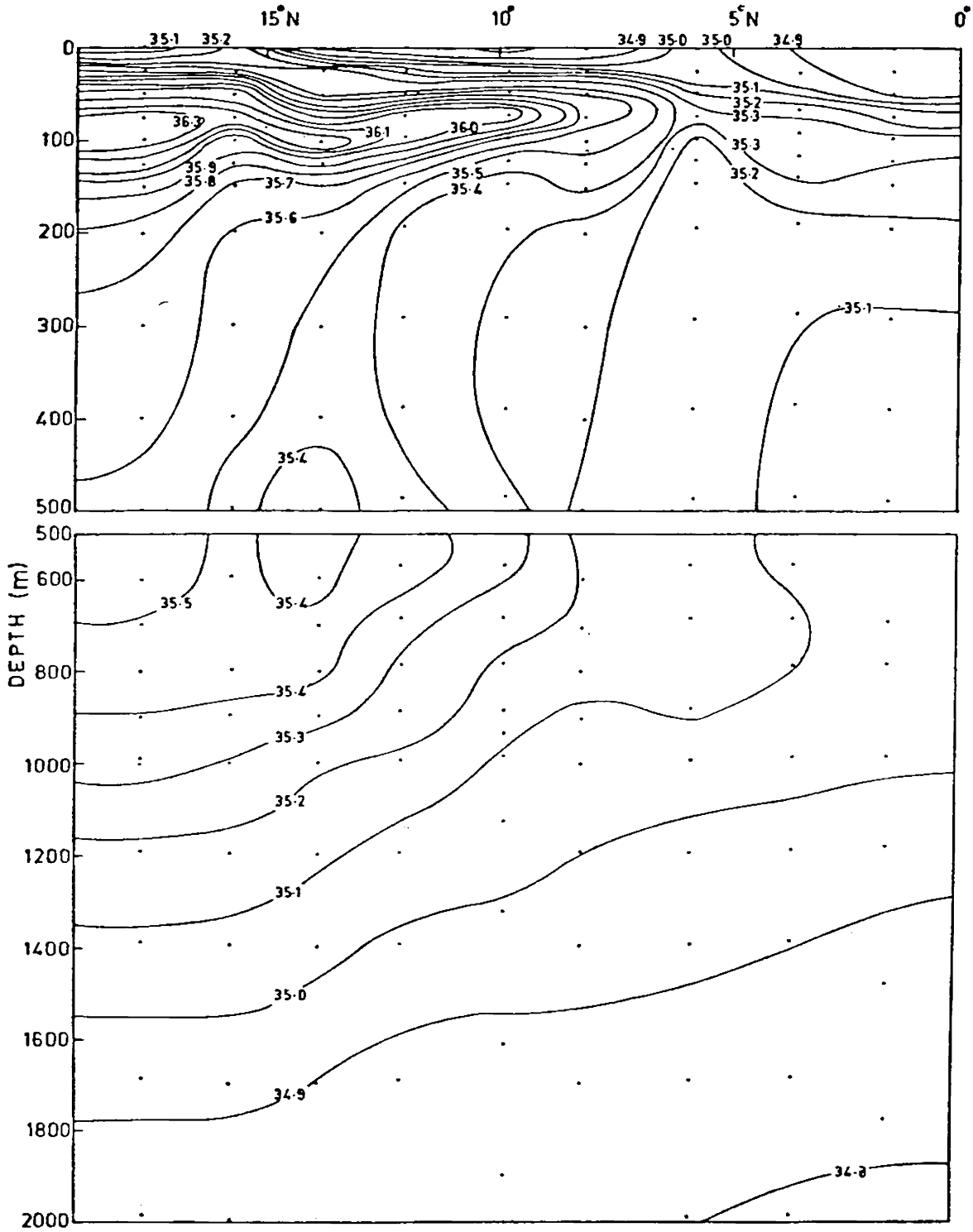

FIG.29: DISTRIBUTION OF SALINITY ALONG SECTION VII

C H A P T E R - IV

CHAPTER - IV

SCATTER DIAGRAMS OF POTENTIAL TEMPERATURE AGAINST SALINITY

Correlation of temperature and salinity, two conservative characteristics of sea water, was first put in a systematic basis by Helland-Hansen (1916) using T-S diagram. This characteristic diagram subsequently became a power tool for the identification of water masses of any oceanic area. In the present chapter it is proposed to study the water characteristics of the intermediate waters in the Arabian Sea using the scatter diagrams of potential temperature against salinity at ten representative areas, shown in Fig. 2. The scatter diagrams are presented in Figs. 30 to 39.

4.1.1. Area 1 - Between 0^{o} to 4^{o}N and 48^{o} to 52^{o}E

The potential temperature-salinity (Θ-S) diagram shows less scatter in the intermediate depths except 100 to 80 cl/t surfaces. Homogeneity is indicated by less scatter in a Θ-S diagram, whereas wide scatter represents heterogeneity. Vertical sections of potential temperature and salinity along the equator reveal homogeneous water in the intermediate layers. A comparison of the distribution of properties on potential thermosteric anomaly surfaces

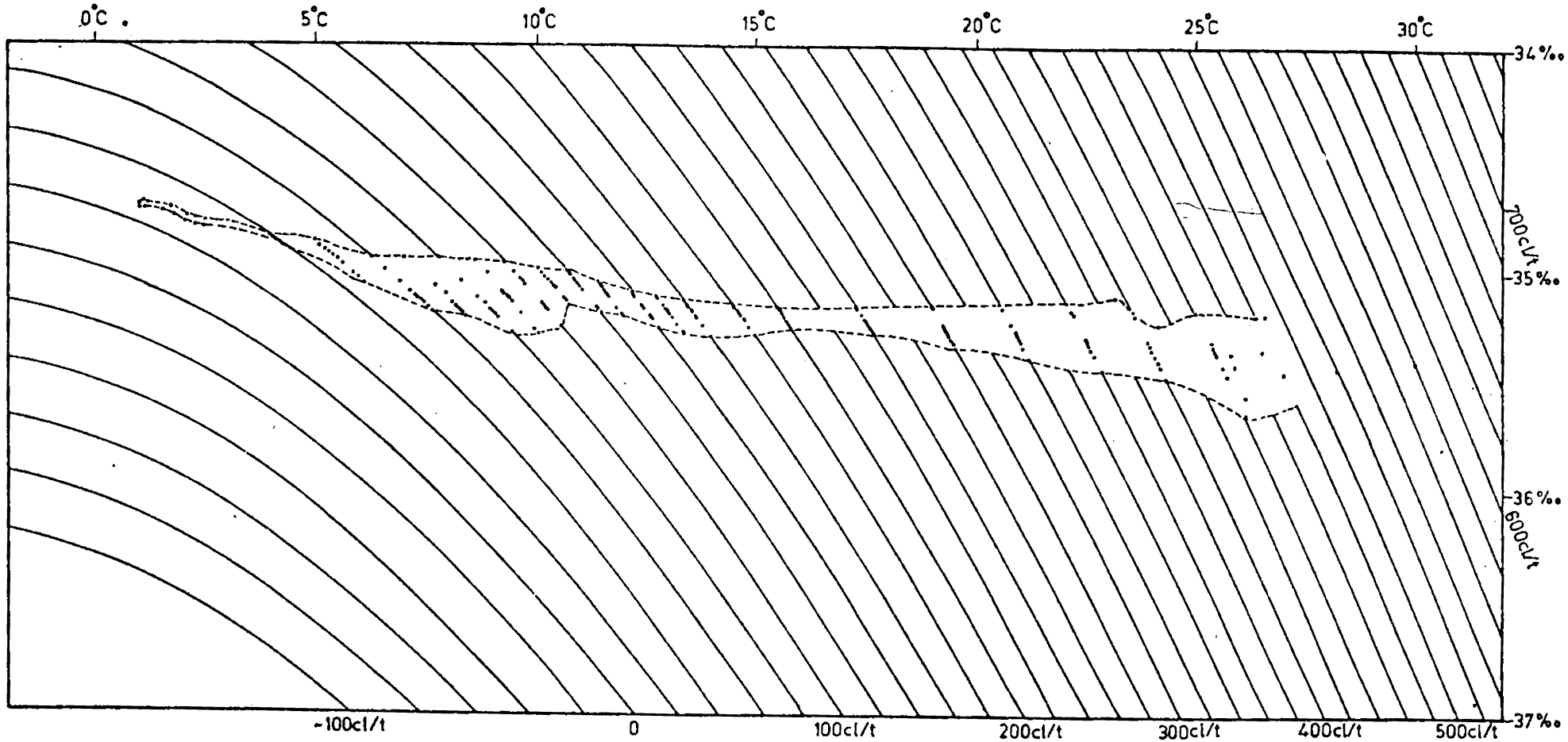

FIG 30 : SCATTER DIAGRAM FOR Θ-S - AREA 1

studied also indicates homogeneous water near the equator. The homogeneity is due to various water types from northern and southern hemispheres, and Pacific Ocean coming into juxtaposition, resulting in lateral as well as vertical mixing (Sharma, 1976).

A close examination of the scatter diagram reveals a weak salinity minimum between 130 and 110-cl/t surfaces. The vertical section of salinity along the equator also exhibits a minimum in the west around the same steric interval. The minimum is due to the influx of water from the south and east.

The heterogeneity noticed between 100 and 80-cl/t surfaces is because of the horizontal advection of Red Sea Water with the maximum salinity of 35.30‰ occurring around 90 to 80-cl/t surfaces. Southward advection of relatively high saline water in the depth range of 500 to 1,000 m, crossing the equator close to the western boundary under the Somali Current was reported by Quadfasel and Schott (1982). Underneath the 40-cl/t surface, the scatter is almost uniform and must be of circumpolar origin (Sharma, 1976).

4.1.2. Area 2 - Between 0° to 4°N and 56° to 60°E

The distribution of potential temperature against salinity exhibits heterogeneity compared to the western area. The heterogeneity may be due to the less mixing of the

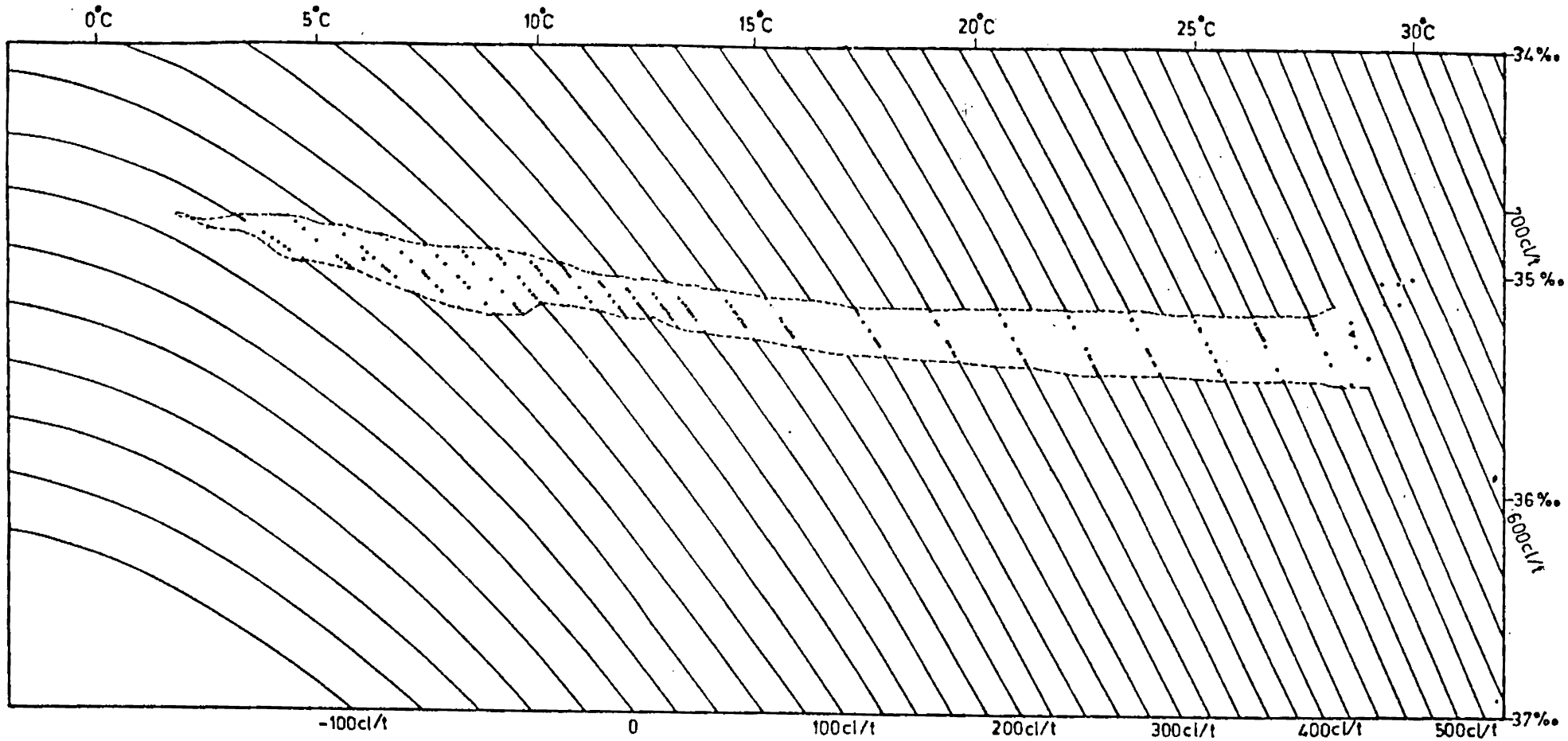

FIG 31 : SCATTER DIAGRAM FOR Θ-S — AREA 2

high salinity water masses from the north and low salinity water masses from the south and east. Just as in the western region, the influence of Red Sea Water is found around 90 to 80-cl/t surfaces, but the salinity maximum is reduced from 35.30 to 35.20‰ . Below the influence of Red Sea Water, relatively wide scatter is probably because of the advection of low salinity water from the south as confirmed in the distribution of properties on 40-cl/t surface.

4.1.3. Area 3 - Between 0° to 4°N and 64° to 68°E

Relatively less scatter is noticed in the intermediate layers, suggesting nearly homogeneous water, though wide scatter is found in the upper layers. The homogeneity is due to the admixture of various water masses from the north, south and east. Red Sea Water is indicated between 100 and 80 cl/t surfaces with the same salinity maximum as that of area 2. Similar to the previous region, relatively more scatter is found below the influence of Red Sea Water.

4.1.4. Area 4 - Between 0° to 4°N and 72° to 76°E

The spread of Θ-S reveals homogeneity in the intermediate depths. The homogeneity may be because of the vertical mixing which is in agreement with the significant vertical mixing, suggested in the distribution of properties on potential thermosteric anomaly surfaces in

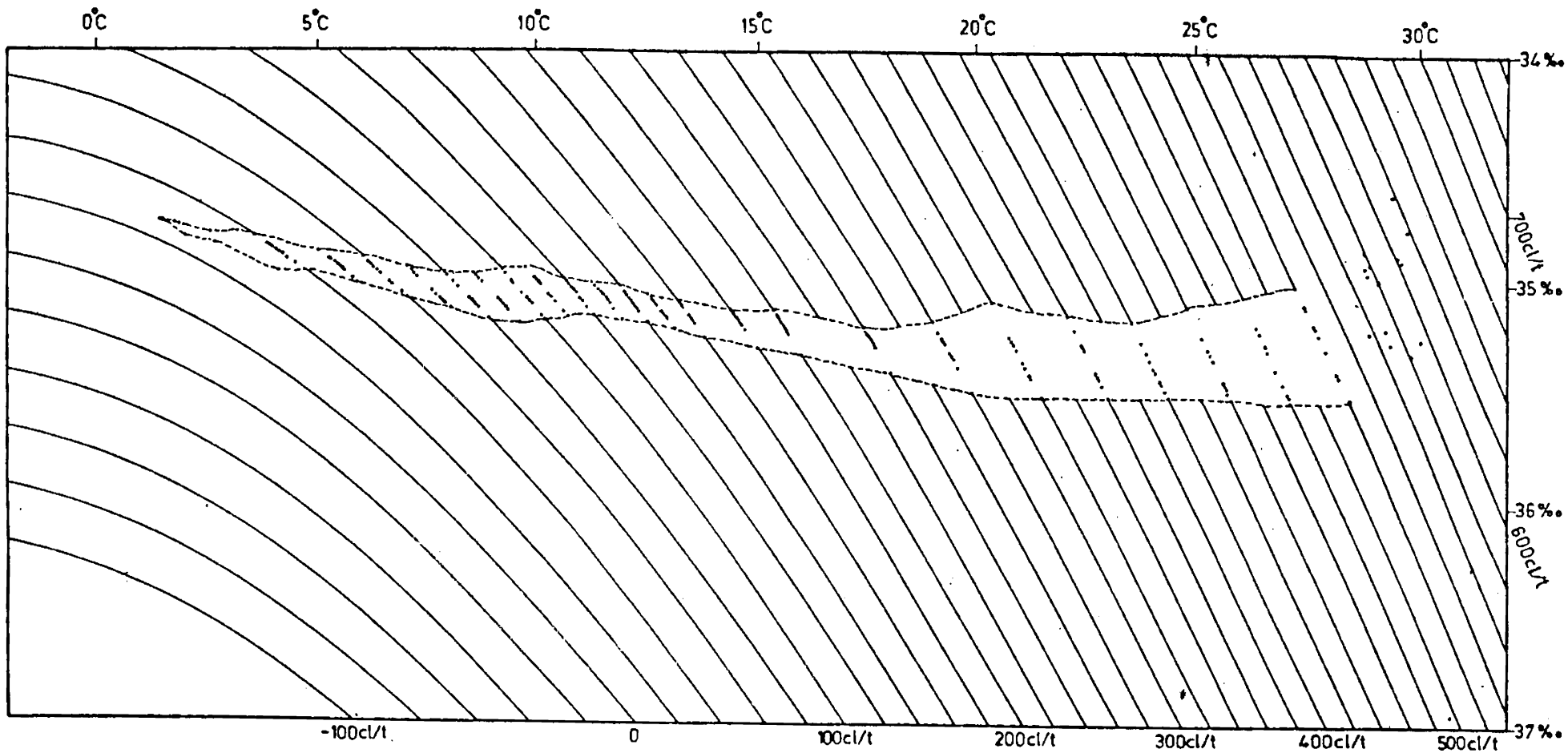

FIG 32 : SCATTER DIAGRAM FOR Θ-S - AREA 3

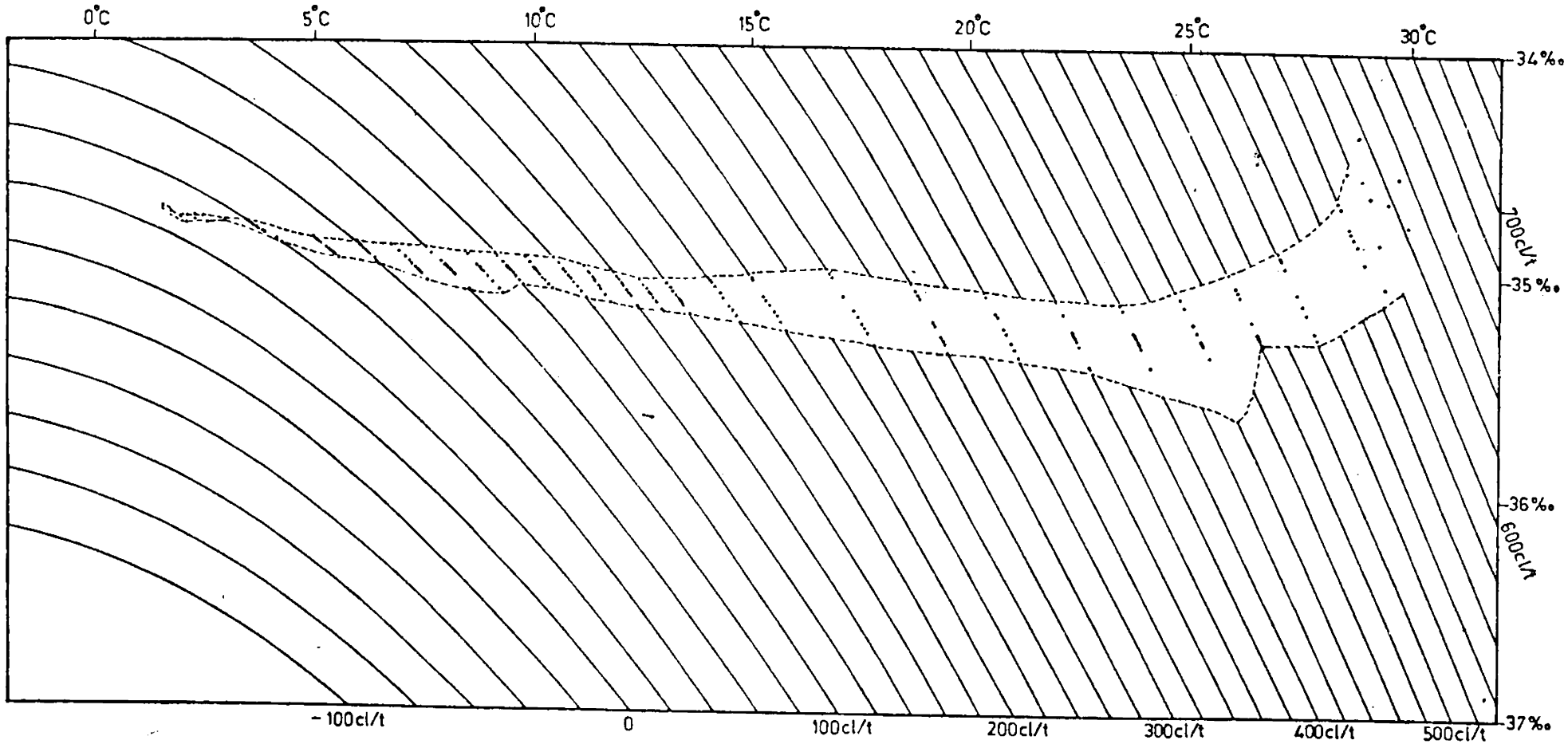

FIG 33 : SCATTER DIAGRAM FOR Θ-S - AREA 4

the southeastern Arabian Sea. The influence of Red Sea Water is less conspicuous in the area compared to the three western areas and is found around 90 to 80-cl/t surfaces with the salinity maximum further reduced to 35.12‰ . The waters below 40-cl/t surface is homogeneous and of circumpolar origin, just as could be inferred in the westernmost region also.

4.1.5. Area 5 - Between 7° to 11°N and 52° to 56°E

The distribution of potential temperature against salinity displays heterogeneity as a consequence of strong horizontal advection of various water masses. Between 200 and 100-cl/t surfaces, the points are scattered within the salinity range of 35.14 to 35.42‰ . Compared to the equatorial areas, the influence of Red Sea Water is very predominant in this area because of the proximity to its source. Higher salinity around 35.55‰ is encountered in the range of 90 to 80-cl/t surfaces and the wide scatter indicates the horizontal advection of Red Sea Water which is in confirmation with the strong horizontal mixing found in the distribution of properties on the isanosteric surfaces and in the vertical section along 10°N. Below 60-cl/t surface, there is less scatter and the water is homogeneous.

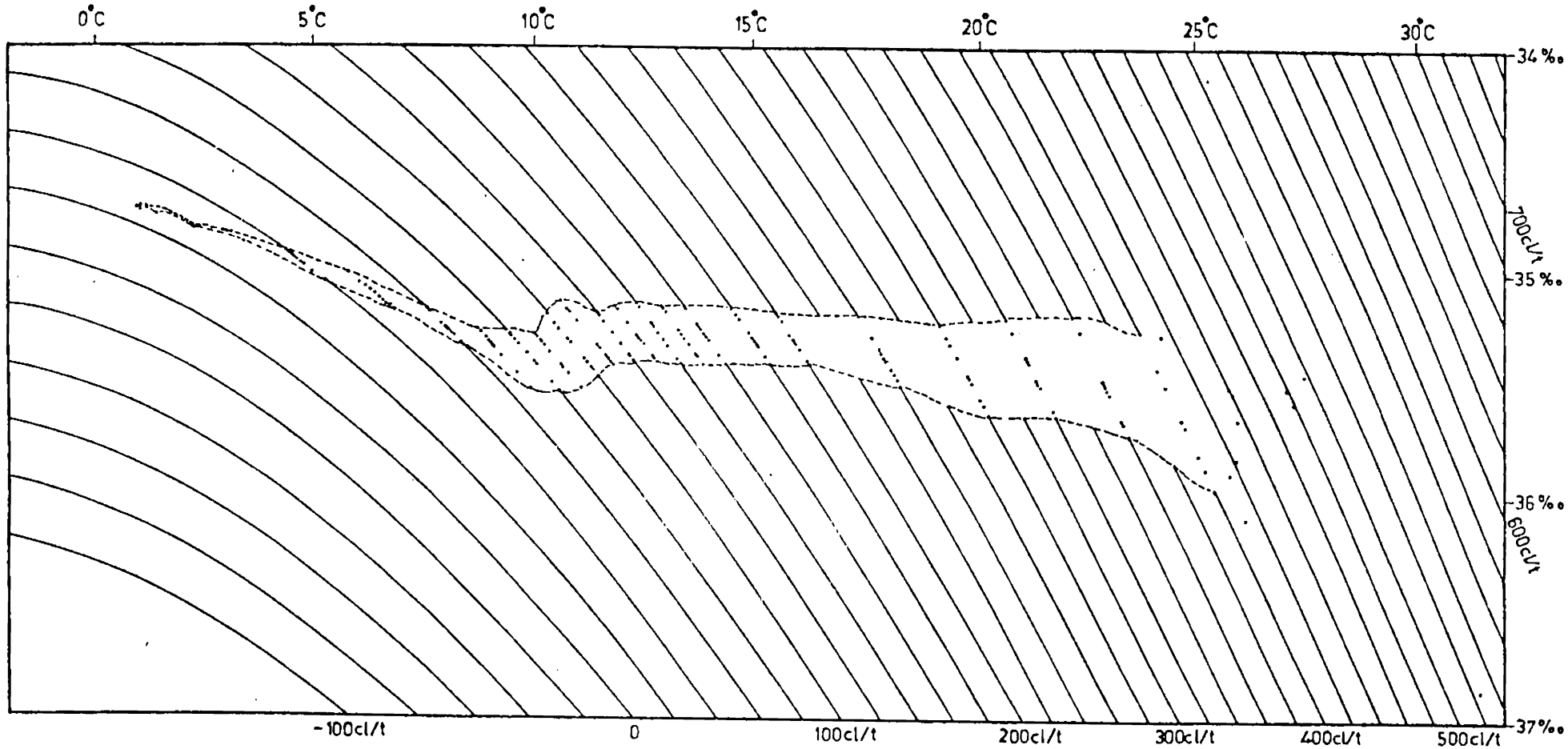

FIG 34 : SCATTER DIAGRAM FOR Θ-S - AREA 5

4.1.6. Area 6 - Between 7° to 11°N and 60° to 64°E

The spread of θ-S reveals relatively heterogeneous water in the intermediate layers. Salinities greater than 36.00‰ in the upper layers is because of the presence of the Arabian Sea Water. The heterogeneity in the intermediate layers indicates the horizontal advection of the waters as found in the vertical section along 10°N, but its intensity is reduced compared to the western area. Red Sea Water is also observed between 100 and 80-cl/t surfaces, but the salinity maximum is lowered to 35.42‰ from the western area. The horizontal spread of the Red Sea Water is in confirmation with the horizontal mixing indicated on the isanosteric surfaces and vertical section of salinity along 10°N. Scatter is less below 40-cl/t surface suggesting homogeneous water.

4.1.7. Area 7 - Between 7° to 11°N and 68° to 72°E

Many features of this region resemble to that of the western area. The wide scatter in the upper layers is because of the influence of Arabian Sea and Bay of Bengal waters. Similar to the two western areas. Red Sea Water is noticed between 100 and 80-cl/t surfaces with the same salinity maximum as that of area 6. The horizontal spreading

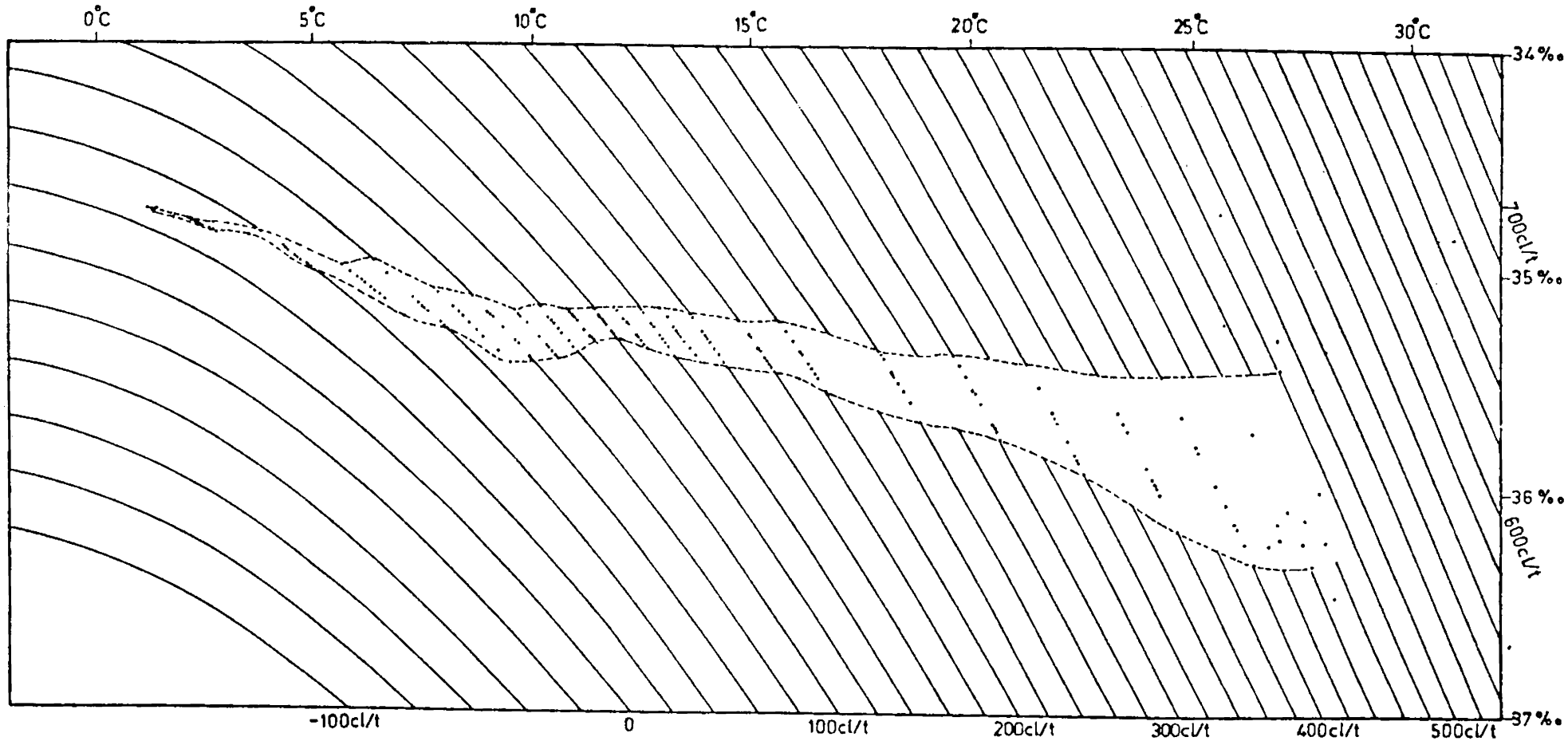

FIG 35 : SCATTER DIAGRAM FOR Θ-S - AREA 6

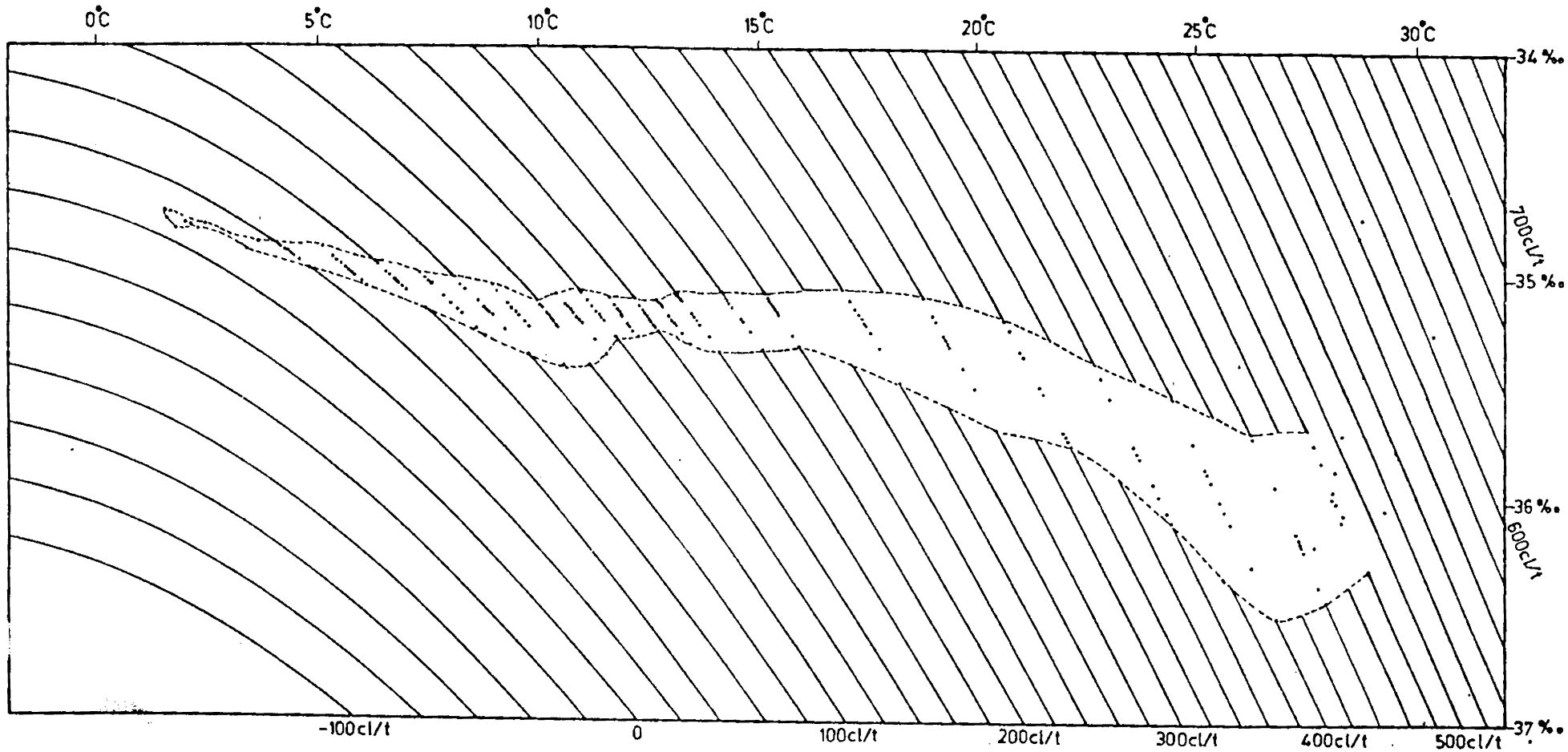

FIG 36 : SCATTER DIAGRAM FOR Θ-S - AREA 7

in the intermediate layers is in agreement with the horizontal mixing revealed from the isanosteric surfaces and vertical section of salinity along 10^{o}N.

4.1.8. Area 8 - Between 14^{o} to 18^{o}N and 56^{o} to 60^{o}E

The distribution of potential temperature against salinity is quite different from the other areas studied. The salinity maximum noticed below 100-cl/t surface as a significant feature in the previous areas is not evident, indicating the absence of Red Sea Water.

The scatter is relatively less, showing homogeneity in the intermediate layers, though more scatter is noticed in the upper layers. The salinity in the intermediate layers is higher (greater than 35.50‰), compared to the other areas studied. The salinity maximum of 35.79‰ noticed at 130-cl/t surface is related to the influence of Persian Gulf Water, eventhough it is less conspicuous. Below 100-cl/t surface, the range of salinity decreases with depth, particularly below 60-cl/t surface.

4.1.9. Area 9 - Between 14^{o} to 18^{o}N and 64^{o} to 68^{o}E

The spread of Θ-S exhibits heterogeneity caused by the horizontal spreading of Persian Gulf Water. The Arabian Sea Water is depicted in the upper layers with salinity

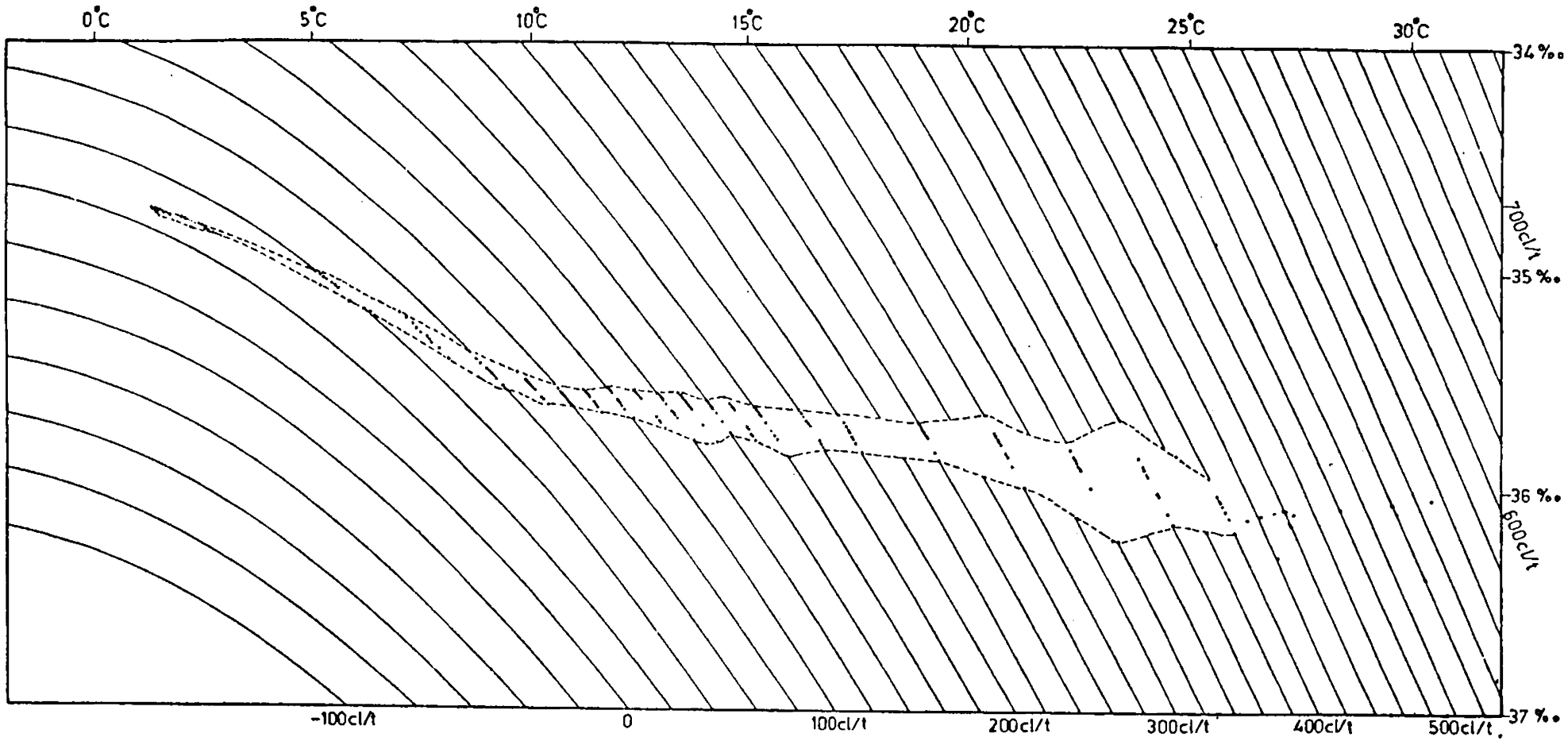

FIG 37 : SCATTER DIAGRAM FOR Θ-S - AREA 8

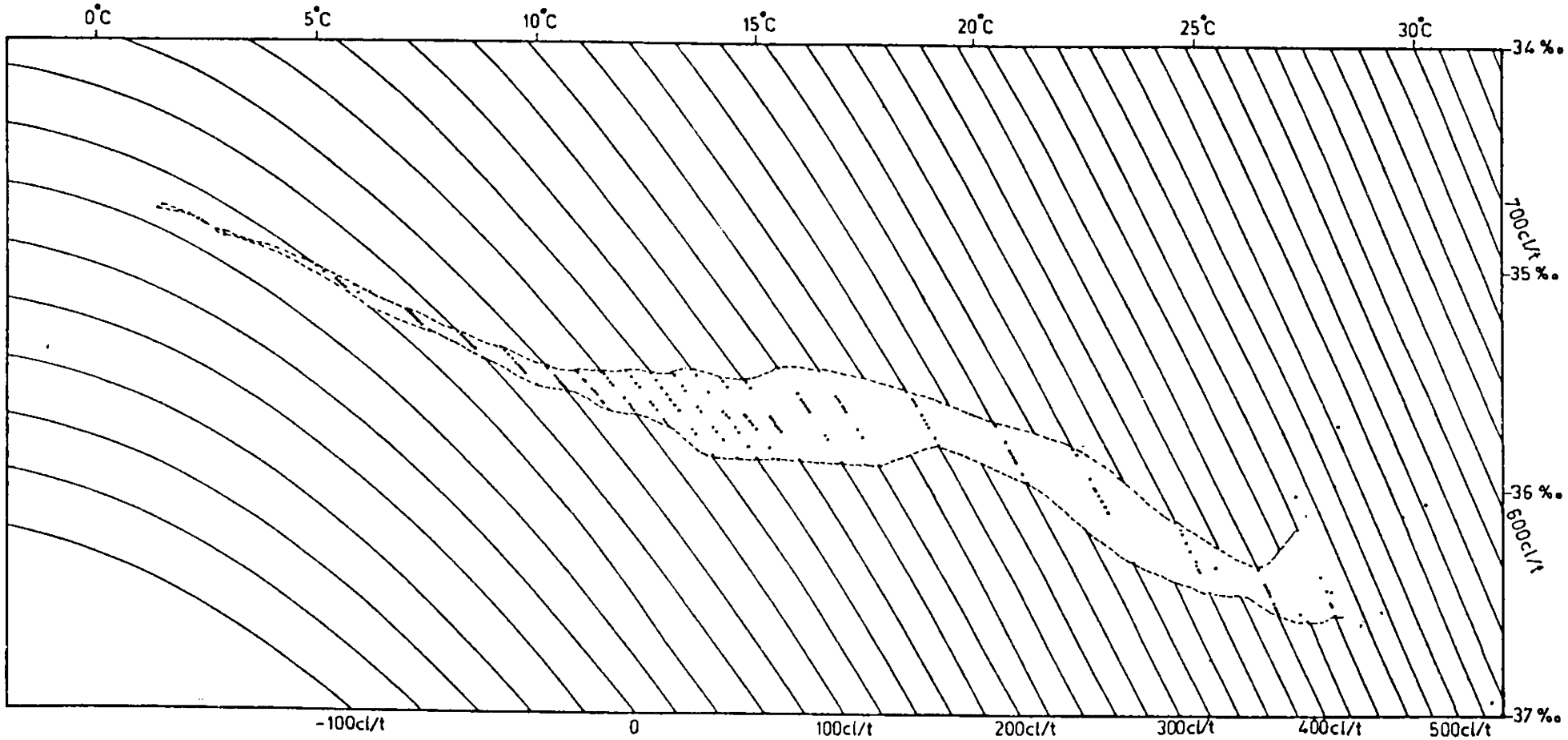

FIG 38 : SCATTER DIAGRAM FOR Θ-S - AREA 9

values .. greater than 36.60‰ . The absence of salinity maximum around 100 to 80-cl/t surfaces confirms that Red Sea Water influence is found only south of 14°N. Similar to the western region, the distribution is homogeneous below 100-cl/t surface.

4.1.10. Area 10 - Between 21° to 25°N and 60° to 64°E

The potential temperature-salinity diagrams reveals wide scatter between 180 and 120-cl/t surfaces, indicating the horizontal spreading of Persian Gulf Water with the maximum salinity value of 36.50‰ at 160-cl/t surface. The spreading of Persian Gulf Water is in confirmation with the spreading and mixing of Persian Gulf Water reported by Premchand (1982) in the northern Arabian Sea. The higher isanosteric surface at which Persian Gulf Water is noticed because of the nearness to its source.

Wide scatter in the surface water compared to the subsurface layers with the salinity range of 36.10 to 36.80‰ is due to the Arabian Sea Water. Below 120-cl/t surface, the distribution is almost homogeneous indicating vertical mixing as found on the isanosteric surfaces and in the section along 20°N.

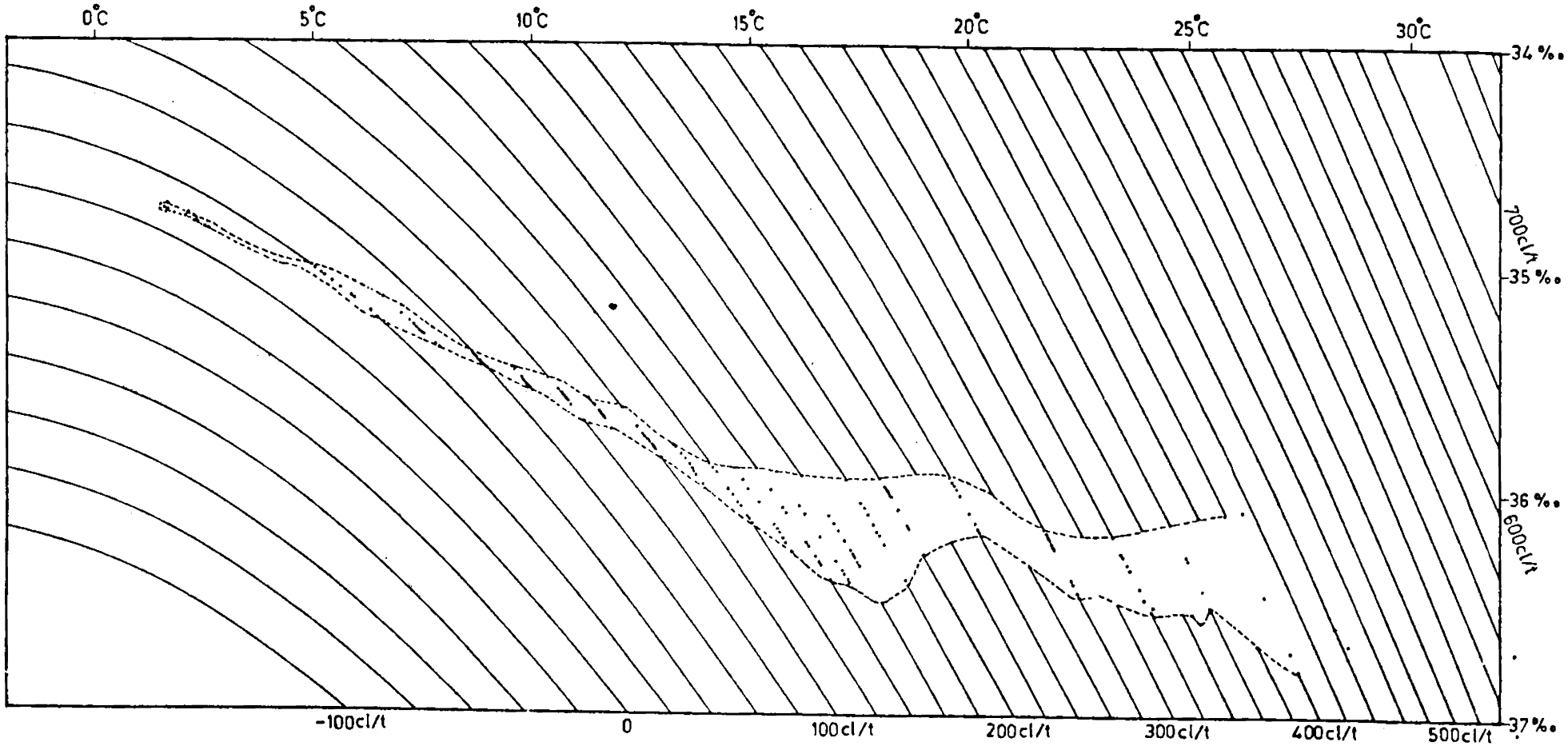

FIG 39 : SCATTER DIAGRAM FOR θ-S — - AREA 10

C H A P T E R – V

CHAPTER - V

DISTRIBUTION OF POTENTIAL VORTICITY BETWEEN DIFFERENT STERIC SURFACES

Potential vorticity is a local measure of vertical homogeneity of a water mass and it is conserved in the absence of vertical mixing. Therefore it gives an indication of water masses and current structure. Hence, the potential vorticity maps between different steric surfaces are presented in this chapter in Figs 40 to 42 to study the water characteristics and current structure of the intermediate waters in the Arabian Sea.

5.1.1. Potential vorticity between 110 and 90 cl/t surfaces

In the interior of the ocean, for large scale processes, relative vorticity is negligible compared to planetary vorticity as mentioned in chapter one. As a result, potential vorticity increases towards higher latitudes (in the northern hemisphere) at a particular level, in the absence of any significant differences in water characteristics. However, in the Arabian Sea, potential vorticity between 110 and 90 cl/t surfaces increases with latitude upto $6^{\circ}N$ and shows a northward decrease in the southeast of Socotra Island and again

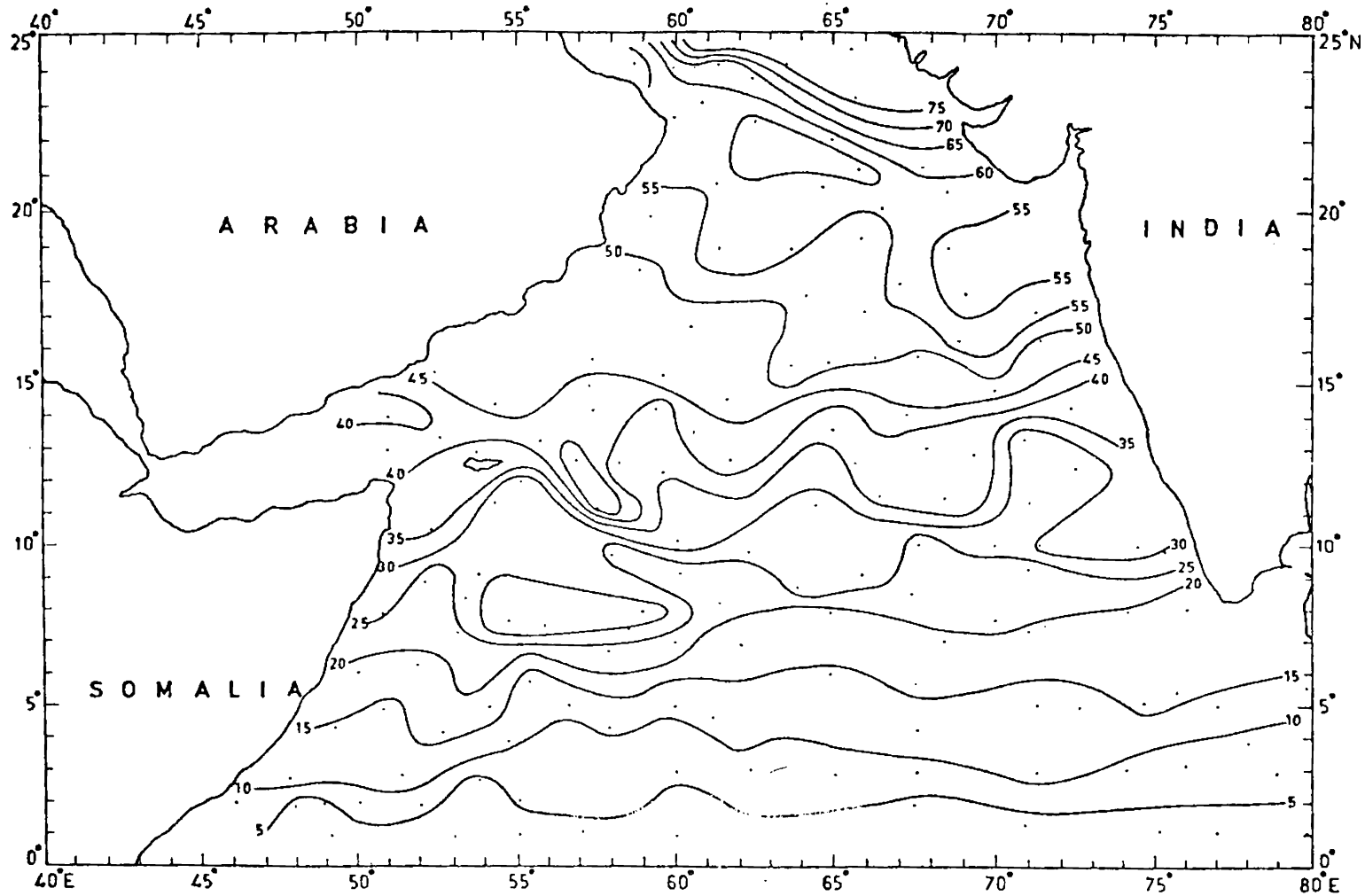

FIG 40 : POTENTIAL VORTICITY (10^{-14} cm^{-1} s^{-1}) BETWEEN 110 AND 90 cl/t SURFACES

increases towards north. Similar northward decrease in potential vorticity is seen off the southwest coast of India and in the western part of the northern Arabian Sea. These areas are potentially baroclinically unstable (McDowell et al., 1982). Intense horizontal mixing is noticed at these areas in the distribution of properties on 100-cl/t surface and in the vertical sections of salinity. In regions of intense horizontal mixing, baroclinic instabilities can be developed if the mixing is not uniform in all places, resulting in the formation of distinct water characteristics at different places within the regions of horizontal mixing.

Similar northward decrease in potential vorticity is observed in the North Atlantic Ocean by McDowell et al. (1982). Stramma (1984) also reported such a situation on the equatorial side of the subtropical gyre in the North Atlantic Ocean.

From the comparison between the potential vorticity of the layer and the distribution of acceleration potential on 100-cl/t surface, it is inferred that some of the closed eddy type circulation are formed due to the manifestations of baroclinic instability prevailing in these areas. It is well known

that baroclinic instability is one of the main reasons for eddy formation in the sea (Gill et al., 1974; Orlanski and Cox, 1973; Pedlosky, 1974, 1975; Orlansky, 1969) apart from topographic effects.

The distribution of potential vorticity of the layer also indicates southward flow along the Somali Coast which is confirmed on the distribution of acceleration potential. In general, it is found that the geostrophic flow is consistent with the distribution of the potential vorticity (Stramma, 1984).

Strong gradients in the distribution of potential vorticity observed off the northern Somali Coast, eastern and northern Arabian Sea indicate that the waters are relatively more heterogeneous as seen in the scatter diagrams. Such areas coincide with the regions of intense horizontal mixing as revealed in the distribution of properties on 100-cl/t surface and in the vertical sections of salinity. Hence, the heterogeneity inferred from the distribution of potential vorticity is because of strong horizontal mixing.

On the contrary, the waters are more homogeneous near the equator and off the southeast coast of Arabia as evident from the relatively weak gradients in the

potential vorticity distribution. The homogeneity is because of vertical mixing as confirmed in the distribution of salinity on 100-cl/t surface, in the vertical sections of salinity and in the scatter diagrams.

The distribution of potential vorticity, in general, resembles that of the salinity distribution on 100-cl/t surface. Sarmiento et al. (1982) also found such features in the North Atlantic Ocean.

5.1.2. Potential vorticity between 90 and 70 cl/t surfaces

The distribution of potential vorticity between 90 and 70 cl/t surfaces is more or less similar to the upper layer. Northward decrease in potential vorticity is noticed in the southeast of Socotra Island, north-eastern and northern Arabian Sea, indicating the baroclinic instability conditions. Relatively strong gradients in potential vorticity are seen in the northern and eastern Arabian Sea and in the southeast of Socotra Island suggesting heterogeneous water. The heterogeneity is because of the horizontal mixing as noticed in the distributions of salinity on 80-cl/t surface, in the vertical sections of salinity and in the scatter diagrams. Comparatively weak gradients are observed in the central and southeastern Arabian Sea indicating homogeneous water as a result of vertical mixing which is in confirmation with the results inferred from the previous chapters.

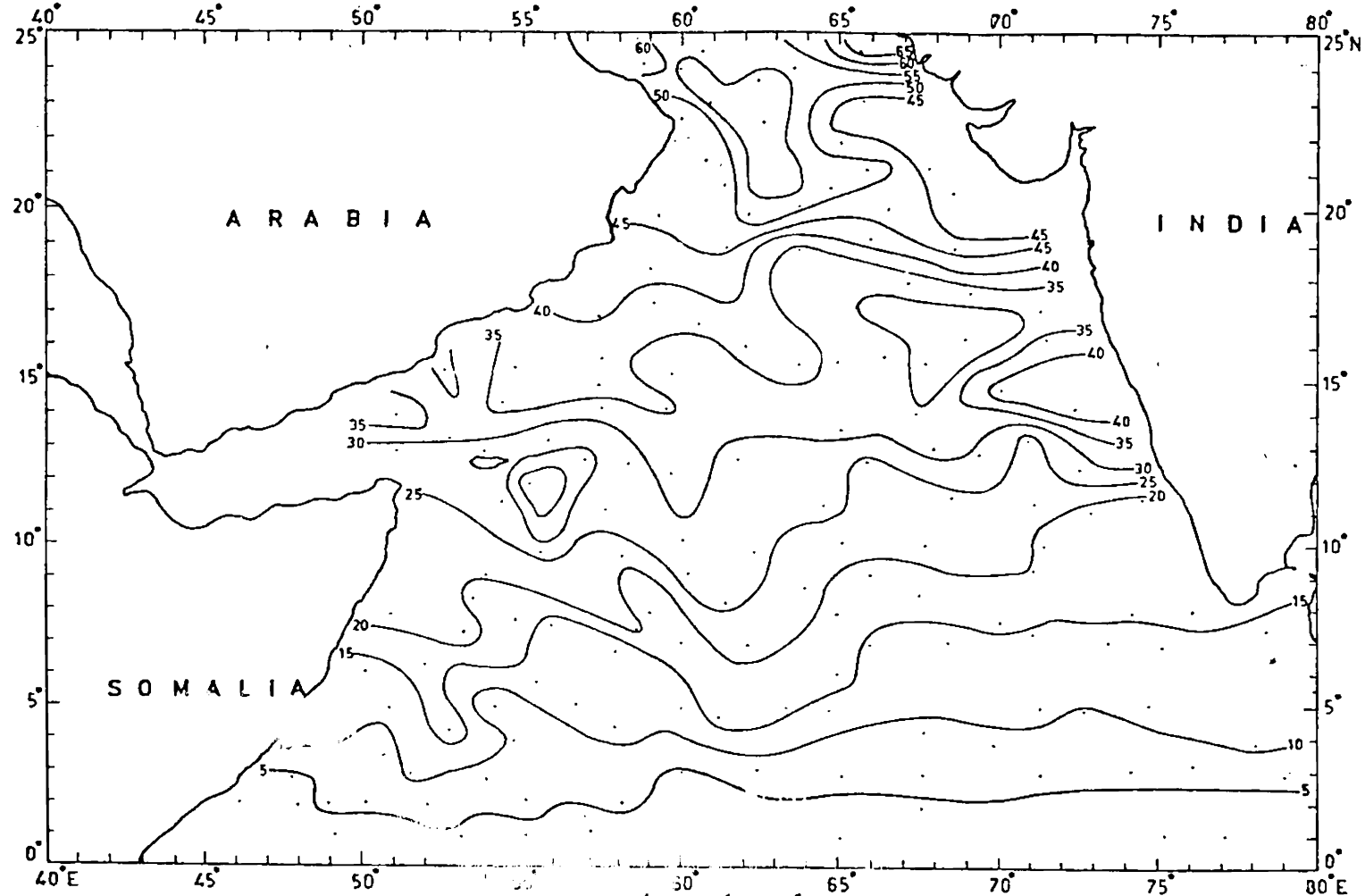

FIG 41 : POTENTIAL VORTICITY (10^{-4} cm^{-1} s^{-1}) BETWEEN 90 AND 70 cl/t SURFACES

5.1.3. Potential vorticity between 70 and 50 cl/t surfaces

Almost all the features noticed between 70 and 50 cl/t surfaces are similar to the upper layers, but the gradients are generally weak. Regions of baroclinic instability are found south of Socotra Island, northern and northeastern Arabian Sea as indicated by the northward decrease in potential vorticity.

As in the upper two layers, gradients in potential vorticity are relatively higher south of Socotra Island and in the eastern Arabian Sea indicating heterogeneity. Such a condition coincides with the horizontal mixing noticed in the distribution of properties in the previous chapters. On the contrary, comparatively weak gradients are seen near the equator, suggesting homogeneity as a result of vertical mixing.

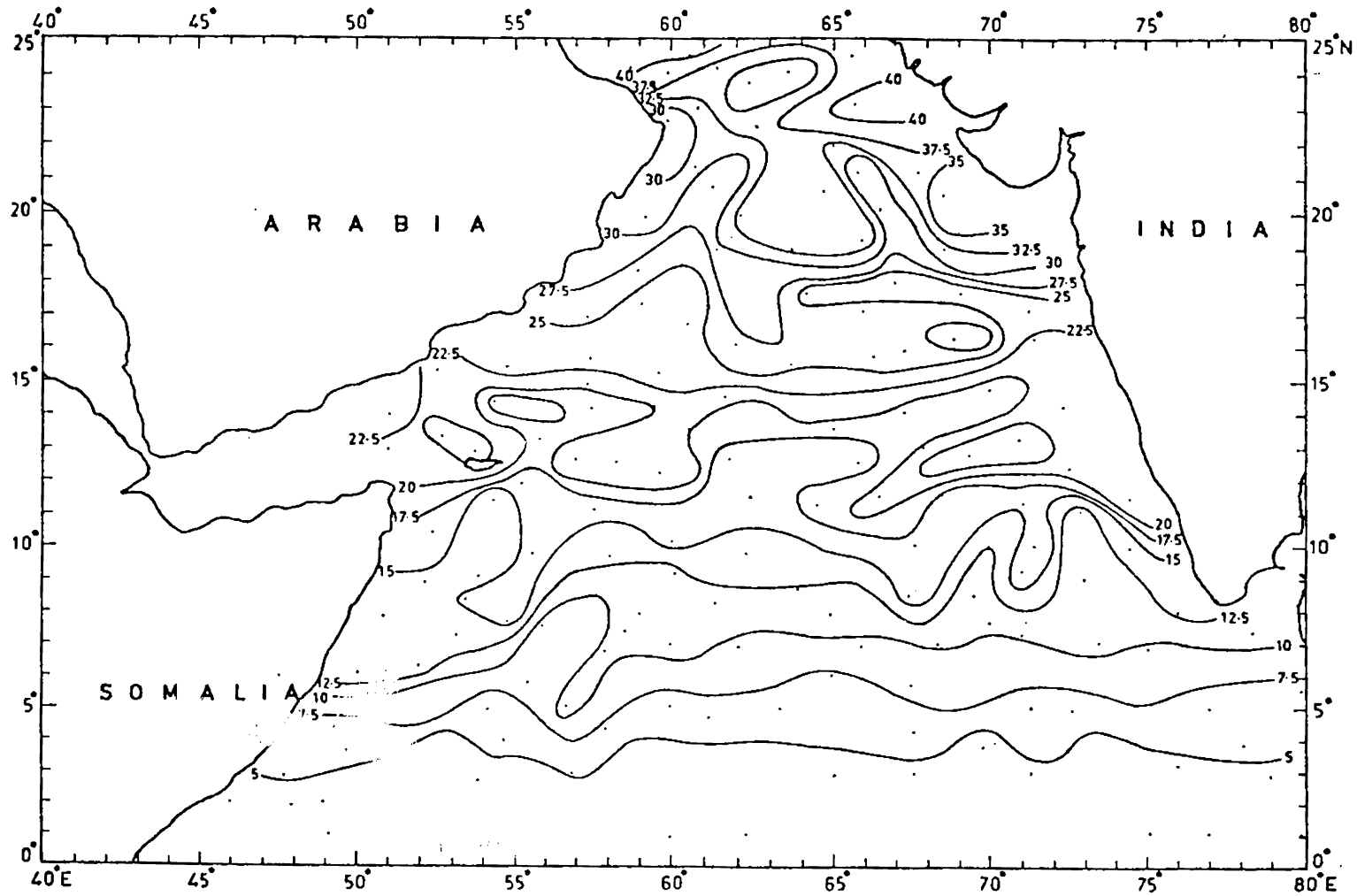

FIG 42 : POTENTIAL VORTICITY (10^{-14} cm^{-1} s^{-1}) BETWEEN 70 AND 50 cl/t SURFACES

C H A P T E R - VI

CHAPTER - VI

SUMMARY AND CONCLUSIONS

The present thesis is an outcome of a study of the water characteristics and current structure of the intermediate waters in the Arabian Sea carried out by the author. The study is accomplished by presenting the topography of different isanosteric surfaces of the intermediate waters and the distribution of acceleration potential and salinity on these surfaces, besides presenting the vertical sections along different latitudes and longitudes in the Arabian Sea. The water characteristics are also studied by working out the scatter diagrams of potential temperature against salinity for different representative areas in the Arabian Sea. An attempt is also made to present the potential vorticity between different steric levels to understand the circulation and mixing processes. Data collected during the International Indian Ocean Expedition (IIOE) and subsequently in the Arabian Sea are used for the study. The area covered north of the equator upto the border of Asian Continent, excluding the Red Sea and Persian Gulf is considered.

Constant potential thermosteric anomaly surfaces of 100, 80, 60 and 40-cl/t, covering the intermediate waters, are chosen to study the water characteristics and current structure. The topography, acceleration potential and salinity maps are prepared for the above surfaces. Since, temperature on an isanosteric surface is uniquely defined by salinity, the salinity maps can alternatively be used as temperature maps. The geostrophic flow along the isanosteric surfaces was deduced from the gradient of acceleration potential using 2,000 db as the reference pressure.

Five zonal and two meridional sections of potential temperature and salinity are presented. Scatter diagrams of potential temperature against salinity are plotted for ten representative areas in the Arabian Sea. Potential vorticity is computed using a novel method, introduced by McDowell et al. (1982), from the hydrographic measurements of the potential density alone.

From the distribution of properties on potential thermosteric anomaly surfaces, it is clear that zonal flow near the equator, meridional flow along the Somali Coast and off the southwest coast of

India prevail on the upper three surfaces, whereas meridional flow predominates on the lower surface. A westward flowing undercurrent near the equator between 45° and 75°E is revealed on the distribution of acceleration potential. North of the westerly undercurrent, an easterly flow of about 200 km wide is evident. The topography as well as the distribution of salinity confirms the above zonal flows while advection of low saline water from the southern hemisphere is noted on the lower surfaces.

Southward undercurrent along the Somali Coast and southerly flow along the southwest coast of India are noticed on the distribution of acceleration potential and in the distribution of salinity maps. Besides, an anticyclonic flow pattern is noted near the southern Somali Coast.

The circulation, suggested by the topography is agreeing with the pattern of acceleration potential. The troughs and ridges on the topography maps, in many cases, are associated with the boundaries of the currents on the acceleration potential map. A striking feature on the topography as well as on the distribution of acceleration potential is the occurrence of number of lows and highs indicating cyclonic and anticyclonic eddies.

The spatial variation of salinity is significant on the upper three surfaces while it is much less on the lower surface. The lower salinities are noticed near the equator whereas high salinity values are found in the northwestern Arabian Sea. In general, salinity decreases from north to south and from west to east on all the four surfaces.

An interesting feature is the rapid decrease of salinity from the central western Arabian Sea towards south and southeast on the upper two surfaces suggesting the horizontal advection of Red Sea Water. Besides, isolated cells of low and high salinity values are found in different regions of the Arabian Sea.

The horizontal gradients in salinity are relatively higher in the central western and eastern Arabian Sea coinciding with the lower thickness between the potential thermosteric anomaly surfaces where horizontal mixing predominates due to higher stability. On the contrary, less horizontal salinity gradients are noticed in the southeastern and northern Arabian Sea where greater thickness between the isanosteric surfaces indicating the prominence of vertical mixing because of lower stability.

The horizontal variation of temperature is less in the intermediate depths in the zonal sections whereas it is significant in the meridional sections. A southerly flow off the southwest coast of India and along the Somali Coast are indicated in the zonal temperature sections as revealed on the distribution of acceleration potential. Similarly, westerly flow near the equator is suggested at intermediate depths in the two meridional sections as found on the acceleration potential of the upper three surfaces.

Homogeneous water is noticed in the intermediate layers in the vertical section of salinity along the equator. The influence of Pacific Ocean Water is observed in the western region of the equatorial section as a weak salinity minimum.

The horizontal spreading of Red Sea Water is predominant along 10^{o}N whereas it is restricted to the western region of the sections along 5^{o} and 15^{o}N. Homogeneous water is found east of the Red Sea Water in the above three sections as a result of the admixture of various water masses. Bay of Bengal Water is noticed in the upper layers in the eastern part of the above sections.

The influence of Persian Gulf Water is found in the two northern zonal sections in the upper layers below the Arabian Sea Water. A notable feature is the conspicuous absence of Red Sea Water in the northern Arabian Sea, north of 15°N.

The horizontal advection of Red Sea Water from the north and low saline water from the south are well depicted in the two meridional sections. The water characteristics and cross-sectional flow pattern indicated in the vertical sections of salinity and potential temperature are in close agreement with the distribution of properties revealed on the potential thermosteric anomaly surfaces.

The scatter diagrams of potential temperature against salinity indicate homogeneous water near the equator except the region bounded by 56° to 60°E which exhibits **heterogeneity**. The heterogeneity is due to the advection of different water masses from north and south. The influence of Red Sea Water is noticed around 100 to 80-cl/t surfaces in most of the areas near the equator. Relatively wide spread around 40-cl/t surface in the equatorial region of the central Arabian Sea suggests the northward advection of water from the south as revealed in the distribution of properties on 40-cl/t surface.

The distribution of potential temperature against salinity exhibits heterogeneity between 7^{o} and $11^{o}N$ as a consequence of the horizontal advection of various water masses. Heterogeneity is more in the west than in the east. Red Sea Water noticed around 80 to 100-cl/t surfaces as a prominent salinity maximum decreases towards east. The horizontal spreading of the Red Sea Water suggested in these areas is in confirmation with the distribution of properties on the isanosteric surfaces and the vertical sections of salinity.

The spread of potential temperature against salinity is relatively less between 14^{o} and $18^{o}N$. The spreading of Arabian Sea Water and Persian Gulf Water are noticed in the upper layers. The absence of any salinity maximum below 100-cl/t surface confirms that the influence of Red Sea Water is felt only south of $14^{o}N$ in the Arabian Sea.

The Persian Gulf Water is indicated in the northern most area with Arabian Sea Water above and homogeneous water below. The homogeneity below 120-cl/t surface is the result of vertical mixing as found in the sections of salinity. Below 60-cl/t surface the range of salinity variation is less.

In general, the water characteristics suggested from the scatter diagrams conform with that found on the distribution of properties on potential thermosteric anomaly surfaces and in the vertical sections of salinity and potential temperature.

From the distribution of potential vorticity between different steric surfaces, it is evident that baroclinic instability prevails off the southeast coast of Socotra Island, southwest coast of India, northern and northeastern Arabian Sea. Intense horizontal mixing is noticed at these areas in the distribution of properties on isanosteric surfaces, in the vertical sections of salinity and in the scatter diagrams. In regions of intense horizontal mixing, baroclinic instabilities can be developed if the mixing is not uniform in all places, resulting in the formation of distinct water characteristics at different places within the regions of horizontal mixing. It is clear that some of the closed eddy type circulation are formed due to the manifestations of baroclinic instability prevailing in these areas. It is also found that the geostrophic flow deduced from the gradient of acceleration potential, in general, is consistent with the distribution of potential vorticity.

Relatively strong gradients in potential vorticity seen in the southeast of Socotra Island, northern and eastern Arabian Sea indicate heterogeneity which coincides with the regions of horizontal mixing as revealed in the distribution of properties on the isanosteric surfaces, in the vertical sections of salinity and in the scatter diagrams.

On the contrary, weak gradients in potential vorticity noticed near the equator, southeast coast of Arabia and central Arabian Sea suggest homogeneity as a result of vertical mixing which is in conformity with the distribution of properties in the vertical sections of salinity and scatter diagrams.

In general, the distribution of potential vorticity resembles that of the salinity distribution.

The intermediate waters of the Arabian Sea, a part of the North Indian Ocean have less interaction with waters of the others except in the south, probably, a consequence of closed boundary on its northern border. There is less renewal of water other than horizontal and vertical mixing confined to the same region unlike in the other regions of the world oceans at similar latitudes.

Both in the Atlantic and Pacific Oceans the intermediate waters have certain conspicuous characteristics. Prominent among them are (1) Step structure in the vertical profiles of temperature and salinity (2) Renewal of waters from the Arctic in the north and the Antarctic in the south (3)Predominence of Western and Eastern Boundary Currents which are the counter meridional flows, responsible for the renewal of waters.

Of these prominent characteristics , the renewal of water is obviously absent in the Arabian Sea. But it is not immediately clear whether the step structure and Western and Eastern Boundary Currents prevail in the Arabian Sea even at lower scale of action. To identify them, further studies at closer network with moored buoy stations for current measurements and STD data that provides continuous profiles, enabling the study of finer structure are to be carried out.

REFERENCES

REFERENCES

*Behringer, D.W. (1972). Investigations of large-scale oceanic circulation patterns using historical hydrographic data. Ph.D. dissertation, Univ. California, San Diego.

Bruce, J.G. (1968). Comparison of near surface dynamic topography during the two monsoons in the western Indian Ocean. Deep Sea Res., 15, 665-677.

Bruce, J.G. (1970). Notes on the Somali Current system during the southwest monsoon. J. Geophys. Res., 75, 4170-4173.

Bruce, J.G. and G.H. Volkmann (1969). Some measurements of currents off the Somali Coast during the northeast monsoon. J. Geophys. Res., 74, 1958-1967.

Clowes, A.J. and G.E.R. Deacon (1935). The deep-water circulation of the Indian Ocean, Nature, 136, 936-938.

Duing, W. (1970). The Monsoon Regime of the currents in the Indian Ocean. East-West Center Press, University of Hawaii, 68 pp.

Duing, W. (1977). Large-scale eddies in the Somali Current. Geophys. Res. Lett., 4, 155-158.

Duing, W. and W.D. Schwill (1967). Ausbreitung and Vermischung des salzreichen Wassers aus dem Roten Meer and aus dem Persischen Golf. Meteor. Forsch. Erg., A 3, 44-66.

Federov, K.N. (1978). The thermohaline fine structure of the ocean (English translation). Pergamon Mar.Ser., No.2, Pergamon Press, 170 pp.

Fofonoff, N.P. (1962). Physical properties of sea water. In : The Sea. 1, M.N.Hill Ed., Interscience, New York - London, 1-30.

Gallagher, J.F. (1966). The variability of water masses in the Indian Ocean. National Oceanographic Data Center, General Series, Publ. G-11, Washington,D.C., 74 pp.

Gill, A.E., J.S.A.Green and A.J. Simmons (1974). Energy partition in the large-scale ocean circulation and the production of mid-ocean eddies. Deep Sea Res., 21, 499-528.

Godfrey, J.S. and T.J. Golding (1981). The Sverdrup relation in the Indian Ocean, and the effect of Pacific-Indian Ocean throughflow on Indian Ocean circulation and on the East Australian Current. J. Phys. Oceanogr., 11, 771-779.

Hamon, B.V. (1967). Medium-scale temperature and salinity structure in the upper 1,500 m in the Indian Ocean. Deep Sea Res., 14, 169-182.

*Helland-Hansen, B. (1916). Nogen Hydrografiske Metoder, Forh. Skand. Naturf. Mote. 357-359.

*Hisard,P. and P. Rual (1970). Courant equatorial intermediaire de I' Ocean Pacifique et contrecourants adjacents. Cah. ORSTOM, ser Oceanogr., 8, 21-45.

Krause, G. (1968). Struktur und Verteilung des Wassers aus dem Roten Meer im Nordwestern des Indischen ozeans. Meteor. Forsch. Erg., A 4, 77-100.

Leetmaa, A., D.R. Quadfasel and D. Wilson (1982). Development of the flow field during the onset of the Somali Current, 1979. J. Phys. Oceanogr., 12, 1325-1342.

*Levy, E., A. Spencer, G. Needell, G. Hund and J.R. Luyten (1982). A compilation of moored current meter data, White Horse profiles and associated oceanographic observations, Vol. XXIX (INDEX, 1979). Tech. Rep., WHOI, 82-16.

Luther, M.E. and J.J. O'Brien (1985). A model of the seasonal circulation in the Arabian Sea forced by observed winds. Prog. Oceanogr., 14, 353-385.

Luyten, J.R. and J.S. Swallow (1976). Equatorial undercurrents. Deep. Sea Res., 23, 999-1001.

Luyten, J.R., M. Fieux, and J. Gonella (1980). Equatorial currents in the western Indian Ocean. Science, 209, 600-603.

*Moller, L. (1929). Die Zirculation des Indischen Ozeans. Veroff. Inst. Meeresk. Univ. Berl., H.21, 48 pp.

Montgomery, R.B. (1937). A suggested method for representing gradient flow in isentropic surfaces. Bull. Amer. Met. Soc., 18, 210-212.

Montgomery, R.B. (1938). Circulation in the upper layers of southern North Atlantic deduced with use of isentropic analysis. Pap. Phys. Oceanogr. & Met., 6, No.2, 55 pp.

Montgomery, R.B. and A.F. Spilhaus (1941). Examples and outline of certain modifications in upper-air analysis. J. Aero. Sci., 8, 276-283.

Montgomery, R.B. and W.S. Wooster (1954). Thermosteric anomaly and the analysis of serial oceanographic data. Deep Sea Res., 2, 63-70.

Montgomery, R.B. and E.D. Stroup (1962). Equatorial waters and currents at 150°W in July-August 1952. Johns Hopk. Oceanogr. Stud., 1, 68 pp

Orlanski, I. (1969). The influence of bottom topography on the stability of jets in a baroclinic fluid. J. Atmos. Sci., 26, 1216-1232.

Orlanski, I. and M. Cox (1973). Baroclinic instability in ocean currents. Geophys. Fluid Dyn., 4, 297-332.

Parr, A.E. (1938). Isopycnic analysis of current flow by means of identifying properties. J. Mar. Res., 1, 133-154.

Pedlosky, J. (1974). The stability of currents in the atmosphere : Part I. J. Atmos. Sci., 21, 201-219.

Pedlosky, J. (1975). The development of thermal anomalies in a coupled ocean-atmosphere model. J. Atmos. Sci., 32, 1501-1514.

Premchand, K. (1982). Spreading and mixing of the Persian Gulf Water in the northern Arabian Sea. Indian J. Mar. Sci., 11, 321-326.

Pond, S. and G.L. Pickard (1983). Introductory dynamical oceanography. Pergamon Press. 2nd Ed., 329 pp.

Quadfasel, D.R. and F. Schott (1982). Water mass distributions at intermediate layers off the Somali Coast during the onset of southwest monsoon 1979. J. Phys. Oceanogr., 12, 1358-1372.

Quadfasel, D.R. and F. Schott (1983). Southward subsurface flow below the Somali Current. J. Geophys. Res., 88, 5973-5979.

Reid, J.L. (1965). Intermediate waters of the Pacific Ocean. Johns Hopk. Oceanogr. Stud., 2, 85 pp.

Robinson, M.K. (1967). Arabian Sea. In, Encyclopedia of Oceanography edited by R.W. Fairbridge, Reinhold Publ. Corp., New York, 1, 40-43.

Rochford, D.J. (1961). Hydrology of the Indian Ocean-I. The water masses in the intermediate depths of the southeast Indian Ocean. Aust. J. Mar. Freshw. Res., 12, 129-149.

Rochford, D.J. (1964). Salinity maxima in the upper 1,000 m metres of the North Indian Ocean. Aust. J. Mar. Freshw. Res., 15, 1-24.

Rochford, D.J. (1966). Distribution of Banda Intermediate Water in the Indian Ocean. Aust. J. Mar. Freshw. Res., 17, 61-76.

Saramiento, J.L., C.G. Rooth and W. Roether (1982). The North Atlantic tritium distribution in 1972. J. Geophys. Res., 87, 8047-8056.

Sastry, J.S. and R.S. D'Souza (1972). Oceanography of the Arabian Sea during the southwest monsoon season, Part III - Salinity. Ind. J. Met. Geophys., 23, 479-490.

*Schott, G. (1926). Die Tiefwasserbewegungen des Indischen Ozeans. Ann. Hydrograph. Maritimen Meteorol., 12, 417-431.

Schott, F. (1983). Monsoon response of the Somali Current and associated upwelling. Prog. Oceanogr., 12, 357-381.

Schott, F. and D.R. Quadfasel (1982). Variability of the Somali Current System during the onset of the southwest monsoon, 1979. J. Phys. Oceanogr., 12, 1343-1357.

Sharma, G.S. (1972). Water characteristics at 200-cl/t in the intertropical Indian Ocean during the southwest monsoon, J. Mar. Res., 30, 102-111.

Sharma,G.S. (1976). Transequatorial movement of water masses in the Indian Ocean. J. Mar. Res., 34, 143-154.

Sharma, G.S.,A.D. Gouveia and S. Satyendranath (1978). Incursion of the Pacific Ocean Water into the Indian Ocean. Proc. Indian Acad. Sci., 87, 29-45.

*Spencer, A., K.O'Neill and J.R.Luyten (1980). A compilation of moored current meter data, White Horse profiles and associated oceanographic observations (Indian Ocean Array 1979). WHOI Tech. Rep. 80-41, 46 pp.

Stramma, L. (1984). Geostrophic transport in the warm water sphere of the eastern subtropical North Atlantic. J. Mar. Res., 42, 537=558.

Sverdrup, H.U., M.W. Johnson and R.H. Fleming (1942). The oceans, their physics, chemistry and general biology. Prentece-Hall, New York, 1087 pp.

Swallow, J.C. (1980). The Indian Ocean Experiment : Introduction. Science, 209, 588.

Swallow, J.C. (1984). Physical oceanography of the Indian Ocean. Deep Sea Res., 31, 639-650.

Swallow, J.C. and J.G. Bruce (1966). Current measurements off the Somali Coast during the southwest monsoon of 1964. Deep Sea Res., 13, 861-888.

Taft,B.A. (1963). Distribution of salinity and dissolved oxygen on surfaces of uniform potential specific volume in the South Atlantic, South Pacific and Indian Oceans. J. Mar. Res., 21, 129-146.

Talley, L.D. and M.S. McCartney (1982). Distribution and circulation of Labrador Sea Water. J. Phys. Oceanogr., 12, 1189-1205.

*Thomsen, H. (1933). The circulation in the depths of the Indian Ocean. J. du Conseil, Conseil Perm. International pour l' Exploration de la Mer, 8, 315-317.

*Thomsen, H. (1935). Enstehung und verbreitungeiniger charakteristisenen water masses in dem Indischen und Sudlichen Pazifischean O'zean. Ann. Hydrol. Birl., 63, 293-305.

Tsuchiya, M. (1968). Upper waters of the intertropical Pacific Ocean. Johns Hopk. Oceanogr. Stud., 4, 50 pp.

Warren, B.A. (1978). Bottom water transport through the southwest Indian Ridge. Deep Sea Res., 25, 315-322.

Warren, B.A. (1981). Transindian hydrographic section of Lat. 18°S. Property distribution and circulation in the South Indian Ocean. Deep Sea Res., 28, 759-788.

Warren, B.A., H. Stommel and J.C. Swallow (1966). Water masses and patterns of flow in the Somali Basin during the southwest monsoon of 1964, Deep Sea Res., 13, 825-860.

Wooster, W.S., M.B. Schaefer and M.K. Robinson (1967). Atlas of the Arabian Sea for Fishery Oceanography. Inst. Mar. Resources, Univ. California, IMR Ref. 67-12.

Wyrtki, K. (1957). The water exchange between the Pacific and Indian Oceans in relation to upwelling process. Proc. Pacif. Cong., 16, 61-66.

Wyrtki, K. (1961). Physical Oceanography of the Southeast Asian waters. Naga Rep., 2, Univ. California Press, 195 pp.

Wyrtki, K. (1971). Oceanographic atlas of the International Indian Ocean Expedition. Washington, D.C. National Sci. Foundation, 531 pp.

Wyrtki, K. (1973). Physical oceanography of the Indian Ocean, In Ecological Studies, Analysis and Synthesis, B. Zeitzsehel, Ed., Springer-Verlag, 3, 18-36.

---

* Not referred in original